Aberrant Intracellular Calcium Cycling in the Heart

Mechanistic Insights into Catecholaminergic Polymorphic Ventricular Tachycardia and Heart Failure

Jere Paavola

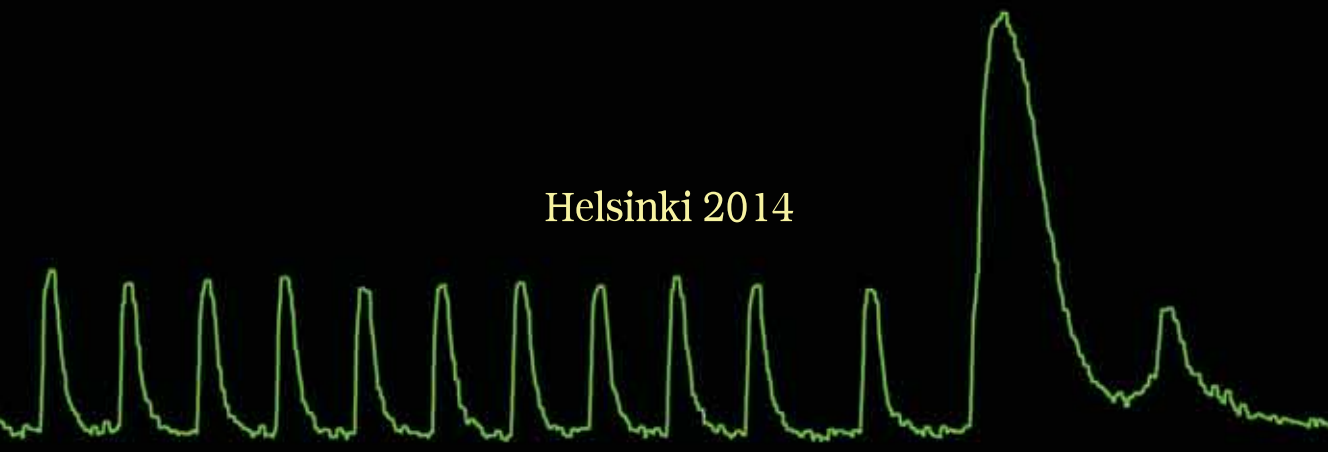

Helsinki 2014

Aberrant Intracellular Calcium Cycling in the Heart

Mechanistic Insights into Catecholaminergic Polymorphic Ventricular Tachycardia and Heart Failure

Jere Paavola

ACADEMIC DISSERTATION

To be publicly discussed, with the permission of the Faculty of Medicine, University of Helsinki, in Lecture Hall 3, Biomedicum Helsinki, Haartmaninkatu 8, Helsinki, on March 28th 2014 at 12 noon

From the Unit of Cardiovascular Research,
Minerva Foundation Institute for Medical Research
&
Department of Cardiology,
Helsinki University Central Hospital

Faculty of Medicine, University of Helsinki, Finland

Helsinki 2014

Supervisors

Professor **Matti Viitasalo**
Department of Cardiology
Helsinki University Central Hospital
University of Helsinki
Helsinki, Finland

Associate Professor **Mika Laine**
Department of Cardiology
Helsinki University Central Hospital
University of Helsinki
Helsinki, Finland

Reviewers

Associate Professor **Kari Ylitalo**
Department of Cardiology
Institute of Clinical Medicine
University of Oulu
Oulu, Finland

Associate Professor **Pasi Tavi**
Department of Biotechnology and Molecular Medicine
A.I. Virtanen Institute for Molecular Sciences
University of Eastern Finland
Kuopio, Finland

Discussed with

Professor **Stephan E. Lehnart**
Heart Research Center Göttingen
Department of Cardiology and Pulmonology
University Medical Center Göttingen, Germany
Georg-August University Göttingen, Germany

ISBN 978-952-10-9761-4 (paperback)
ISBN 978-952-10-9762-1 (PDF)
http://ethesis.helsinki.fi
Printing: Unigrafia
Helsinki 2014

There are strings in the human heart that had better not be vibrated
- Charles Dickens

Author's contact information:

Photo: © Márk Tassy

Jere Paavola

Unit of Cardiovascular Research
Minerva Foundation Institute for Medical Research
Biomedicum Helsinki 2U
Tukholmankatu 8
00290 Helsinki
Finland
Mobile +358 50 443 1337
Fax +358 9 191 25701
E-mail: jere.paavola@helsinki.fi

Table of Contents

List of original publications

This thesis is based on the following studies, referred to in the text by their Roman numerals:

I **Paavola J**, Viitasalo M, Laitinen-Forsblom PJ, Pasternack M, Swan H, Tikkanen I, Toivonen L, Kontula K, Laine M. Mutant ryanodine receptors in catecholaminergic polymorphic ventricular tachycardia generate delayed afterdepolarizations due to increased propensity to Ca^{2+} waves.
Eur Heart J. 2007 May;28(9):1135-42. Epub 2007 Mar 8.

II Kujala K*, **Paavola J***, Lahti A, Larsson K, Pekkanen-Mattila M, Viitasalo M, Lahtinen AM, Toivonen L, Kontula K, Swan H, Laine M, Silvennoinen O, Aalto-Setälä K. Cell model of catecholaminergic polymorphic ventricular tachycardia reveals early and delayed afterdepolarizations. **PLoS One**. 2012;7(9):e44660. Epub 2012 Sep 4.

III **Paavola J**, Väänänen H, Larsson K, Kujala K, Toivonen L, Kontula K, Laine M, Aalto-Setälä K, Swan H, Viitasalo M. Distinct depolarization and repolarization changes in catecholaminergic polymorphic ventricular tachycardia: A study from cellular Ca^{2+} handling and action potentials to clinical monophasic action potentials and electrocardiography.
Submitted manuscript.

IV **Paavola J**, Schliffke S, Rossetti S, Kuo IY, Yuan S, Sun Z, Harris PC, Torres VE, Ehrlich BE. Polycystin-2 mutations lead to impaired calcium cycling in the heart and predispose to dilated cardiomyopathy.
J Mol Cell Cardiol. 2013 May;58:199-208. Epub 2013 Jan 30.

* These authors contributed equally to this work.

Abstract

Heart disease is the biggest killer world-wide, causing a quarter of all deaths. During the past two decades, it has also risen above infectious diseases as the leading cause of years of life lost. Heart failure, characterized by weak pump function of the heart, and disturbances in heart rhythm (arrhythmias) are common and interrelated mechanisms underlying cardiac mortality.

Intracellular calcium ions are crucial to contraction and relaxation of the heart muscle, as well as to control of its rhythm. How calcium is handled and regulated is thus essential to normal cardiac function, and disturbances in these processes can have catastrophic consequences. Understanding the mechanisms of these disturbances is important for improving disease prevention, diagnosis, and management. The studies in this thesis focus on two conditions where cardiac calcium handling is impaired. Studies I – III examine the mechanisms of a genetic arrhythmia disease named catecholaminergic polymorphic ventricular tachycardia (CPVT), which is characterized by stress-induced ventricular tachycardia in a structurally normal heart. Study IV investigates cardiac function in a model of another genetic disease, autosomal dominant polycystic kidney disease (ADPKD). This systemic disease mainly affects the kidneys, and the mechanisms of the concomitant decline in cardiac function have thus far remained underinvestigated.

We evaluated clinical data on cardiac function of CPVT patients, including 24h electrocardiograms, intracardiac monophasic action potential recordings, and exercise stress tests. We used cell models to study the underlying disease mechanisms in detail. During conditions of stress, CPVT cells showed increased spontaneous and irregular release of calcium from within the intracellular stores through the cardiac ryanodine receptors. These receptors, which function as intracellular calcium release channels, harbor the disease-causing mutation. The spontaneous release of calcium led to changes in the membrane potential of the cells, manifested as afterdepolarizations during the resting phase of the cardiac cycle. These afterdepolarizations were reproduced in the clinical monophasic action potential recordings of CPVT patients, and were shown to trigger arrhythmias in these patients. Changes in intracellular calcium alter the membrane potential, and these changes are reflected on the electrocardiogram. Thus, irregularities that might correspond to those observed in the cell model were then investigated in 24h electrocardiograms of CPVT patients. Increased irregularity of cardiac repolarization was found in the CPVT

patients. Such irregularity was greater in the electrocardiograms of CPVT patients with a history of more severe arrhythmic events. Additionally, we found slowed depolarization in response to stress in CPVT cells and patients, suggesting reduced conduction velocity might contribute to an arrhythmic substrate in these patients.

Cardiac function in ADPKD caused by mutations in polycystin-2, another intracellular calcium channel, was investigated in a zebrafish model lacking expression of the polycystin-2 protein. The zebrafish lacking polycystin-2 showed signs of heart failure, including reduced cardiac output, edema, and arrhythmias. Hearts, which were then examined in more detail *ex vivo*, showed impaired cycling of intracellular calcium, which is likely to underlie the cardiac dysfunction observed *in vivo*. The association of ADPKD with idiopathic dilated cardiomyopathy (IDCM) was examined using the Mayo ADPKD Mutation Database, which contains data on genotyped ADPKD patients. Examination of the ADPKD Database showed IDCM to be very common among ADPKD patients. IDCM was most prevalent in patients with mutations in polycystin-2, suggesting impaired calcium cycling as a potential pathomechanism.

Studies I-III shed new light on mechanisms of arrhythmias in CPVT and related conditions, opening the way for future studies on arrhythmia risk and therapeutic evaluation. Furthermore, the results encourage pursuing the novel stem cell models for studying pathomechanisms and therapeutics. Study IV showed an association between ADPKD and IDCM. The zebrafish model suggested impaired calcium cycling as an underlying mechanism, highlighting the usefulness of zebrafish as a model in cardiac research.

Tiivistelmä – Finnish summary

Sydänsairaudet ovat maailmanlaajuisesti yleisin kuolinsyy, aiheuttaen neljänneksen kuolemista. Kahden viime vuosikymmenen aikana ne ovat ohittaneet tartuntataudit suurimpana menetyttyjen elinvuosien aiheuttajana. Sydämen vajaatoiminta ja rytmihäiriöt ovat sydänkuolleisuuden taustalla olevia yleisiä ja toisiinsa liittyviä mekanismeja.

Solunsisäiset kalsiumionit ovat elintärkeitä sekä sydämen supistuvuuden ja relaksaation, että sen rytmin säätelyn kannalta. Kalsiumin tiukka säätely on siten sydämen normaalin toiminnan edellytys, ja tämän säätelyn häiriöillä voi olla vakavia seuraamuksia. Näiden häiriöiden mekanismien ymmärtäminen on tärkeää sairauksien ehkäisyn, diagnostiikan ja hoidon kannalta. Tämän väitöskirjan osatyöt paneutuvat kahteen sairauteen, joissa sydämen solunsisäisen kalsiumin säätely on häiriintynyt. Osatyöt I – III tutkivat katekoliaminergisen monimuotoisen kammiotiheälyöntisyyden (CPVT) mekanismeja. Tämä perinnöllinen rytmihäiriösairaus aiheuttaa henkeä uhkaavaakin kammiotiheälyöntisyyttä stressin yhteydessä rakenteellisesti terveessä sydämessä. Osatyössä IV tutkitaan sydämen toimintaa liittyen autosomissa vallitsevasti periytyvään munuaisten monirakkulatautiin (ADPKD). Tämä perinnöllinen systeeminen sairaus vaikuttaa oleellisesti munuaisiin, mutta samanaikainen sydämen toiminnan heikkeneminen on jäänyt vähemmälle huomiolle.

Arvioimme sydämen toimintaa CPVT-potilailla käyttäen menetelminä sydänsähkökäyrän pitkäaikaisnauhoitusta, sydämen rasituskoetta ja elektrofysiologista tutkimusta, johon sisältyi oikean kammion aktiopotentiaalimittaus. Lisäksi käytimme solumalleja mekanismien yksityiskohtaiseen selvittämiseen. CPVT:n taustalla ovat mutaatiot sydämen ryanodiinireseptorissa, joka on kalsiumin säätelyssä oleellinen solunsisäinen kalsiumkanava. Stressin yhteydessä CPVT-soluissa esiintyi lisääntynyttä spontaania ja epäsäännöllistä kalsiumin vapautumista solunsisäisistä varastoista mutatoituneiden ryanodiinireseptorien läpi. Tämä johti solukalvon jännitteen muutoksiin, jotka havaittiin sydämen lepovaiheen aikana ilmenevinä jälkidepolarisaatioina. Vastaavia jälkidepolarisaatioita havaittiin myös CPVT-potilaiden aktiopotentiaalimittauksissa, missä ne ajoittain laukaisivat kammiolisälyöntejä. Solunsisäisen kalsiumpitoisuuden muutokset vaikuttavat solukalvon jännitteeseen, mikä taas heijastuu sydänsähkökäyrään. Tämän vuoksi solumallissa todettua kalsiumpitoisuuden vaihtelua vastaavia

muutoksia tutkittiin CPVT-potilaiden sydänsähkökäyrissä. Vastaavasti, myös sydämen repolarisaation vaihtelu oli lisääntynyt CPVT-potilailla. Tämä vaihtelu oli suurempaa niiden CPVT-potilaiden sydänsähkökäyrissä, joilla oli aiemmin todettuja vakavia rytmihäiriötapahtumia. Tämän lisäksi löysimme CPVT-soluilla ja -potilailla stressin yhteydessä hidastuvaa depolarisaatiota, viitaten hidastuneen sähköisen johtumisen mahdolliseen osuuteen rythmihäiriölttiutta lisäävänä tekijänä näillä potilailla.

Tutkimme sydämen toimintaa polykystiini-2:n mutaatioista aiheutuvassa ADPKD-mallissa. Käytetyltä seeprakalamallilta puuttuu polykysteiini-2-proteiini, joka normaalisti muodostaa solunsisäisen kalsiumkanavan. ADPKD:n yhteyttä tuntemattomasta syystä johtuvaan laajentavaan sydänlihassairauteen (IDCM) tarkasteltiin Mayo-klinikan ADPKD tietokannasta, joka sisältää tietoa genotyypatuista ADPKD-potilaista. Seeprakalamallissa todettiin sydämen vajaatoimintaan viittaavina löydöksinä alentunut sydämen minuuttitilavuus, turvotusta ja rytmihäiriöitä. Kalojen sydämiä tutkittiin tarkemmin kuvantamalla solunsisäistä kalsiumia, jonka säätelyn havaittiin olevan heikentynyttä ADPKD-kaloilla sopien havaitun sydämen vajaatoiminnan syyksi. Mayo-klinikan tietokannassa IDCM oli yleinen diagnoosi ADPKD-potilaiden keskuudessa. Vallitsevuus etenkin polykystiini-2-mutaatioita kantavien ADPKD-potilaiden keskuudessa oli yleistä, viitaten heikentyneeseen kalsiumin säätelyyn mahdollisena tautimekanismina.

Osatyöt I – III tuovat uutta tietoa CPVT:n ja senkaltaisten tautitilojen yhteydessä esiintyvien rytmihäiriöiden mekanismeista, avaten samalla tien tuleville rytmihäiriöriskiin ja hoidon tehon arviointiin liittyville tutkimuksille. Lisäksi tulokset kannustavat jatkamaan uusien solumallien käyttöä tautimekanismeihin ja hoitoihin liittyvissä tutkimuksissa. Osatyö IV:ssä havaittiin yhteys ADPKD:n ja IDCM:n välillä. Tutkimukset seeprakalamallilla viittaavat heikentyneeseen solunsisäisen kalsiumin säätelyyn taustalla olevana mekanismina, samalla alleviivaten seeprakalamallin käyttökelpoisuutta sydäntutkimuksessa.

Abbreviations

ADPKD	autosomal dominant polycystic kidney disease
AM	acetoxymethyl
AP	action potential
APD	action potential duration
AV	atrioventricular
bpm	beats per minute
$[Ca^{2+}]_i$	intracellular calcium concentration
Calstabin2	FKBP12.6, RyR2 stabilizing protein
CaMKII	Ca^{2+}/calmodulin-dependent protein kinase II
CASQ2	cardiac calsequestrin protein
CASQ2	cardiac calsequestrin gene
CDM	complex demodulation
CPVT	catecholaminergic polymorphic ventricular tachycardia
DAD	delayed afterdepolarization
DCM	dilated cardiomyopathy
dpf	days post fertilization
EAD	early afterdepolarization
ECG	electrocardiogram
hpf	hours post fertilization
ICD	implantable cardioverter defibrillator
$I_{Ca,L}$	L-type calcium current
IDCM	idiopathic dilated cardiomyopathy
I_{K1}	inwardly rectifying potassium current
I_{Kr}	rapid delayed rectifying potassium current
I_{Ks}	slow delayed rectifying potassium current
I_{Na}	sodium current
I_{NCX}	sodium-calcium exchanger current
iPSC	induced pluripotent stem cell
$I_{to,f}$	fast transient outward potassium current
$I_{to,s}$	slow transient outward potassium current
LTCC	L-type calcium channel

MAP	monophasic action potential
MAPD	monophasic action potential duration
MMA	modified moving average
NCX	sodium-calcium exchanger channel
PC1	polycystin-1 protein
PC2	polycystin-2 protein
PCR	polymerase chain reaction
PKA	protein kinase A
PKD1	polycystic kidney disease type 1
PKD1	polycystin-1 gene (human)
PKD2	polycystic kidney disease type 2
PKD2	polycystin-2 gene (human)
pkd2	polycystin-2 gene (zebrafish)
PLB	phospholamban
PVC	premature ventricular contraction
QT	QT interval
QTVI	QT variability index
RyR2	ryanodine receptor type 2 protein
RyR2	ryanodine receptor type 2 gene (human)
SCD	sudden cardiac death
SERCA2a	sarcoplasmic reticulum Ca^{2+} ATPase
SR	sarcoplasmic reticulum
STV	short-term variability
TRPP1	transient receptor potential polycystic 1, polycystin-1
TRPP2	transient receptor potential polycystic 2, polycystin-2
T-tubule	transverse tubule
TWA	T-wave alternans
UWA	U-wave alternans
VF	ventricular fibrillation
VT	ventricular tachycardia
WT	wildtype

Introduction

Globally, heart disease is the number one cause of mortality and years of life lost. It is not just the elderly who are directly affected: in women aged 15 – 49, cardiovascular disease is the third biggest killer after HIV/AIDS and a group of other non-communicable diseases. In men aged 15 – 49, it is the biggest killer (Lozano et al. 2012). Besides being the biggest single killer, ischemic heart disease often leads to declined cardiac function and heart failure. In patients with heart failure, loss of adequate pump function and sudden cardiac death (SCD) due mainly to ventricular arrhythmias are equally common causes of mortality (Tomaselli et al. 1994). The hard work of scientists over the last decades has tremendously improved our understanding of the mechanisms behind failing cardiac function and lethal arrhythmias. Yet, much remains incompletely understood.

A common thread linking impaired pump function of the heart to lethal arrhythmias has started to emerge: abnormal intracellular Ca^{2+} handling (Laurita et al. 2008b, Aistrup et al. 2011). Ca^{2+} is essential for muscle contraction. However, when it gets mishandled, it is not just the contraction and relaxation that are affected. Ca^{2+} can also trigger, sustain, and perpetuate arrhythmias, with possibly disastruous consequences.

In this thesis, I present the results of our investigations on the mechanistic role of intracellular Ca^{2+} cycling in pathology linked to arrhythmias in catecholaminergic polymorphic ventricular tachycardia (CPVT) and cardiac dysfunction in autosomal dominant polycystic kidney disease (ADPKD). Both diseases are inherited conditions that in addition to investigating disease-specific pathomechanisms, offer the possibility of gaining a better understanding of disease processes linked to abnormal intracellular Ca^{2+} handling more broadly.

Studies I – III focus on the mechanisms of arrhythmias in CPVT. Clinical data including monophasic action potential (MAP) recordings, electrocardiograms (ECG), and exercise stress tests, are combined with investigation of the disease at the molecular and cellular levels by using traditional and modern cell models. The arrhythmias in CPVT resemble those seen in patients with heart failure. Therefore the implications of these findings touch a far broader population than those suffering from this fairly rare genetic condition.

Study IV examines cardic function in ADPKD using a zebrafish model and clinical data on ADPKD patients. Based on detailed investigation of *in vivo* and *ex vivo* cardiac function in the model organism, clinical data on ADPKD patients are examined for the prevalence of heart failure. ADPKD is the most common inherited kidney disease and is associated with substantial cardiovascular morbidity and mortality. The mechanisms of cardiac dysfunction in these patients remain underinvestigated and poorly understood.

In all four studies, basic research methods are combined with clinical patient data in an attempt to bridge the gap between basic research and the clinic, helping to translate insights gained in the lab to benefit the patients. Before presenting and discussing our findings, I review the essential concepts and take a look at where we currently stand in our understanding of the role of Ca^{2+} in arrhythmias and heart failure.

Review of literature

ELECTRICAL ACTIVITY OF THE HEART

1.1 The cardiac action potential and its conduction

The heart pumps blood around the circulatory system, hence facilitating the delivery of oxygen and nutrients to target tissues all over the body and the removal of waste products from them. To achieve this, the heart contracts and relaxes rhythmically. The rhythmic action is based on the generation of action potentials (AP), which are the fundamental manifestations of electrical activity in the heart. Action potentials are short cyclic events resulting from the transfer of various ions between the outside and inside of the cells through specialized channels on the cellular plasma membrane of the cardiomyocytes, known as the sarcolemma (Nerbonne et al. 2005). The movement of ions results in changes of membrane potential that are in the order of 100 millivolts (mV). Under normal conditions, APs are generated in specialized pacemaker cells of the sinoatrial node, located in the right atrium of the heart. Thus the

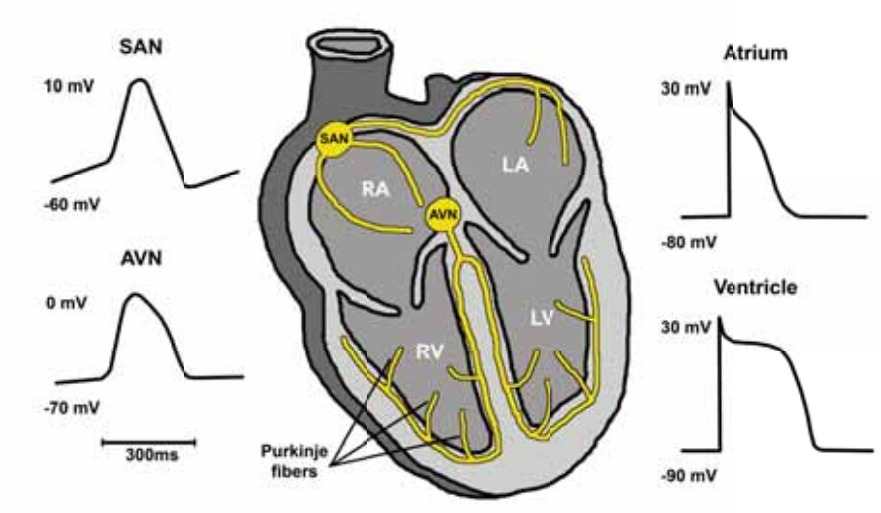

Figure 1. A simplified schematic of the heart's electrical conduction system (yellow) and typical AP characteristics of different cell types. SAN = sinoatrial node, AVN = atrioventricular node, RA = right atrium, LA = left atrium, RV = right ventricle, LV = left ventricle.

expression: “sinus rhythm”. The APs reach neighboring cells by sarcolemmal channels called gap junctions, which permit the flow of current, enabling propagation (Rohr 2004). The APs are conducted through the atria into the atrioventricular (AV) node, located between the atria and the ventricles. From the AV node, the only conductive route between the atria and the ventricles under normal conditions, the APs travel along Purkinje fibers to finally achieve synchronized excitation of the ventricular myocardium. The Purkinje cells are modified cardiomyocytes, capable of rapid conduction. Due to the differential expression of ion channels, the shape and duration of the AP varies greatly based on the type of heart cell in question, as demonstrated in figure 1.

1.2 Sarcolemmal ion channels and currents in the cardiomyocyte

Here I shall concentrate on the ventricular AP, as it is most essential to this study. The AP is generally divided into four phases (figure 2). Each phase is characterized by a distinct combination of tightly controlled ion currents (Amin et al. 2010). These ion currents result from the opening and closing (known as gating) of sarcolemmal ion channels (Grant 2009). The gating of relevant cardiac ion channels is dependent on the membrane potential. As the membrane potential reaches a certain threshold, these channels open or close. Closure of the channels is associated with a period of inactivation, which underlies refractoriness during which the channels are unable to re-activate (open). The current amplitude through an ion channel is determined by its conductivity and by the membrane potential. Currents through ion channels in which the current amplitude does not increase linearly with its conductivity are known as rectifying currents. In such channels conductivity varies depending on the membrane potential. Ions tend to move down their concentration gradient. At equilibrium potential, referred to as the Nernst potential, the net current across the membrane is zero. The equilibrium potential of a specific ion depends on its concentrations inside and outside the cell, as well as on the temperature. During the resting phase of the ventricular cardiomyocyte (phase 4), the membrane potential is typically -90 mV, with the inside of the cell being negatively charged. The negative resting potential is largely due to the inwardly rectifying potassium current (I_{K1}), resulting from K^+ ions flowing out of the cell, and is close to the equilibrium potential for K^+. When an AP reaches the cell, Na^+ and some Ca^{2+} ions flow into it from neighboring cells via gap junctions, increasing the membrane potential, hence partly depolarizing the cell. When the cell reaches a threshold potential of about -70 mV, the fast, voltage-

gated Na^+ channels open resulting in an inward sodium current (I_{Na}) (phase 0). At the same time, the inwardly rectifying K^+ channels close, helping to move the potential from the negative K^+ equilibrium potential towards the positive Na^+ equilibrium potential. This causes the voltage-gated Na^+ channels to close and transient K^+ channels to briefly open, producing a hyperpolarizing notch to the AP due to fast and slow transient outward K^+ currents ($I_{to,f}$ and $I_{to,s}$)(phase 1). Phase 2 is referred to as the plateau phase, resulting from a balance between inward L-type Ca^{2+} current ($I_{Ca,L}$) through the voltage-gated, L-type calcium channels (LTCC) that open at -40 mV, and the outward K^+ currents through the slow and rapid delayed rectifying K^+ channels (I_{Ks} and I_{Kr}). The long plateau phase is distinctive for the ventricular AP and contributes to physiologically appropriate sustained muscle contraction. Phase 3 of the AP is characterized by rapid repolarization. LTCCs close, while the slow delayed rectifying K^+ channels remain open. As repolarization progresses, more rapid delayed rectifying K^+ channels open, and now also the inwardly rectifying K^+ channels open, producing I_{K1}. At -85 mV, the delayed rectifying K^+ channels close, but the I_{K1} continues passing K^+ ions out of the cell, contributing to the resting membrane potential during phase 4 of the AP.

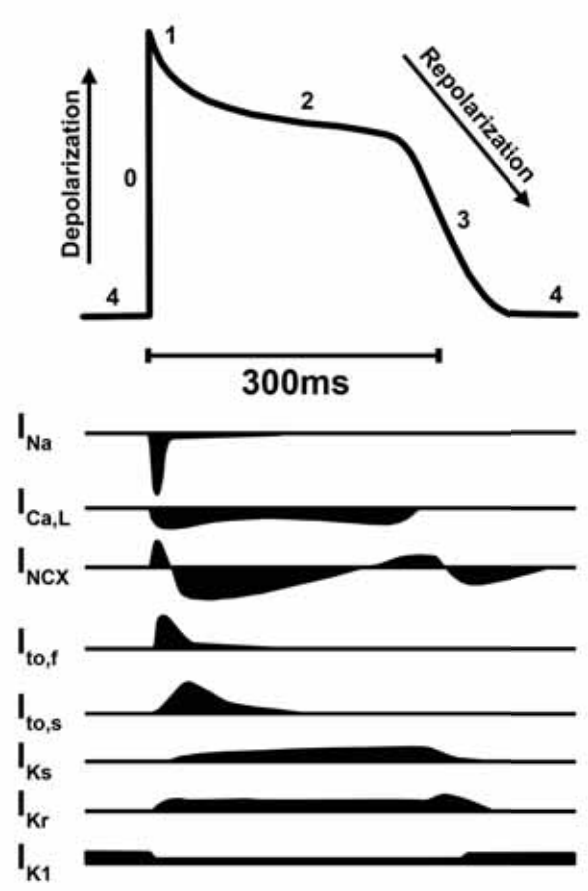

Figure 2. AP shape in an adult human ventricular cardiomyo-cyte, showing its four phases and essential underlying ionic currents. Downward currents indicate depolarizing currents and upward currents repolarizing ones. Modified from (Nerbonne et al. 2005).

The resting membrane potential is also maintained by the Na^+/K^+ pump, which in an energy consuming process actively removes three Na^+ ions from the cell in exchange for every two K+ ions entering the cell, also helping to maintain the concentrations of these ions. Additionally, the sodium-calcium exchanger current (I_{NCX}) contributes to the AP in potentially important ways, as is discussed below (Bers 2002).

FROM ELECTRICAL EXCITATION TO MECHANICAL CONTRACTION

1.3 Excitation-contraction coupling

The process of translating the electrical excitation in the form of depolarizing current of the AP into muscle contraction of the cardiac chambers is referred to as excitation-contraction coupling. To understand how it works, we must follow and understand the movements of the crucial messenger – calcium (Bers 2002).

1.4 Calcium cycling – meet the key players

Transverse tubules (T-tubules) are invaginations of the sarcolemma. They make up most of the sarcolemmal area and enable rapid communication between the sarcolemma and intracellular structures (ter Keurs 2012, Ferrantini et al. 2013). Most sarcolemmal ion channels are concentrated to the T-tubules. During the plateau of the AP, Ca^{2+} enters the cell via voltage-gated LTCCs as an inward Ca^{2+} current ($I_{Ca,L}$) as shown in figure 2. This entry of Ca^{2+} triggers a much larger release of Ca^{2+} from the sarcoplasmic reticulum (SR) in a process called calcium-induced calcium release (figure 3). The SR is an intracellular organelle specialized in storage and cycling of Ca^{2+}. The release of Ca^{2+} from the SR into the cytosol takes place via specialized calcium channels on the SR membrane, the cardiac ryanodine receptors (RyR2), which are organized into close physical contact with the LTCCs of the sarcolemma. The high concentration of free intracellular calcium $[Ca^{2+}]_i$ activates the contractile apparatus. Cardiac calsequestrin (CASQ2) functions as a Ca^{2+} buffer in the SR, and triadin anchors it to RyR2 (Guo et al. 1995, Zhang et al. 1997). Unphosphorylated FKBP12.6 (calstabin2) binds to RyR2, stabilizing its function (Marx et al. 2000). For muscle relaxation to take place, $[Ca^{2+}]_i$ must fall. This is achieved by pumping Ca^{2+} out of the cytosol. Most of it is pumped back into the SR by the SR Ca^{2+} ATPase (SERCA2a). SERCA2a is inhibited by unphosphorylated

phospholamban (PLB). Ca^{2+} also leaves the cytosol via the sodium-calcium exchanger channel (NCX), one Ca^{2+} ion in exchange for three Na^{+} ions entering from the extracellular space. Additionally, minor amounts of Ca^{2+} are removed by the sarcolemmal Ca^{2+} ATPase and the mitochondrial Ca^{2+} uniporter (Bers 2002). These fast cyclic increases and decreases in $[Ca^{2+}]_i$ are known as Ca^{2+} transients. The SR membrane also harbors additional Ca^{2+} channels. The inositol 1,4,5-trisphosphate receptors (IP3R) are important in cardiac development, signaling, and also play roles in pathophysiology (Kockskamper et al. 2008, Signore et al. 2013). Additionally, polycystin-2 (PC2) is known to form a Ca^{2+}-activated Ca^{2+} channel on the SR membrane (Koulen et al. 2002).

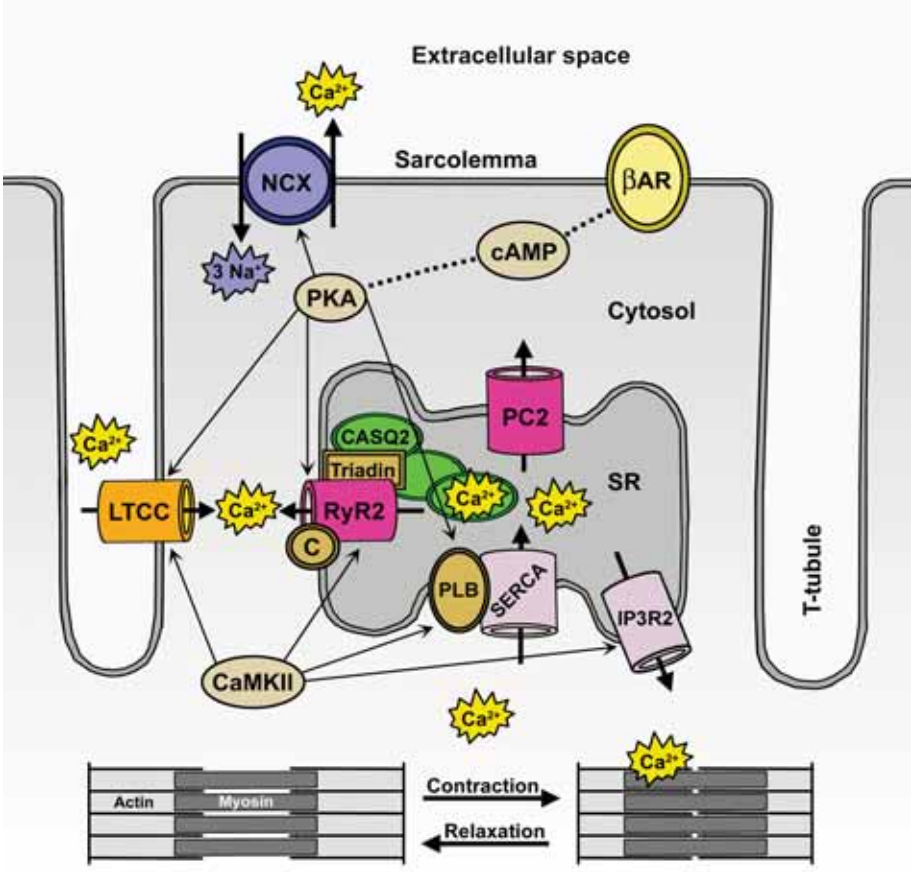

Figure 3. Calcium cycling in the cardiomyocyte. LTCC = L-type Ca^{2+} channel, CaMKII = Ca^{2+}/calmodulin-dependent protein kinase II, NCX = Sodium-calcium exchanger, C = Calstabin2 (FKBP12.6), PKA = Protein kinase A, RyR2 = Cardiac ryanodine receptor, CASQ2 = Cardiac calsequestrin, SERCA = Sarcoplasmic reticulum Ca^{2+} ATPase, PLB = Phospholamban, PC2 = Polycystin-2, cAMP = Cyclic adenosine monophosphate, SR = Sarcoplasmic reticulum, IP3R2 = Type 2 inositol 1,4,5-trisphosphate receptor, βAR = Beta-adrenergic receptor, T-tubule = Transverse tubule.

The function of these key proteins in Ca^{2+} cycling is modulated by Ca^{2+}/calmodulin-dependent protein kinase II (CaMKII), which phosphorylates RyR2, increasing Ca^{2+} transient magnitude and spontaneous Ca^{2+} release from the SR. CaMKII also phosphorylates PLB, relieving its inhibition of SERCA2a and thus increasing SR Ca^{2+} reuptake, and LTCC, increasing $I_{Ca,L}$ (Yuan et al. 1994, Maier et al. 2007). Furthermore, CaMKII modulates Na^{+} channels, K^{+} channels, and inositol 1,4,5-trisphosphate receptors (IP3R), which are also expressed on the nuclear envelope, where they colocalize with CaMKII and contribute to regulation of gene transcription (Bers et al. 2009). CaMKII is activated by a rise in $[Ca^{2+}]_i$, which can be due to reactive oxygen species, β-adrenergic receptor stimulation, angiotensin II, aldosterone, or hyperglycemia (Luo et al. 2013).

Another essential regulator on cardiac Ca^{2+} cycling is protein kinase A (PKA). Circulating catecholamines epinephrine, released by the adrenal glands, and norepinephrine, released by the sympathetic neurons, bind and activate β-adrenergic receptors on the sarcolemma. Activation of these G protein-coupled receptors increases adenylyl cyclase activity, resulting in conversion of ATP to cyclic adenosine monophosphate (cAMP), which in turn activates PKA (Krebs 1989, Sassone-Corsi 2012). PKA phosphorylates numerous target proteins, e.g. PLB, LTCC, RyR2, and likely NCX, increasing the frequency and amplitude of intracellular Ca^{2+} transients (Hain et al. 1995, Zhang et al. 2009b). This translates to increased heart rate and contractility, classic manifestations of the sympathetic fight or flight response. Importantly, PKA phosphorylatin of troponin I desensitizes troponin C to Ca^{2+}, enabling rapid relaxation and maintenance of Ca^{2+} cycling at rapid heart rates (Li et al. 2000)

1.5 Calcium in heart muscle contraction and relaxation

Elevated $[Ca^{2+}]_i$ during systole activates the myofilaments to contract. Ca^{2+} binds to troponin C, which goes on to move tropomyosin aside, exposing myosin cross-bridges, which bind to actin. Energy in the form of ATP is then converted to movement of the actin-myosin filaments relative to each other, resulting in sarcomere shortening. As Ca^{2+} is pumped out of the cytosol, it dissociates from troponin C, causing relaxation (Bers 2008). In addition to accelerating $[Ca^{2+}]_i$ decay, relaxation can be accelerated by PKA-mediated phosphorylation of troponin I that accelerates unbinding of Ca^{2+} from troponin C, as mentioned above (Li et al. 2000).

1.6 Interplay between calcium and membrane voltage

What makes the role of Ca^{2+} very interesting and important is its ability to modulate membrane potential (Laurita et al. 2008b). When NCX operates in forward mode, three Na^+ ions enter the cell for every removed Ca^{2+} ion. This creates a positive inward (depolarizing) current and tends to increase AP duration (APD). NCX can also operate in reverse mode, removing three Na^+ ions for every entered Ca^{2+} ion. This repolarizes the cell and tends to shorten APD. Therefore, increased $[Ca^{2+}]_i$ will typically increase APD. This relationship is known as positive calcium to voltage coupling. However, because NCX function depends on membrane potential and Na^+ in addition to Ca^{2+}, its effect on APD may be difficult to predict under changing conditions. For example, during VT the intracellular Na^+ concentration may rise and lead to reverse mode operation of NCX, which is more rapid than inactivation of LTCC. The resulting inflow on Ca^{2+} may cause Ca^{2+}-induced Ca^{2+} release, sustaining or perpetuating the arrhytmia.

LTCC opening is regulated by negative feedback, where $[Ca^{2+}]_i$ will inactivate LTCC, thus shortening APD. High $[Ca^{2+}]_i$ also increases I_{Ks}, also shortening APD. This contrary relationship is called negative calcium to voltage coupling. The effect of $[Ca^{2+}]_i$ on the membrane potential will therefore depend on the relative amount and activity of available NCX and LTCC, as well as the Na^+ concentration and membrane potential. Additionally, high $[Ca^{2+}]_i$ reduces I_{Na}, decreasing maximal upslope velocity of the AP (phase 0)(Casini et al. 2009). High $[Ca^{2+}]_i$ also decreases conduction velocity of APs between cells by closing gap junctions (Peracchia 2004).

WHEN CALCIUM GOES ROGUE – Failures of rhythm and pumping

The essential pump function of the heart may be compromised by disturbances in its rhythm or the ability to contract and relax in a way that maintains sufficient blood pressure for perfusion of target tissues. Impaired calcium handling is implicated in pathologies involving both rhythm and contraction/relaxation of the heart.

1.7 Mechanisms of ventricular arrhythmias – with a focus on calcium

Cardiac arrhythmias can be divided into passive (e.g. AV block) and active ones (Antzelevitch et al. 2008, Issa et al. 2012). I will focus on active ventricular arrhythmias, which can be mechanistically divided into abnormal impulse formation and abnormal impulse conduction. Disorders of impulse formation include abnormal automaticity and triggered activity, which encompasses early afterdepolarizations (EAD) and delayed afterdepolarizations (DAD). Disorders of impulse conduction refer to block and reentry, which can be anatomical or functional (figure 4) (Antzelevitch et al. 2008, Issa et al. 2012).

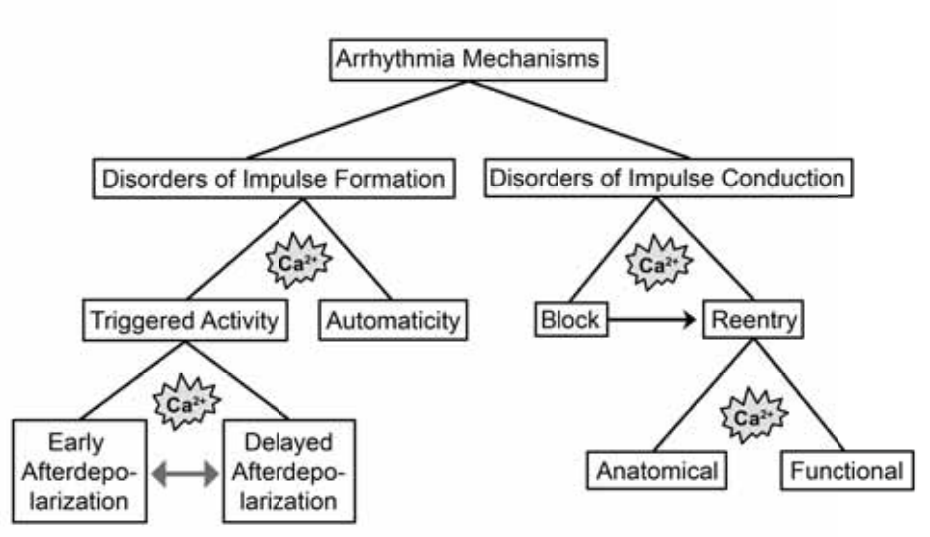

Figure 4. Mechanisms of cardiac arrhythmias, with an emphasis on active ventricular tachyarrhythmias. Ca^{2+} plays a key mechanistic role at multiple levels, as marked on the chart. The double-headed arrow signifies mechanistic similarities between EADs and DADs, with Ca^{2+} as the common denominator.

1.7.1 Automaticity

Cardiac cells possess an intrinsic capability to spontaneously generate APs, referred to as automaticity. Under normal conditions, sinoatrial node cells have the highest rate, and are therefore in charge of setting the rhythm, pacemaking. Cardiomyoctes elsewhere in the heart also have pacemaker capability, with decreasing intrinsic rate the further they are from the sinoatrial node. The pacemaking rate is controlled by the autonomic nervous system and by extracellular ion concentrations, namely K^+. Abnormal automaticity may arise un-

der conditions of higher resting membrane potential, such as ischemia. The pacemaking rate is proportional to the resting membrane potential. Hence abnormal automaticity results in high rates of pacemaking. Release of Ca^{2+} from the SR may be mechanistically important in abnormal automaticity, and lead to depolarizing currents through activation of NCX, similar to the mechanism of DADs. Abnormal automaticity is not likely responsible for the majority of ventricular tachyarrhythmias, but it can be an initiating factor to arrhythmias sustained by reentrant mechanisms. In practise, it is difficult to mechanistically distinguish abnormal automaticity from localized reentrant mechanisms, as well as from triggered activity (Antzelevitch et al. 2008).

1.7.2 Early afterdepolarizations

EADs are depolarizing oscillations in membrane potential that take place during repolarization, at phase 2 or 3 of the AP (figure 5). Prolongation of APD predisposes to EADs. For example, in patients with long QT syndrome, EAD-induced triggered activity is considered the factor that initiates torsades de pointes, a potentially lethal form of ventricular tachycardia (VT). Additionally, multiple other factors predispose to EAD, among them electrolyte abnormalities, hypoxia, catecholamines, and heart failure. At the cellular level, EADs are associated with reduced repolarizing K^+ currents, increased Ca^{2+} current, increased NCX activity, and increased late Na^+ current (Antzelevitch et al. 2008). It is well established that the upslope of the EAD is due to $I_{Ca,L}$, making LTCC recovery from inactivation followed by its activation a prerequisite for EAD-induced triggered activity (January et al. 1992).

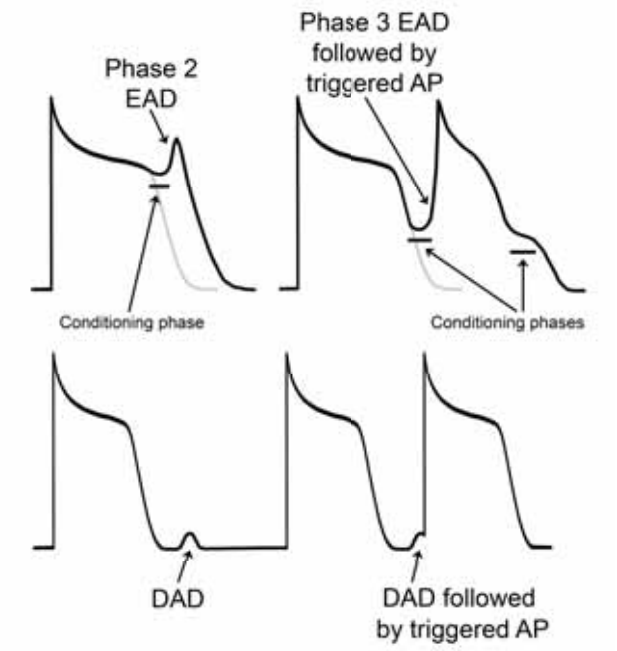

Figure 5. EADs occur before the end of repolarization. They are preceded by conditioning phases, transient delays in repolarization due to inward currents. DADs occur after the completion of repolarization. Both EADs and DADs will trigger an AP if they reach threshold voltage. This is called triggered activity.

Less clear are the mechanisms accounting for the so called "conditioning phase", which is a transient delay of repolarization deemed necessary for EAD formation. An emerging view centers on $[Ca^{2+}]_i$ as the key contributor to the conditioning phase of EADs and highlights the similarity to DADs (Volders et al. 2000). Intracellular Ca^{2+} overload or spontaneous SR Ca^{2+} release activates NCX, which is the source of the depolarizing current that leads to LTCC activation (Volders et al. 1997, Choi et al. 2002). Additionally, phase 3 EADs that occur below the threshold potential for LTCC activation (< ~ -35mV), appear NCX-mediated and are thus mechanistically similar to DADs (Patterson et al. 1990, Xu et al. 1996, Spencer et al. 2003). Recently, late phase 3 EADs have been described associated with shortened APD following the end of rapid activation (e.g. termination of atrial fibrillation). These late phase 3 EADs are distinguished by the associated normal SR Ca^{2+} release, as opposed to spontaneous release in other forms of afterdepolarizations (Burashnikov et al. 2006).

1.7.3 Delayed afterdepolarizations

DADs are depolarizing oscillations in membrane potential that follow an AP and occur after completion of repolarization, in phase 4 (figure 5). If depolarization reaches a threshold, it will induce an AP. This is called triggered activity. DADs occur under conditions of high $[Ca^{2+}]_i$, such as during high plasma concentrations of digitalis or catecholamines. As discussed above, catecholamines raise $[Ca^{2+}]_i$ by PKA-mediated phosphorylation of target proteins. NCX pumps one Ca^{2+} ion out of the cell in exchange for three Na^+ ions, resulting in a positive inward (depolarizing) current, manifested as a DAD. As RyR2 is the channel responsible for the large release of Ca^{2+} from the SR, regulation of RyR2 function is crucial to development of DADs. DADs and DAD-induced triggered activity are thus mechanistically implicated in multiple forms of VT. DAD-induced triggered activity is observed under conditions of normal RyR2 function (digitalis toxicity), as well as under conditions of abnormal RyR2 function, such as in patients with heart failure or mutations in RyR2, as will be discussed below (Laurita et al. 2008b).

1.7.4 Block and reentry

Conduction block, or wavebreak, is a prerequisite for reentry (Antzelevitch et al. 2008). Block can be caused by anatomical or functional heterogeneities, as is the case with reentry itself. In reentry, the electrical impulse persists in the cardiac tissue beyond the tissue's refractory period, thus reexciting the same tissue. A classical example of anatomical reentry is the formation of a reentrant loop between the atria and ventricles using the AV node and an accessory

conduction pathway between the atria and ventricles, as happens in Wolff-Parkinson-White syndrome (Al-Khatib et al. 1999). Other examples of anatomical factors include scar tissue following a myocardial infarct, or fibrosis in a hypertrophied heart. Such fibrosis may arise due to apoptosis and necrosis of cardiomyocytes in response to elevation of $[Ca^{2+}]_i$, demonstrating how dysregulated Ca^{2+} contributes even to an anatomical substrate for arrhythmias (Demaurex et al. 2003, Chen et al. 2005, Nakayama et al. 2007, Dorn 2009). Functional block typically occurs when the propagating impulse encounters a refractory region that has not yet recovered from previous excitation. This is underlied by spatial heterogeinities of the refractory period. A newer concept is the restitution hypothesis, which predicts block to occur when the slope of the APD restitution curve is greater than one. This is determined by plotting the APD against the preceding diastolic interval (Taggart et al. 2008). More recently, also restitution of conduction velocity has been shown to influence conduction block (Weiss et al. 2005). However, the most recent evidence points toward an essential role for Ca^{2+} cycling heterogeneities as the underlying cause behind dyssynchrony and alterations in membrane potential leading to conduction block and reentry (Chudin et al. 1999, Omichi et al. 2004). This type of alternating pattern of the AP has been associated with wavebreak and ventricular fibrillation (VF) (Pastore et al. 1999). Alternans is discussed in more detail below.

In addition to conduction block, prerequisites for reentry include a vulnerable substrate with heterogeinities in conduction and refractoriness, and a trigger in the form of an EAD, DAD, abnormal automaticity, or reflective or type 2 reentrant excitation (Antzelevitch et al. 2008). A vulnerable substrate may comprise anatomic or functional heterogeneities, highlighted by reduced conduction velocity and shortened APD. In the case of a trigger at a vulnerable time and place, this shortened wavelength (= conduction velocity x refractory period) allows the excitation to reenter a part of tissue that has regained excitability, leading to circuitous propagation of the impulse. Models for functional reentry include the leading circle, figure of eight, and spiral wave (rotor). Spiral wave formation is considered important in the degeneration of monomorphic VT to polymorphic VT and VF (Davidenko 1993, Samie et al. 2001). Aberrant Ca^{2+} cycling is implicated in this process. Elevated $[Ca^{2+}]_i$ and spatial heterogeinities in $[Ca^{2+}]_i$ translate via the NCX to heterogeinities of APD. In regions of prolonged APD, encountering the incoming spiral wave results in decreased conduction velocity, block, and wavebreak (Chudin et al. 1999).

1.7.5 Alternans

Calcium alternans is defined as the beat-to-beat alternation of intracellular calcium transient magnitude (large-small-large-small etc.) and corresponds to APD alternans (short-long-short-long etc). For long, it was thought that Ca^{2+} alternans was secondary to APD alternans (Koller et al. 1998, Watanabe et al. 2001). However, recently Ca^{2+} has emerged as the key player behind arrhythmogenic cardiac alternans (Pruvot et al. 2004, Laurita et al. 2008b, Narayan et al. 2008, Bayer et al. 2010, Gaeta et al. 2012). Alternans can occur at a subcellular, cellular, and tissue level. When tissue level alternans is in phase, meaning that adjacent regions of the heart show similar APD at a given time, it is referred to as concordant alternans. When alternans falls out of phase between adjacent regions, long APD in one region and short APD in another, it is called discordant alternans (figure 6).

It is this discordant alternans that is thought to be arrhythmogenic by increasing spatial heterogeneities of APD and thus predisposing to conduction block and reentry (figure 7) (Wilson et al. 2007).

Several factors may influence the development of Ca^{2+} alternans, which develops when one or more key components of the Ca^{2+} cycling machinery fails to maintain a sufficient rate of Ca^{2+} cycling. Alternans may be due to impaired SR Ca^{2+} release. There are controversial findings about whether or not this is associated with alternans of SR Ca^{2+} content (Shiferaw et al. 2003, Diaz et al. 2004, Picht et al. 2006).

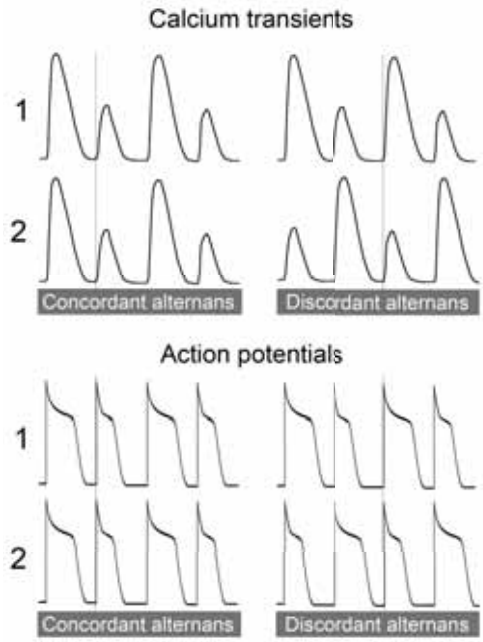

Figure 6. Drawing of simultaneous intracellular Ca^{2+} transients and APs demonstrating concordant and discordant cardiac alternans. Numbers 1 and 2 refer to adjacent regions of cardiac tissue. In concordant alternans, the adjacent regions oscillate in phase, whereas in discordant alternans the adjacent regions are out of phase. This type of spatially discordant alternans predisposes to block and reentry.

Some findings implicate slow recovery from inactivation of RyR2, such that full recovery is reached only after every other beat, resulting in an alternating magnitude of Ca^{2+} release (Picht et al. 2006, Restrepo et al. 2008). Overall, most evidence associates Ca^{2+} alternans with decreased RyR2 open probability and increased refractoriness of the channels (Diaz et al. 2002, Xie et al. 2008a, Nivala et al. 2012). However, others have found increased RyR2 open probability to produce Ca^{2+} alternans (Lehnart et al. 2006). Findings in heart failure implicate impaired SR Ca^{2+} reuptake by SERCA2a in development of Ca^{2+} alternans (Pieske et al. 1995).

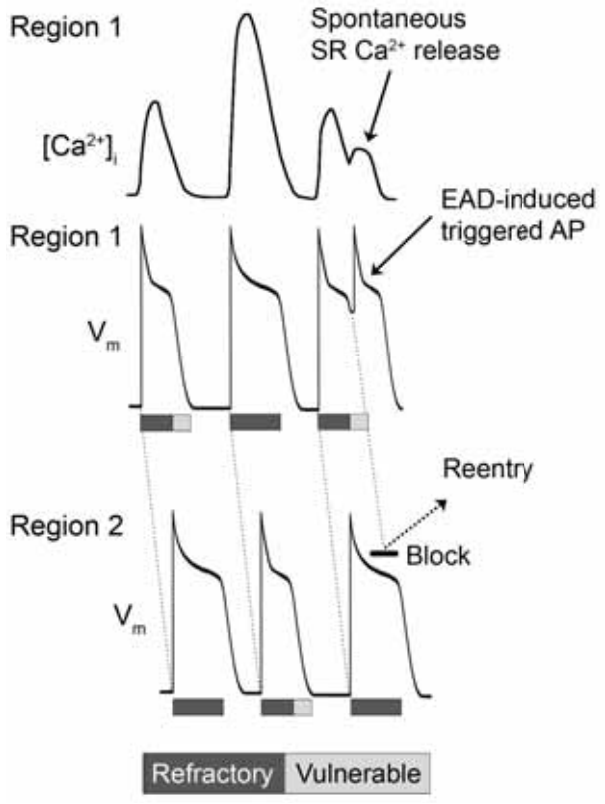

Figure 7. Spontaneous SR Ca^{2+} release in region 1 of the ventricle results in an EAD that induces an AP, which is the trigger initiating reentry. A vulnerable substrate is created by spatially discordant APD alternans between adjacent ventricular regions 1 and 2. The trigger in region 1 occurs at a vulnerable time when region 2 is still refractory. This leads to conduction block and initates a reentrant arrhythmia. V_m = membrane potential.

1.8 Calcium in heart failure

Globally, heart disease is the number one cause of mortality and years of life lost (Lozano et al. 2012). Heart failure occurs when the heart fails to sufficiently perform its function of pumping blood around the circulatory system to meet the needs of the body. It is often caused by ischemic heart disease, high blood pressure, valvular disease, or cardiomyopathy (McMurray et al. 2005). Almost half of heart failure patients suffer SCD mainly due to ventricular tachyarrhythmias, putting SCD on par with failure of pump function as a cause of mortality in heart failure (Cohn et al. 1991, Tomaselli et al. 1994). In the

past decades, the essential role of impaired calcium handling has been recognized as a key factor behind both weakened cardiac pump function and arrhythmias in the failing heart (Gwathmey et al. 1987, Beuckelmann et al. 1992, Hasenfuss et al. 2002).

1.8.1 Arrhythmias and contractile dysfunction

In the acutely failing heart sympathetic activation is an adaptive response meant to maintain sufficient perfusion of target tissues. However, prolonged sympathetic activation turns maladaptive and contributes to progression of heart failure. High plasma norepinephrine levels are a strong marker of poor prognosis (Cohn et al. 1984). As discussed above, sympathetic activation leads to high $[Ca^{2+}]_i$, promoting arrhythmias in multiple ways (figure 8). In heart failure, the expression and activity of multiple Ca^{2+} cycling proteins is altered (Hasenfuss et al. 2002, Del Monte et al. 2008). The levels of LTCC are essentially unchanged, but their coupling with RyR2 in the junctional SR may be defective. This may be due to loss of organized T-tubule structure resulting in dyssycronous Ca^{2+} release and impaired contractility (Song et al. 2006, Wagner et al. 2012). Many studies have found decreased RyR2 expression levels in failing hearts, but also contradictory findings exist.

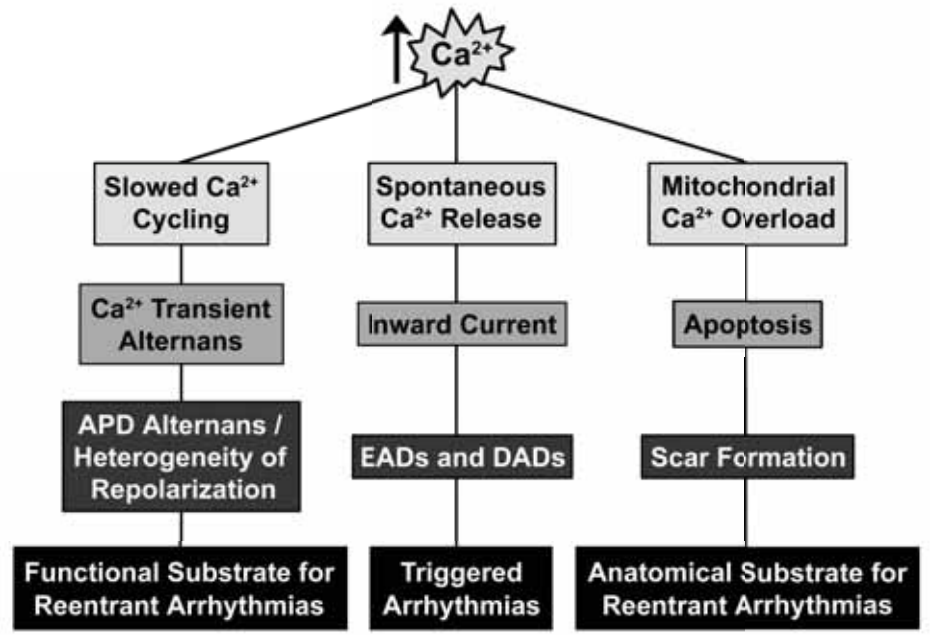

Figure 8. Mechanisms by which high $[Ca^{2+}]_i$ promotes arrhythmias in heart failure. Modified from (Aistrup et al. 2011).

Also the findings on altered RyR2 activity remain controversial. RyR2 is chronically hyperphosphorylated in the failing heart. Under normal conditions, the accessory protein calstabin2 is bound to RyR2, stabilizing the channel. This interaction is modulated by PKA-mediated phosphorylation of RyR2, leading to dissociation of calstabin2 (Marx et al. 2000). The effects of this include an increase in RyR2 Ca^{2+} sensitivity and channel activity, as well as RyR2 uncoupling and dyssynchronized channel function. The resulting diastolic spontaneous Ca^{2+} release may induce triggered arrhythmias and impair contractility/relaxation. However, the role of RyR2 phosphorylation and calstabin2 dissociation remain controversial, and some evidence points to an exacerbating effect of constitutive dephosphrorylation, not phosphorylation, of RyR2 on SR Ca^{2+} leak (Bers et al. 2003, Liu et al. 2014). Decreased expression of SERCA2a is a consistent finding in heart failure and correlates with myocardial function (Hasenfuss et al. 1994, Hasenfuss et al. 2002). Furthermore, inhibition of SERCA2a function by PLB is stronger in failing hearts (Frank et al. 2000). NCX expression levels are increased in heart failure, possibly to compensate for decreased SERCA2a activity, and correlate with diastolic cardiac function (Hasenfuss et al. 1999). The downside of improved diastolic function is an increase in the incidence of I_{NCX}-mediated triggered arrhythmias (Schillinger et al. 2002). Additionally, as the NCX-LTCC balance shifts towards Ca^{2+} extrusion, the SR Ca^{2+} load tends to decrease, resulting in smaller Ca^{2+} transients and decreased force of contraction, a hallmark of the failing heart. As with dyssynchronous Ca^{2+} release and impaired contraction, Ca^{2+} reuptake dyssynchrony may contribute to impaired relaxation in failing hearts (Hohendanner et al. 2013).

Mitochondrial Ca^{2+} is an important regulator of cell metabolism and survival. Mitochondrial Ca^{2+} overload in heart failure leads to increased production of reactive oxygen species, decreased production of energy, and cardiomyocyte apoptosis (Luo et al. 2013). CaMKII regulates this process, as well as many proteins involved in Ca^{2+} cycling, as discussed above. Under the high $[Ca^{2+}]_i$ seen in heart failure, CaMKII may become constitutively activated and promote further progression of heart failure and arrhythmias. Inhibition of CaMKII improves cardiac function in failing hearts (Sossalla et al. 2010). PKA-mediated changes in activity of Ca^{2+} cycling proteins are mainly due to chronically elevated levels of plasma catecholamines in heart failure. However, recent finding suggest that CaMKII-mediated regulation of SR Ca^{2+} release via phosphorylation of RyR2 may be more important than PKA-mediated phosphorylation, especially in the transition from cardiac hypertrophy to failure

(Fischer et al. 2013). CaMKII activation promotes arrhythmias; phosphorylation of LTCCs and Na^+ channels promotes formation of EADs and also predisposes to DADs. Phosphorylation of RyR2s increases SR Ca^{2+} release, promoting DADs. Increased apoptosis and collagen deposition increase structural heterogeneity and predispose to reentrant arrhythmias (Luo et al. 2013).

Many structural proteins of the cytoskeleton and myofilaments, for example ankyrin, titin, and dystrophin, are implicated in impaired Ca^{2+} cycling and contribute to weakened cardiac function and arrhythmias in heart failure (Luo et al. 2013). Overall, it is worth remembering that the development of heart failure is a complex process, which involves changes in expression and function of hundreds if not thousands of different genes.

1.9 Catecholaminergic polymorphic ventricular tachycardia

1.9.1 Characteristics

CPVT is an autosomally inherited syndrome characterized by VT related to mental or physical stress (Laitinen et al. 2001, Priori et al. 2001). Under conditions of sympathetic stimulation these patients present with premature ventricular contractions (PVC), bidirectional VT, polymorphic VT, and SCD in the absence of structural heart disease (Swan et al. 1999) (figure 9). The resting ECG in these patients is normal. Although a history of syncopal events is common, SCD may be the first manifestation. If untreated, the mortality rate may be as high as 50% by 20 years of age (Leenhardt et al. 1995). Early onset of symptoms is associated with severity of the disease. The estimated prevalence of CPVT in the general population is 1 in 10 000. CPVT may account for some cases of unexplained sudden death in children and adolescents (Tester et al. 2007, van der Werf et al. 2010).

1.9.2 Genetic background

The genetic aspect of CPVT was observed already more than half a century ago in a report on sisters with polymorphic ventricular arrhythmias in the absence of structural heart disease (Berg 1960). This was followed by case reports with increasing patient numbers (Reid et al. 1975, Coumel 1978, Leenhardt et al. 1995). Over a decade ago the CPVT phenotype was associated with a disease locus on chromosome 1q42-43 in two Finnish families with an autosomal dominant mode of inheritance (Swan et al. 1999). Soon after, the disease-causing gene was identified as the cardiac ryanodine receptor gene

(*RyR2*)(Laitinen et al. 2001, Priori et al. 2001). Today, well over a hundred different *RyR2* mutations have been linked to CPVT (Medeiros-Domingo et al. 2009). *RyR2* is a large gene of 105 exons. The disease-causing mutations are mostly missense, i.e. amino acid changing mutations and cluster in three well conserved regions: the N-terminal, the central region with the calstabin2 binding domain, and the C-terminal channel forming domain. Approximately 60-70% of patients with a clinical diagnosis of CPVT harbor identifiable mutations in *RyR2* (Cerrone 2004, Medeiros-Domingo et al. 2009).

Around the same time as *RyR2* mutations were linked to CPVT, a recessive form of CPVT in Bedouin families was mapped to chromosome 1p13-21, and soon after, disease-causing homozygous missense mutations were identified in *CASQ2* (Lahat et al. 2001a, Lahat et al. 2001b). The *CASQ2* gene contains 11 exons. To date, over twenty recessively inherited *CASQ2* mutations linked to CPVT have been identified (Leenhardt et al. 2012). Half of these are missense

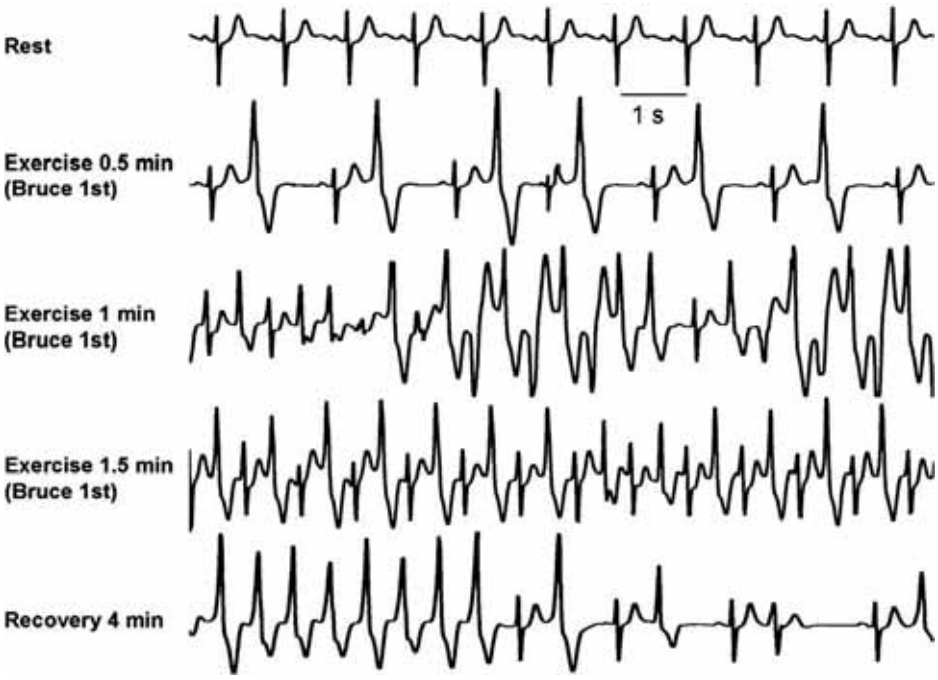

Figure 9. ECG during exercise stress test in a CPVT patient. During exercise worsening ventricular arrhythmias are observed. Bidirectional VT develops after 1 minute of exercise with a sinus heart rate of approximately 120 beats per minute. Arrhythmias rapidly recede during recovery. Adapted with permission from (Liu et al. 2008).

mutations, and the other half are nonsense mutations, leading to truncated proteins. *CASQ2* mutations are found is 3-5% of CPVT patients (Ackerman et al. 2011).

A novel recessive form of CPVT discovered in an Arabic family was mapped to chromosome 7p14-22, but the causative gene remains unknown (Bhuiyan et al. 2007). Recently, yet another autosomal recessive form of CPVT was associated with mutations in triadin in two families (Roux-Buisson et al. 2012). The mutations resulted in the absence of the triadin protein, and also associated with skeletal muscle weakness in one of the patients.

1.9.3 Mechanisms

All known CPVT-causing mutations involve proteins associated with intracellular Ca^{2+} release. The common pathomechanism is thought to be spontaneous leak of Ca^{2+} from the SR under conditions of adrenergic stimulation, resulting in mainly NCX-mediated diastolic inward current, DADs, and triggered arrhythmias. However, several hypotheses exist on the mechanism of the spontaneous Ca^{2+} release (Wehrens 2007, Cerrone et al. 2009). The majority of mechanistic studies have been performed on transgenic mice. Although these transgenic models of RyR2 and CASQ2 have demonstrated arrhythmogenicity, the observed phenotype has not always resembled the human phenotype (Cerrone et al. 2005, Kannankeril et al. 2006, Knollmann et al. 2006, Song et al. 2007, Lehnart et al. 2008).

The magnitude of SR Ca^{2+} release depends steeply on the SR Ca^{2+} content (Bassani et al. 1995). An increase in SR Ca^{2+} content also increases RyR2 open probability, and thus spontaneous Ca^{2+} release, which is a normal phenomenon under conditions of SR Ca^{2+} overload. (Eisner et al. 2013). The so called store overload-induced Ca^{2+} release hypothesis states that CPVT mutations lower this threshold for spontaneous Ca^{2+} release (Jiang et al. 2002b, Jiang et al. 2004, Jiang et al. 2005). Recently, a luminal Ca^{2+}-sensing gate of RyR2 that controls store overload-induced Ca^{2+} release was identified (Chen et al. 2014).

Interactions between different domains of the RyR2 channel are essential for its function. One hypothesis implicates defective interdomain interactions in spontaneous Ca^{2+} release in CPVT. Impaired interaction between the N-terminal and central regions destabilizes the closed state of the channel, resulting in spontaneous Ca^{2+} release (Ikemoto et al. 2002). In CPVT, defective

interdomain interaction leads to spontaneous Ca^{2+} release in a mutation-dependent manner (George et al. 2006, Suetomi et al. 2011).

A third hypothesis accounts spontaneous Ca^{2+} release to increased sensitization of RyR2 to cytosolic Ca^{2+} due to dissociation of the RyR2 stabilizing protein calstabin2 (Marx et al. 2000). According to this hypothesis, RyR2 mutant channels have a weakened interaction with calstabin2, and adrenergic stimulation via PKA-mediated phosphorylation of RyR2 further impairs this interaction, causing dissociation of calstabin2, which leads to increased RyR2 open probability and spontaneous Ca^{2+} release. The benzothiazepine derivatives K201 (JTV519) and its follower S107 restore the impaired RyR2-calstabin2 interaction and rescue the arrhythmogenic CPVT phenotype in mice (Wehrens et al. 2004, Lehnart et al. 2008). However, this hypothesis remains controversial, because other groups have been unable to repeat results regarding the RyR2-calstabin2 interaction (George et al. 2003, Jiang et al. 2005) and the antiarrhythmic effects of K201 (Liu et al. 2006), as well as the dependency of antiarrhythmic effects of K201 on the RyR2-calstabin2 interaction (Hunt et al. 2007). The antiarrhythmic effects of these experimental drugs may be mutation dependent, or have targets other than stabilization of the RyR2-calstabin2 interaction. To make the mechanistic soup of SR Ca^{2+} leak even more complex, new findings indicate that SR Ca^{2+} leak is exacerbated by RyR2 dephosphorylation, a finding opposing previous studies that implicate increased RyR2 phosphorylation in SR Ca^{2+} leak (Liu et al. 2014).

CASQ2 is a high capacity low affinity Ca^{2+} buffer in the SR, and additionally modulates RyR2 open probability via its interaction with triadin and junctin (Györke et al. 2004, Györke et al. 2008). Mutations in *CASQ2* are likely to cause CPVT by various mechanisms (Faggioni et al. 2012). The loss of functional CASQ2 may release the inhibitory effect on RyR2 and lead to spontaneous Ca^{2+} release independent of the free SR Ca^{2+} concentration. Secondly, the absence of CASQ2 SR Ca^{2+} buffering will increase free SR Ca^{2+} concentration and thus spontaneous Ca^{2+} release (Kornyeyev et al. 2012). Additionally, the absence of CASQ2 leads to structural SR remodelling and downregulation of triadin and junction, leading to spontaneous Ca^{2+} release (Knollmann et al. 2006). Absence of triadin was recently linked to CPVT, highlighting its importance in maintaining normal SR Ca^{2+} release (Roux-Buisson et al. 2012).

1.9.4 Management and challenges

A CPVT diagnosis is followed by comprehensive genetic testing (*RyR2* and *CASQ2*), screening of family members, and counseling (Ackerman et al. 2011, van der Werf et al. 2013). Patients are advised on exercise restriction, and the importance of drug compliance is emphasized. β-blocker treatment is started, typically with a long-acting compound that lacks sympathomimetic activity, such as nadolol (Hayashi et al. 2009). Also propranolol is widely used. For prevention of arrhythmias, it is important to titrate the β-blocker to the highest tolerable dose. Even on β-blocker therapy event rates remain significant with estimated 8-year rates for arrhythmic events at 37.2%, near fatal events at 15.3%, and fatal events at 6.4% (van der Werf et al. 2012). Carvedilol may be a good alternative in the future, based on its recently discovered ability to directly decrease RyR2 open probability (Zhou et al. 2011).

Importantly, if arrhythmic events occur on β-blocker therapy, treatment must be boosted. Supplementing β-blocker therapy with flecainide is recommended as the next step (van der Werf et al. 2013). Flecainide was found to directly inhibit RyR2, and its ability to suppress arrhythmic events in small clinical studies is encouraging (Watanabe et al. 2009, van der Werf et al. 2011). Although the LTCC-blocker verapamil together with a β-blocker was effective in reducing ventricular arrhythmias during exercise stress testing (Swan et al. 2005, Rosso et al. 2007), in a long term follow-up the combination failed to prevent significant ventricular arrhythmias (Rosso et al. 2010). Drugs of possible therapeutic value in the future include propafenone (Hwang et al. 2011), K201 (JTV519) (Lehnart et al. 2004a), and the CaMKII inhibitor KN-93 (Liu et al. 2011).

If patients are not arrhythmia-free despite optimized drug therapy, left cardiac sympathetic denervation may be performed. In this procedure, the lower half of the left stellate ganglion and the thoracic ganglia Th2-4 are removed to prevent norepinephrine release in the heart (Odero et al. 2010). The role of this technique in the management of drug-resistant CPVT remains unclear. Long-term follow-up data are lacking, while short-term results in small sets of patients seem promising (Wilde et al. 2008, Collura et al. 2009, Schneider et al. 2013). The technique is mastered only by a limited number of surgeons worldwide, restricting its availability (Leenhardt et al. 2012). Some authors consider it the next line of treatment after optimizing drug therapy (van der Werf et al. 2013), while others see it as an experimental approach following implantable

cardioverter defibrillator (ICD) treatment to reduce ICD shocks in patients with persistent arrhythmic storms (Liu et al. 2008).

Also the role of ICD therapy is unclear. The official recommendation is to implant an ICD for CPVT patients with a history of sustained VT or VF, and to consider it for asymptomatic patients with a heavy familial burden of early mortality. Additionally, hemodynamically untolerated VT or syncope on β-blocker therapy is an indication for ICD implantation (Epstein et al. 2013). However, the proarrhythmic effect of ICD shocks has recently raised concern (Mohamed et al. 2006, Palanca et al. 2006, Pizzale et al. 2008), and prompted some to recommend ICD implantation only as a last resort after other available treatments have proven inadequate (Garratt et al. 2010, van der Werf et al. 2013). Optimal ICD programming in these patients remains extremely difficult (Roses-Noguer et al. 2013).

Factors that complicate the diagnosis and management of CPVT patients and their family members include highly variable disease penetrance, hence the lack of established genotype-phenotype correlations, and the high proportion of *de novo* mutations (Leenhardt et al. 2012). In the future improving risk stratification for CPVT patients and their relatives is of utmost importance.

1.10 Autosomal dominant polycystic kidney disease – with a focus on cardiac manifestations

1.10.1 Characteristics

ADPKD is a genetic disease characterized by the development of multiple bilateral renal cysts and numerous extrarenal manifestations (Gabow 1993, Torres et al. 2007) (figure 10).

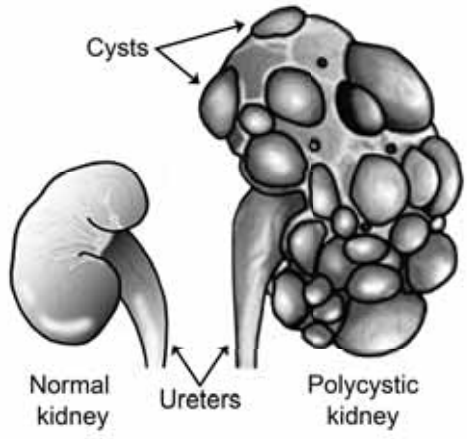

Figure 10. Comparison of normal kidney anatomy with that of a polycystic kidney, which is enlarged and contains multiple cysts in varying stages of development. Modified from www.kidney.niddk.nih.gov.

The cysts grow in number and size, and affect renal function usually between the 4th and 6th decades of life. At this point the kidneys are usually very cystic and enlarged, Annually the total kidney volume increases by approximately 5% and glomerular filtration rate decreases by approximately 5mL/min (Klahr et al. 1995, Grantham et al. 2006). Kidney and cyst volumes are the strongest known predictors of renal failure. In progressed disease, a cyst-filled kidney can weigh 10-15kg, 100-fold the weight of a normal healthy kidney. The progression to end-stage renal disease, defined as renal failure needing replacement therapy (GFR < 15mL/min/1.73m^2), occurs on average during the 6th to 8th decades of life (Hateboer et al. 1999). The disease tends to progress faster in men.

ADPKD patients often develop cysts and other manifestations in multiple organs, reflecting the systemic nature of the disease (Torres et al. 2007). Cysts may form in the liver, pancreas, seminal vesicles, and arachnoid membrane. Other extrarenal manifestations include intracranial arterial elongation and aneurysms, aortic root dilatation and aneurysms, diverticulosis, and hernias of the abdominal wall (Pirson 2010). Most of the adult patients experience renal pain, mainly due to infections, stones, hemorrage, and cysts (Bajwa et al. 2004). With the availability of modern renal replacement therapies, cardiovascular diseases have become a major cause of morbidity and the most common cause of mortality in ADPKD patients (Fick et al. 1995, Perrone et al. 2001, Ecder 2013). Interestingly, patients usually become hypertensive before impairment of renal function. Half of the patients develop high blood pressure (>140/90 mmHg) before 35 years of age (Kelleher et al. 2004). Also other cardiovascular abnormalities manifest early in the course of the disease. Young patients with normal blood pressure and renal function show endothelial dysfunction, impaired coronary flow reserve, increased carotid intima-media thickness, arterial stiffness, and biventricular diastolic dysfunction (Bardaji et al. 1998, Oflaz et al. 2005, Ecder 2013). Furthermore, hypertension and left ventricular hypertrophy commonly contribute to cardiovascular complications in these patients (Chapman et al. 1997). Additionally, mitral-valve prolapse is seen in one out of four patients (Hossack et al. 1988, Lumiaho et al. 2001).

ADPKD is seen world-wide with a prevalence varying between 1 in 400 to 1 in 4000, making it the most common inherited kidney disease (Torres et al. 2007). Recent figures from south-west Germany put the overall prevalence of ADPKD at approximately 1 in 3000 (Neumann et al. 2013). Disease severity varies significantly between and within families, reflecting the important role

of modifying factors, which may be either genetic and/or environmental (Geberth et al. 1995, Persu et al. 2004).

1.10.2 Genetic background

The autosomal dominant pattern of inheritance of the disease was recognized more than half a century ago (Dalgaard 1957). In the 1980s the disease was linked to chromosome 16, but soon after it was realized that not all families show this linkage, suggesting that also other loci are implicated (Reeders et al. 1985, Kimberling et al. 1988, Romeo et al. 1988). In the 1990s two disease-causing genes were identified. Mutations in *PKD1*, which encodes the protein polycystin-1 (PC1), previously also known as transient receptor potential polycystic 1 (TRPP1), account for approximately 85% of cases (Hughes et al. 1995). Mutations in *PKD2*, which encodes the protein PC2, also known as transient receptor potential polycystic 2 (TRPP2), account for most of the rest, approximately 10-15% of the cases (Mochizuki et al. 1996). Likely disease-causing mutations can be identified in approximately 90% of patients (Rossetti et al. 2007). The proportion of *de novo* mutations is approximately 10%. A small amount of cases may be caused by a yet unknown locus. However, a recent re-analysis of PKD families failed to find evidence of a third ADPKD locus (Paul et al. 2013).

PKD1 is located at the chromosomal locus 16p13.3 and consists of 46 exons (Consortium 1995, Hughes et al. 1995). Its protein product PC1 forms a membrane protein with 11 transmembrane domains. The Mayo ADPKD Mutation Database (http://pkdb.mayo.edu) contains nearly 2000 *PKD1* gene variants (January 2014) (Gout et al. 2007). Roughly half appear to be pathogenic, and most of these are nonsense or frameshift mutations, leading to truncated proteins. *PKD2* is located at the chromosomal locus 4q21 and consists of 15 exons (Mochizuki et al. 1996, Hayashi et al. 1997). Its product PC2 is a membrane protein with six transmembrane domains. The Mayo ADPKD Mutation Database contains close to 300 *PKD2* gene variants (January 2014). Nearly three quarters of them are suspected to be pathogenic, most of these as well being nonsense or frameshift mutations. Mutations in both genes are spread throughout the gene with no clear clustering to certain regions, meaning they are very heterogeneous and usually private, i.e. confined to a single family (Tan et al. 2011). *PKD1* mutations lead to a more severe disease than *PKD2* mutations. The average onset of end-stage renal disease occurs during the 6th decade of like in PKD1 and 8th decade of life in PKD2 (Hateboer et al. 1999). This is due to earlier disease onset in PKD1, not to faster rate of disease pro-

gression (Harris et al. 2006). The mutation type (missense versus truncating) does not seem to be associated with the phenotype. However, mutations located in the 5' (N-terminal) end of *PKD1* are more commonly associated with vascular manifestations and more severe kidney disease (Rossetti et al. 2002, Rossetti et al. 2003).

1.10.3 Mechanisms

The role of polycystins in the heart remains poorly understood. PC1 has a long extracellular N-terminus, 11 transmembrane regions, and a short C-terminus that interacts with the C-terminus of PC2 (Hughes et al. 1995, Casuscelli et al. 2009). It is expressed in numerous tissues, including the heart (Geng et al. 1997, Ong et al. 1999). PC1 is mainly located on the plasma membrane, but may also be found in primary cilia, cytoplasmic vesicles, endoplasmic reticulum, and nuclei. It interacts with numerous intra- and extracellular proteins (Torres et al. 2009). PC1 is normally located in adherens junctions, where it is thought to regulate the strength of adhesion between adjacent cells by controlling formation of stable adherens junctions in a process induced by a rise in $[Ca^{2+}]_i$ (Boca et al. 2007, Markoff et al. 2007). However, overall PC1 function remains incompletely understood.

PC2 is less than a fourth the size of PC1. It has short C- and N-termini and six transmembrane regions. Also PC2 is ubiquitously expressed, including myocardial and endocardial cells (Ong et al. 1999). It forms a non-selective Ca^{2+}-regulated cation-channel that is mainly located on the endoplasmic reticulum/SR membrane and the primary cilia, where it colocalizes with PC1 (Vassilev et al. 2001, Koulen et al. 2002, Geng et al. 2006). In rat, PC2, but not PC1, was found on the sarcolemma of ventricular myocytes, suggesting it can function independently of PC1 (Volk et al. 2003). PC2 functions as an intracellular Ca^{2+} channel that regulates $[Ca^{2+}]_i$, as well as a receptor-operated channel on the plasma membrane and a mechanosensitive channel on the ciliary membrane (Qian et al. 2003, Anyatonwu et al. 2004, Tsiokas et al. 2007). PC2 is known to interact with numerous proteins involved in intracellular Ca^{2+} handling (Torres et al. 2009). Interestingly, the C-terminus of PC2 is shown to inhibit RyR2 in its open state, thus inhibiting RyR2 channel activity. In PC2-deficient cardiomyocytes, the loss of inhibition of RyR2 by PC2 led to small frequent spontaneous Ca^{2+} transients and reduced SR Ca^{2+} stores (Anyatonwu et al. 2007). PC2 modulates also IP3R channel activity, and IP3R can activate PC2 channel function (Sammels et al. 2010, Mekahli et al. 2012). Syntaxin 5 inactivates PC2, preventing endoplasmic reticulum Ca^{2+} leak (Geng et al.

2008). Of interest is the interaction of PC2 with the cytoskeleton and its components troponin I (Li et al. 2003b), tropomyosin-1 (Li et al. 2003a), hax-1 (Gallagher et al. 2000), and filamin (Wang et al. 2012), some of which are implicated in heart failure. In the progression of polycystic kidney disease, evidence for the important roles of $[Ca^{2+}]_i$ and cAMP signaling is mounting (Torres et al. 2009). ADPKD cysts show reduced $[Ca^{2+}]_i$ and endoplasmic reticulum Ca^{2+} stores (Xu et al. 2007). Is is thought that abnormal Ca^{2+} homeostasis in ADPKD accounts for the accumulation of cAMP, which promotes cell proliferation and fluid secretion into cysts (Torres et al. 2006).

To summarize, in addition to an important role in progression of kidney disease via cyst expansion and increased cell proliferation and apoptosis (Torres et al. 2009, Abdul-Majeed et al. 2011, Mekahli et al. 2013), Ca^{2+}-mediated mechanisms may also turn out to have a role in ADPKD-associated cardiac pathology.

1.10.4 Management and challenges

Current management is aimed at preventing and treating the various complications of the disease (Torres et al. 2007). Until very recently, there have not been treatments that slow kidney disease progression (Grantham 2008). Management of hypertension is essential. ACE inhibitors and angiotensin receptor blockers may be more effective than other types of antihypertensive agents at preventing end-organ damage (Schrier et al. 2003). Complications that may need management include pain, urinary tract infections, hematuria, kidney stones, end-stage renal disease, intracranial aneurysms, and diverticulitis.

Preclinical studies showed that the antidiuretic hormone arginine vasopressin and its second messenger cAMP promote cyst growth and decline of renal function that can be prevented when vasopressin is eliminated or its effect blocked (Gattone et al. 2003, Wang et al. 2008). Recently, the vasopressin V_2-receptor antagonist tolvaptan was shown to slow the increase in total kidney volume and decrease the decline of kidney function in ADPKD patients (Torres et al. 2012). There are currently over a dozen ongoing clinical trials for ADPKD (http://clinicaltrials.gov). Thus mechanistically relevant drugs look set to change the treatment of ADPKD in the upcoming decades (Chang et al. 2012). For this to happen, a deeper understanding of the molecular level pathomechanisms of this systemic disease is necessary.

MODELS AND TOOLS TO STUDY CARDIAC ELECTRICAL ACTIVITY AND CALCIUM HANDLING

Having the right tools is necessary to study and understand cardiac physiology. In recent years the methodological toolkit has been strengthened by powerful methods that open new possibilities to deepen our understanding of how the heart works and fails.

1.11 At the cellular level

1.11.1 Patch-clamp and calcium imaging in individual cardiomyocytes

In the 1970s, the German cell physiologists Erwin Neher and Bert Sakmann developed a technique to measure ion channel currents in cells by using a glass micropipette (Neher et al. 1978). This technique came to be known as patch-clamp (Hamill et al. 1981), and earned Neher and Sakmann the Nobel Prize in Physiology or Medicine in 1991. To measure ion currents, the glass micropipette, which has an opening in the range of 1μm at its tip, is brought into tightly sealed contact with the cell membrane. The micropipette contains an electrode and a solution of desired contents. The tight seal, formed by applying suction to the micropipette, electronically isolates the membrane patch from the external environment and enables stable recording of electric currents across this patch of membrane. Many variations of the patch-clamp technique exist. To investigate changes in current or voltage across the entire cell membrane, the whole-cell patch technique is applied (Hamill et al. 1981). After forming a seal between the cell membrane and the micropipette, further suction is applied to rupture the patch membrane. Now the inside of the micropipette, which usually contains solution matched to intracellular solution, forms a contiguous space with the inside of the cell. An alternative way to perforate many small holes into the membrane is by applying chemical agents such as amphotericin-B. This variation is called the perforated patch method. In current-clamp mode, changes in voltage across the plasma membrane of the whole cell can be recorded as the current is held constant. Patch-clamp remains the gold standard method of cellular electrophysiology.

Ca^{2+} is a universal second messenger involved in the process of life from fertilization to apoptosis. The accurate measurement of Ca^{2+} levels in living cells

has been the goal of scientists for decades. The first successful attempts were in the 1960s (Ridgway et al. 1967). A big leap came in the 1980s when a variety of fluorescent Ca^{2+} indicator dyes were developed by the Tsien lab (Tsien 1980, Grynkiewicz et al. 1985). Upon binding to Ca^{2+}, these dyes emit fluorescent light, allowing the measurement of $[Ca^{2+}]_i$ (Paredes et al. 2008, Adams 2010). The dyes are usually loaded into cells as lipophilic acetoxymethyl (AM) esters. Inside the cells, esterases cleave off the AM-group, thus trapping the dye inside the cell and exposing its Ca^{2+} binding carboxyl groups. Changes in $[Ca^{2+}]_i$ in individual cells or even whole organs can be imaged with fluorescence microscopy and sensitive cameras. These dyes have proven to be reliable tools, explaining their skyrocketing popularity. Additionally, intracellular Ca^{2+} can be measured with genetically encoded indicators and calcium-sensitive photoproteins (Brini 2008, McCombs et al. 2008).

1.11.2 Induced pluripotent stem cells – a novel source of cardiomyocytes

Physiological studies on mechanisms of genetic diseases have largely been based on transgenic animal models and in vitro experiments involving transfection with mutated human genes. The applicability of results obtained with these model systems to human disease often remains uncertain. Furthermore, an identical genotype regarding a gene of interest can lead to large variation in phenotype between individuals, largely due to unknown genetic and environmental modifiers. These issues have occasionally made interpretation of results obtained with traditional methods challenging, and conclusions difficult to draw. On the other hand, isolation and culture of human adult cardiomyocytes has proved difficult.

Scientists were filled with new excitement some years ago, as the Japanese geneticist Shinya Yamanaha and colleaques reported they could reprogram differentiated adult mouse cells back to a pluripotent state by using a cocktail of four transcription factors (Takahashi et al. 2006). These cells came to be known as induced pluripotent stem cells (iPSC). Very soon after this, similar findings were reported using adult human cells (Takahashi et al. 2007, Yu et al. 2007). Yamanaha shared the 2012 Nobel Prize in Physiology or Medicine for this discovery. The ability to differentiate cardiomyocytes from iPSCs now enables the study of patient- and disease specific human cells *in vitro* (Zhang et al. 2009a, Mummery et al. 2012) (figure 11). It also bypasses the ethical issues associated with human embryonic stem cells.

This new technology opens a multitude of possibilities for studying inherited diseases. The pathomechanisms can be investigated at the cellular and molecular levels in a human cell model. IPSC-derived cells may be used as tools to deliver *in vitro* optimized personalized treatment by screening for safest and most effective compounds for that individual. The cells may be used for drug discovery and toxicology screening and to gain a deeper understanding of how genotype affects drug responses. This is especially relevant with cardiomyocytes, as for all drugs, adverse effects on the heart are the most common cause of approval delay and withdrawal from the market (Mordwinkin et al. 2013).

However, many issues need to be addressed before iPSC technology becomes a firmly established tool in these fields (Knollmann 2013, Li et al. 2013a, Priori et al. 2013, Sinnecker et al. 2013). Current differentiation protocols produce a heterogeneous group of cells that contain many non-cardiomyocytes as well as different types of cardiomyocytes (atrial, pacemaker, ventricular) at various stages of maturation. In addition to heterogeneity of cells produced by a certain iPSC-line, there is great variation between different cell lines produced from the same patient. Phenotypically the cells resemble immature fetal cells more than mature adut cardiomyocytes. This is demonstrated for example by small cell size, lack of T-tubules, depolarized resting membrane potential, spontaneous beating, and weak contractions (please see page 96 for details). Furthermore, a cell model is of limited use in studying organ-level pathologies such as myocardial infarction, heart failure, and developmental defects.

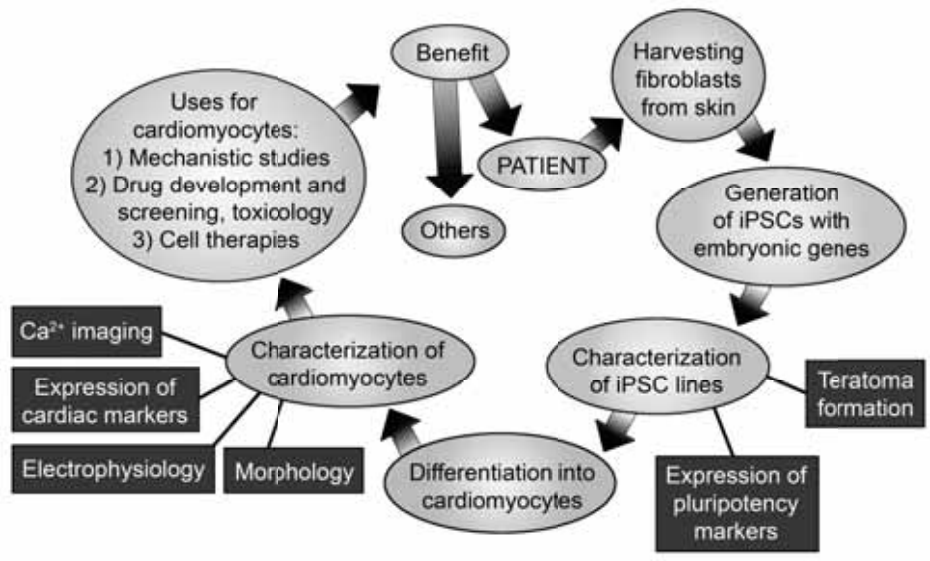

Figure 11. Promises and possibilities of iPSC technology for cardiac patients.

Additionally, cellular reprogramming strategies hold promise for treatment of acquired cardiac diseases including myocardial infarction and heart failure. Cardiac repair and regeneration may be attempted either by cell therapy using iPSC-derived *in vitro* differentiated cardiomyocytes (Yoshida et al. 2011, Okano et al. 2013), or via *in vivo* direct reprogramming of cardiac fibroblasts to myocytes (Addis et al. 2013, Qian et al. 2013). However, here also many challenges remain. Effective *in vivo* reprogramming in humans still seems fairly distant. In addition to the issues listed above, it also raises safety concerns about tumorigenicity and arrhythmogenicity.

1.12 At the tissue level

1.12.1 Calcium and action potential imaging

In addition to single cell measurements, fluorescent Ca^{2+} indicators can be used to record changes in $[Ca^{2+}]_i$ in tissue samples or even whole organs. Similarly, APs can be recorded optically using voltage-sensitive dyes, also known as potentiometric dyes (Cohen et al. 1978). These dyes attach to the cell membrane and respond to a change in electric potential across the membrane with a change in the intensity of fluorescent light they emit. This can be recorded using fluorescent microscopy and sensitive camera equipment. The advantage of voltage-sensitive dyes compared to patch-clamp techniques is the possibility to study AP conduction (speed and direction) in multi-cellular preparations with a non-invasive method. This makes them attractive tools in cardiac research (Herron et al. 2012). Drawbacks include the special recording equipment and laborious optimization of protocols needed mainly due to weakness of the fluorescent signal. Also issues posed by motion artifacts and photodynamic effects need to be addressed. A further alternative for AP measurements is the multi/microelectode array method (Spira et al. 2013).

1.12.2 Monophasic action potential recordings

The first account of MAP recordings dates back to the 19th century, when electrical activity was measured in the frog ventricle (Burdon-Sanderson 1884). Also subsequent techniques relied on producing an injury to the region where MAPs were recorded from. Then it was discovered that simply pressing the electrode against the heart is sufficient to record stable MAPs (Jochim et al. 1935). However, this discovery was practically forgotten after cardiac APs were first recorded from single cells (Draper et al. 1951). In the 1960s and early 70s MAPs were recorded for the first time in humans (Korsgren et al. 1966). The technique relied on suction to maintain tight contact between the

catheter tip and the endocardium, predisposing to air emboli and mechanical injury of the myocardium. The modern contact electrode technique was developed in the early 1980s by Franz and colleagues, enabling safe prolonged measurement of local electrical activity in the heart *in vivo* (Franz 1983).

Typically, MAPs are recorded by introducing the MAP catheter via femoral vein into the right ventricle, or alternatively via femoral artery into the left ventricle (Franz 1991). Under fluoroscopic guidance, the catheter tip is gently brought into contact with the endocardium at a perpendicular angle, and MAPs generally between 10 and 50 mV in amplitude are recorded for up to several hours (figure 12). The tip of the catheter contains a silver-silver chloride MAP electrode. A silver-silver chloride MAP reference electrode is located 5mm proximally from the tip. The location of the platinum pacing electrodes between the MAP electrodes allows low capture thresholds and minimizes pacing artifacts. The catheter tip is flexible for safety, and can be controlled with a thumb lever by the operator. The MAP electrode records electrical activity from a region in its vicinity, likely from a distance of a few millimeters, encompassing a group of cells (Franz 1999). The MAP waveform is almost identical to that of an intracellularly recorded AP, neatly filling the gap between basic electrophysiology and more traditional clinical recordings, such as ECGs (Moore et al. 2007). In addition to research purposes, MAP recordings have many uses in the clinical setting. These include determining effects of drugs, heart rate, and rhythm on APD and refractoriness. Afterdepolarizations can be identified, ablation guided, and the viability of the myocardium assessed during and after ablation. MAPs can detect myocardial ischemia and APD dispersion. Futhermore, MAP recording can be a useful tool in overdrive pacing of atrial flutter to prevent driving the atria into fibrillation.

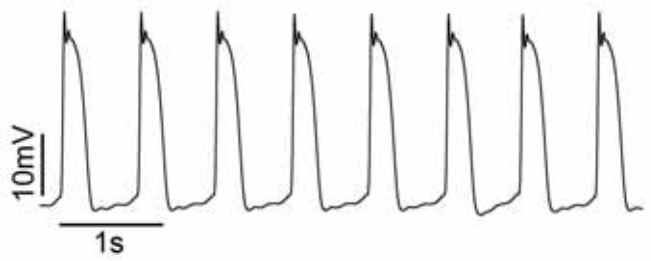

Figure 12. MAP recording from the right ventricular septum in a 10-year-old male.

1.13 At the organism level

1.13.1 Electrocardiograms

The ECG has been a cornerstone of cardiology for over a century (Einthoven 1903). It was the Dutch physiologist Willem Einthoven who, based on previous work, developed the method, named the deflections, and described changes in the ECG under various pathological conditions. For this, he earned the Nobel Prize in Physiology or Medicine in 1924.

The modern 12-lead ECG normally consists of six precordial leads, three limb leads, and three augmented limb leads. The unipolar precordial leads (V1-6) are placed on the chest and view the heart in the horizontal plane. The bipolar limb leads (I-III) are placed on the extremities: I measures the voltage between the left arm and the right arm, II between the left leg and the right arm, and III between the left leg and the left arm. The unipolar augmented limb leads are derived from the three limb leads. In aVR, the right arm is the positive electrode, the left arm and the left leg make up the negative electrode. With similar logic, in aVL the positive electrode is the left arm, and in aVF the positive electrode is the left leg. The limb and augmented limb leads view the heart in the frontal plane. Therefore, leads II, III, and aVF are inferior leads that view the heart from below. Leads I, aVL, V5-6 are lateral leads that view the heart

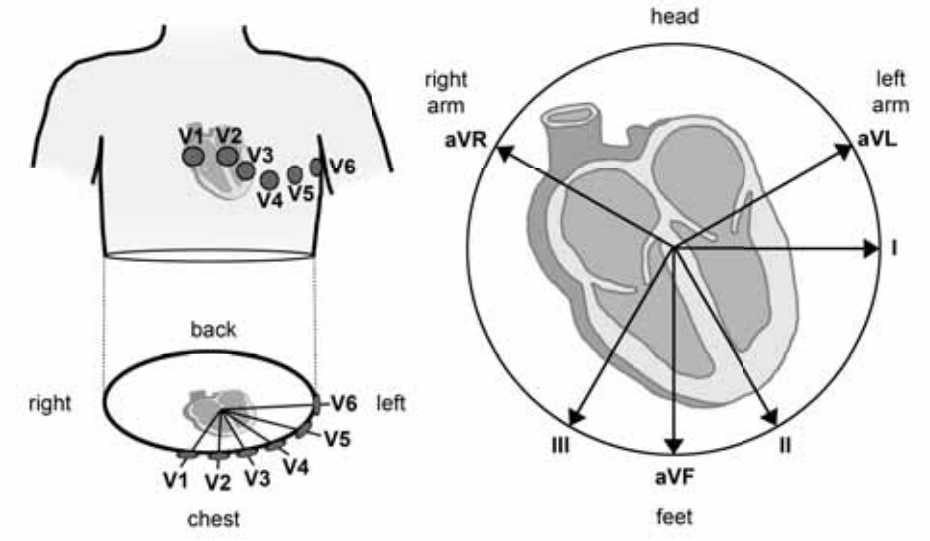

Figure 13. The precordial leads view the heart in the horizontal plane, as shown on the left, whereas the limb and augmented limb leads view the heart in the frontal plane, as shown on the right.

from the left. Leads V1-4 are anterior leads, leads V1-2 look at the right ventricle and leads V3-4 view the interventricular septum (figure 13). When a wave of depolarization is approaching the positive electrode, there is a positive deflection on the ECG. Conversely, when depolarization is moving away from the positive electrode, the deflection is negative. During repolarization, the deflections are in the opposite direction, meaning a wave of repolarization approaching a positive electrode will cause a negative deflection. The amplitude of the deflection is also proportional to the mass of the tissue, therefore

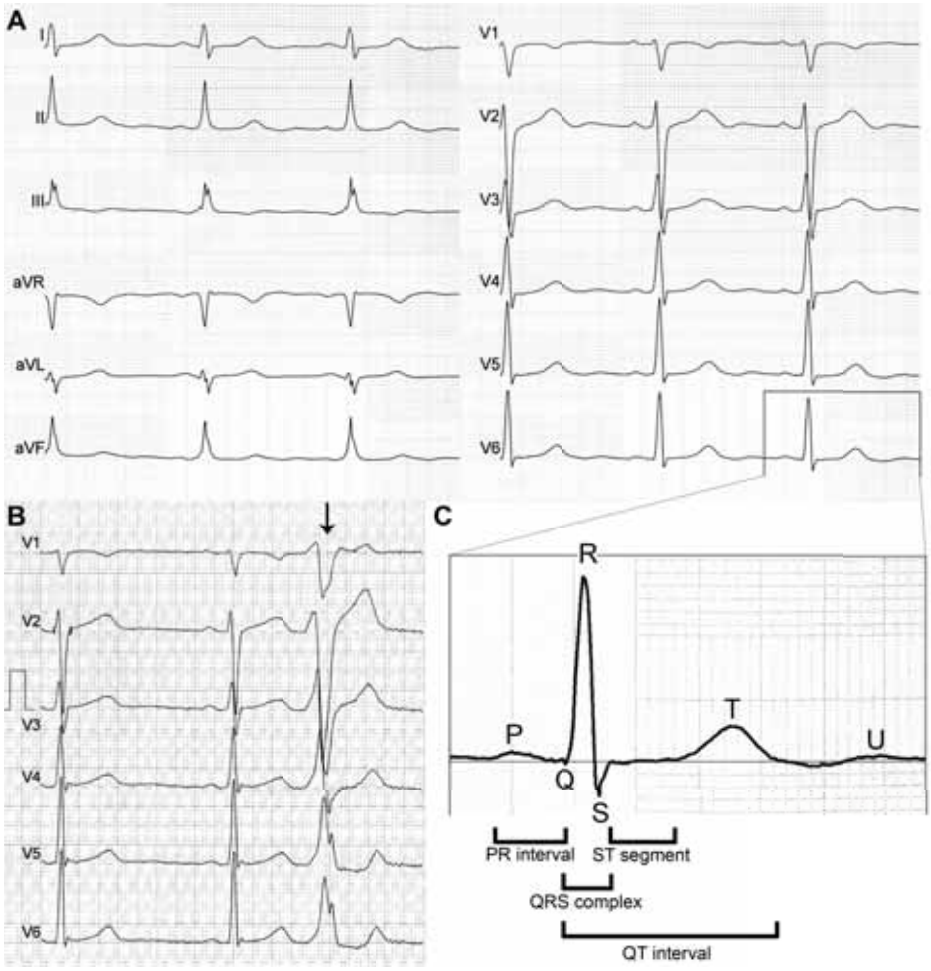

Figure 14. A. Normal 12-lead ECG in a 32-year-old male PhD candidate. **B**. Precordial leads in the same individual showing a PVC (arrow), perhaps a sign of stress related to the upcoming PhD defense. **C**. Nomenclature of essential ECG waves, segments, and intervals.

the much larger ventricles (especially the left one) cause larger defletions than the smaller atria. Because ventricular depolarization progresses from endocardium to epicardium, whereas repolarization progresses from epicardium to endocardium, the deflections caused by both events are toward the same direction.

The depolarization of the atria results in a P-wave. This is followed less than 200 ms later by the depolarization of the ventricles, which is seen on the ECG as the QRS-complex. This is followed by repolarization of the ventricles, showing on the ECG as a T-wave. Atrial repolarization is hidden among the QRS-complex. Occasionally, the T-wave is followed by a small U-wave, the origin of which is debated. A 12-lead ECG and the names of its deflections are shown in figure 14.

1.13.2 Alternans and variability of repolarization

Ventricular repolarization is manifested on the ECG as a T-wave. Its morphology is a reflection of the heterogeneous AP morphologies across the ventricular wall (Yan et al. 1998). Studies on ventricular wedge preparations have revealed these intramural differences in AP morphology (Antzelevitch 2006). Cells on the ventricular epicardium have a prominent phase 1 of the AP and short APD. They are the last to depolarize, but the first to repolarize. Endocar-

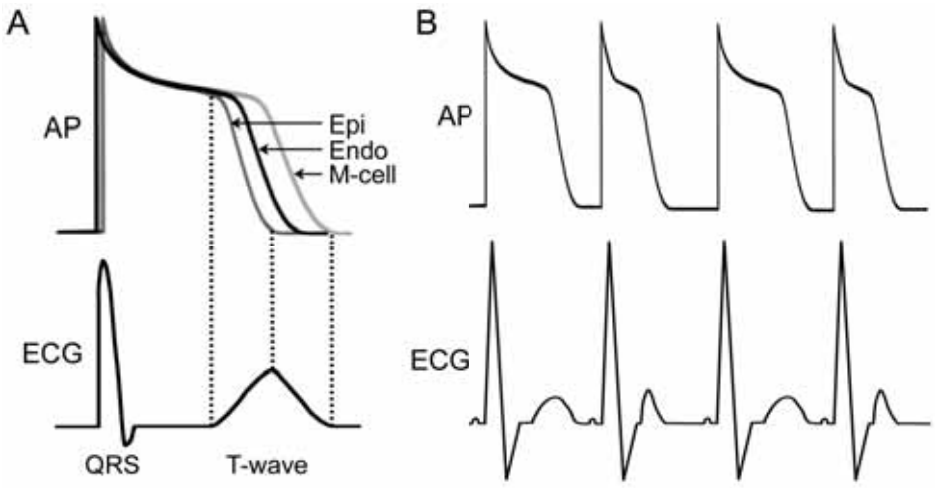

Figure 15. A. A simplified sketch showing how heterogeneity of repolarization across the ventricular wall leads to formation of the T-wave on the surface ECG. Epi = epicardial cells, Endo = endocardial cells, M-cell = mid-myocardial cells. Modified from (Yan et al. 1998). **B**. A simplified sketch showing APD alternans and corresponding exaggerated T-wave alternans on the surface ECG.

dial cells lack a prominent phase 1 of the AP. Cells located deep inside the ventricle wall are called M-cells. They are characterized by a prominent phase 1, and their APs have the ability to prolong significantly with decreasing heart rate and the influence of some drugs (Sicouri et al. 1991). The T-wave begins as the AP plateaus of epicardial and M-cells separate (figure 15A). The peak of the T-wave is marked by the completion of epicardial repolarization. Intramural voltage gradients become fully extinguished as the M-cells are fully repolarized. This is when the T-wave ends.

Alternans of intracellular Ca^{2+} that leads to alternans of APD manifests on the surface ECG as T-wave alternans (TWA) (figure 15B) (Pruvot et al. 2004, Laurita et al. 2008a). TWA is defined as a beat-to-beat alternation in T-wave morphology (shape, amplitude, timing). Often, the definition includes alternation of the ST-segment, T- and U-waves, and is referred to as repolarization alternans (Narayan 2006). The first descriptions of macrovolt TWA date back a hundred years, to the early days of the ECG (Lewis 1911). This type of macroscopic alternans is rare, and from the beginning it was clearly associated with cardiac pathology. In the 1980s sensitive methods to measure microvolt (i.e. not detectable by direct visual inspection) TWA were developed (Adam et al. 1984, Smith et al. 1988). These studies found TWA to associate with VF. Today, TWA has been shown to predict ventricular arrhythmias and SCD in numerous patient groups (Shusterman et al. 2006, Calo et al. 2011). However, also negative findings are reported, and the controversial clinical utility of TWA provokes continued debate (Gupta et al. 2012).

The search for ECG parameters as predictive markers for arrhythmia risk is the focus of intense research efforts. Recently, also non-alternating beat-to-beat variability of repolarization has received attention (Oosterhoff et al. 2011, Varkevisser et al. 2012). Such variability is usually quantified as short-term variability (STV) of APD or the QT interval over a period of 30 – 60 beats. Increased STV has been shown to be a superior predictor of drug-induced arrhythmogenesis than QT prolongation (Abi-Gerges et al. 2010). Additionally, increased STV of QT interval has recently been associated with proarrhythmia in long QT syndrome patients and dilated cardiomyopathy (DCM) patients with heart failure (Hinterseer et al. 2008, Hinterseer et al. 2010). As many questions remain unanswered, the search for optimal prognostic markers for arrhythmia risk goes on (Shusterman et al. 2009).

1.13.3 Zebrafish as a model organism to study human cardiac disease

The last two decades have seen a huge surge in popularity of using zebrafish (*Danio rerio*) as a model for human disease in biomedical research. Zebrafish have proved a useful model to study heart development, mechanisms of inherited and acquired cardiac disease, and in drug development and cardiac toxicity screening (Heideman et al. 2005, Dahme et al. 2009, Bakkers 2011, MacRae 2013). Advantages and disadvantages of zebrafish in cardiac research are listed in table 1.

Table 1. Advantages and disadvantages of using zebrafish to study cardiac disease.

ADVANTAGE	EXPLANATION
Speed	**Hundreds of eggs can be collected on one day's notice. Fish develop rapidly: heart beat in 1 day, fully developed heart in 2 days**
External development	**Allows direct observation of the developing embryo by using normal light microscopy**
Optical transparency	**Non-invasive observation of heart and its function, including heart rate, contractility, cardiac output, blood flow velocity by using normal light microscopy**
Survival without circulation	**Embryonic fish survive for days without circulation, sufficient oxygen and nutrients are supplied by diffusion, allows study of severe cardiac phenotypes**
Similar cardiac physiology	**Heart rate (100–170/min) and action potential duration are more similar to human values than in rodents. However, please see limitations on page 98.**
Simple administration of drugs	**Many drugs can be applied directly to the bath water**
Genetic methods	**Fully sequenced genome. Transgenic fish are increasingly available. Gene silencing with antisense oligos is a well established method**
Affordability	**Costs of husbandry and maintenance are very low compared to mammals**
DISADVANTAGE	**EXPLANATION**
Not a mammal	**Zebrafish is a non-mammalian vertebrate. Results must be interpreted with caution, exciting findings should be confirmed with mammalian models**
Smaller toolkit	**Availability of cell lines, reagents, and transgenic lines is still poorer than in well established rodent models**

Zebrafish originate from freshwater streams in South-East Asia. Females can lay hudreds of eggs weekly. After external fertilization, the development is remarkably rapid. Heart beat initiates 1 day post fertilization (dpf) and the heart is fully formed at 2 dpf. At this stage the fish are 1 – 2 mm long and their heart is approximately 150 µm in diameter. The zebrafish heart is two-chambered, consisting of an atrium and a ventricle (figure 16) (Menke et al. 2011). The embryos hatch from the chorion 2 – 3 dpf and begin their larval life. After their internal yolk reserve is depleted in approximately a week, the young fish must start catching their own food. Zebrafish reach adulthood at three months. The fish grow approximately 3 – 4 cm long and weigh close to 1 g. They can live until approximately five years of age, but for research purposes adult fish aged 6 – 18 months are typically used (figure 17).

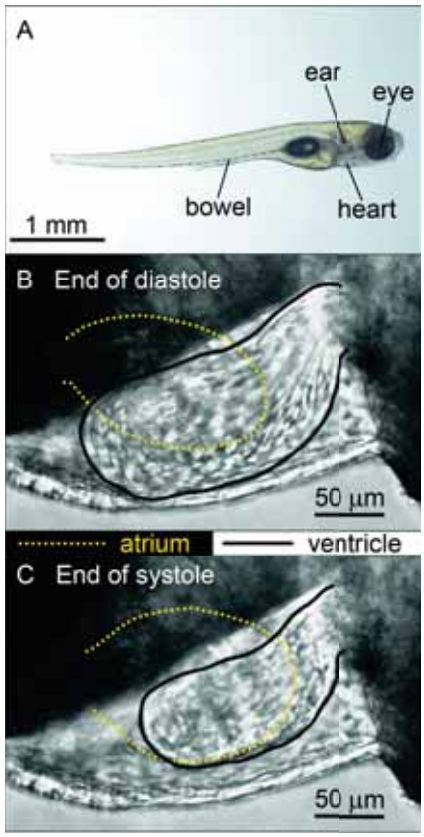

Figure 16. A. Zebrafish larva at 9 dpf. Image by Ivana Kuo, Yale University. **B-C**. Close-up images under a light microscope of an embryonic zebrafish heart at 2 dpf. Outlines of the atrium and ventricle are marked, demonstrating the difference in chamber size between diastole and systole. Images by Juuso Sirén, University of Helsinki.

Figure 17. Adult zebrafish. Photo by Henri Koivula, University of Helsinki.

The genetic tractability of zebrafish is a big factor in its current popularity. It is ideal for phenotype-driven, forward genetics methods. Mutagenesis screens

have been performed for over a decade (Amsterdam et al. 1999). Chemicals, retroviruses, or transposons are used to generate mutations that are then screened and selected for interesting phenotypes (Milan et al. 2008). The causative gene mutations can then be identified with positional cloning. These types of screens are an unbiased way to identify novel genes implicated in cardiac disease. Indeed, numerous cardiac phenotypes and mutations have been identified, providing models for mechanistic and therapeutic studies (Chico et al. 2008, Dahme et al. 2009). Conversely, a known gene of interest can be manipulated to study phenotypic and physiologic consequences. Such reverse genetic methods are most commonly applied by injection of antisense oligonucleotides (morpholinos) into fertilized eggs (Nasevicius et al. 2000, Eisen et al. 2008).

The morpholino will typically block target mRNA translation and result in absence of the target protein for 3 – 5 days. Similarly, desired mRNA may be injected to overexpress a gene of interest. This simple method enables studies on the impact of a single gene on development and physiology in a fast, affordable way. This well established method is a logical next-step to study effects of candidate genes identified in humans in e.g. genome-wide association studies. The recent years have also seen rapid development of targeted mutation and gene-inactivation methods, as well as the emergence of powerful transgenic techniques that allow temporal and spatial control of gene expression in zebrfish (Staudt et al. 2012).

Zebrafish have been used to model a wide variety of cardiac diseases. Congenital heart anomalies are the most common birth defects in humans, occurring in approximately 1% of live births. For example, the zebrafish *gridlock* mutant, which harbors a mutation in the *hey2* gene, offers a model for aortic coarctation (Weinstein et al. 1995). Importantly, an *in vivo* small-molecule screen identified compounds that rescue the disease phenotype by upregulating vascular-endohelial growth factors (Peterson et al. 2004). Furthermore, an illustrative example of the power of zebrafish as model is the discovery of nexilin function and its role in disease (Hassel et al. 2009). Nexilin, previously of unknown function, was identified as a Z-disk protein, and its inactivation in zebrafish using morpholinos led to a DCM phenotype with dilated cardiac chambers and heart failure. Next, human DCM patients were sequenced and mutations in nexilin identified. Overexpression of these human nexilin mutations in zebrafish recapitulated the human disease phenotype. Additionally, zebrafish offers a model for cardiac arrhythmia (Milan et al. 2008). For example, heterozygous mutations in the *kcnh2* gene, which encodes one of the po-

tassium channel subunits important in repolarization, lead to prolonged repolarization (Arnaout et al. 2007). Conversely, gain-of-function mutations in the same gene lead to shortened depolarization (Hassel et al. 2008). These mutants offer models to study human long and short QT syndromes. Importantly, zebrafish respond to QT interval affecting drugs comparably to humans. When given 23 drugs known to prolong the QT interval in humans, 22 of these resulted in a similar QT prolongation in zebrafish (Milan et al. 2003). Remarkably, zebrafish are capable of fully regenerating their heart following injury, hence providing an exciting model to study regeneration (Poss et al. 2002). The first reports used an amputation model, where approximately 20% of the ventricle is excised from the apex. More recently, a cryoinjury-induced myocardial infarction model has been introduced (Chablais et al. 2011, Gonzalez-Rosa et al. 2011). Application of a metal-probe cooled in liquid nitrogen results in the death of approximately 20% of the ventricular myocytes. After both types of injuries, essentially full regeneration ensues in one month.

The above mentioned snap shots demonstrate the versatility and robustness of zebrafish as a model organism in cardiac research.

Aims of the study

I Investigate the mechanisms of ventricular arrhythmia in CPVT by examining cardiac electrophysiology *in vivo* and intracellular Ca^{2+} handling *in vitro*.

II Decipher the cellular level pathomechanims of CPVT by studying electrophysiology and intracellular Ca^{2+} handling in human iPSC-derived cardiomyocytes generated from a CPVT patient carrying a *RyR2* mutation.

III Expand mechanistic studies on cardiomyocytes. Explore depolarization and repolarization in clinical MAP recordings and ECGs of CPVT patients for corresponding manifestations of abnormalities discovered in cell studies.

IV Investigate cardiac function and potential mechanisms of dysfunction in a zebrafish model of PKD with *in vivo* and *ex vivo* techniques. Determine the association between PKD and heart failure in humans.

Patients, materials, and methods

1 Clinical data

1.1 MAP recordings (Studies I – III)

We recruited patients from three Finnish CPVT families that carry known mutations in *RyR2* (P2328S, Q4201R, and V4653F). Out of the 22 affected, over 10-year-old subjects, six refused the electrophysiological study and one had another serious medical condition. Right cardiac catheterization with MAP recording was performed in the remaining 15 patients, and in 12 age-matched controls. The control subjects were recruited from patients being electrophysiologically evaluated after a catheter ablation of accessory AV pathways. 12 consecutive patients were chosen for MAP recording, which was performed at the end of the routine electrophysiological evaluation. All subjects had normal QT intervals, structurally normal hearts, and were not taking any medications known to affect cardiac repolarization. The control subjects were 18 – 50 years old, and were not taking β-blockers. In CPVT patients, β-blockers were discontinued at least five drug half-lives prior to a bicycle ergometer exercise test, which was performed one day before the MAP recording. All protocols were carried out according to institutional guidelines. The research protocol was approved by the Ethics Review Committee of the Department of Medicine, University of Helsinki. All study subjects provided written informed consent.

To study APs and cellular mechanisms of arrhythmias *in vivo*, MAPs were recorded by introduction of a bipolar silver–silver chloride catheter (model 006248, Bard Inc., USA) through the femoral vein. The catheter was attached to the right ventricular septum under fluoroscopic guidance. Additionally, three quadripolar electrophysiological catheters (Bard Inc.) were placed in the right atrium, the AV junction, and the right ventricular apex. Blood pressure from the femoral artery was monitored with a fluid manometer. The MAP signal was amplified and filtered at 0.05 – 250 Hz. Blood pressure and 12-lead ECG were stored digitally at a sampling rate of 1 kHz (Cardiolab, Prucka Engineering, USA).

Stable MAP signal, indicated by noiseless stable amplitude and isopotential baseline at diastole, was recorded in all patients. MAPs were recorded during sinus rhythm and atrial pacing at cycle lengths of 600, 500, and 400 ms. First,

a baseline was recorded, followed by infusion of incrementally increasing concentrations of epinephrine. For safety reasons, the maximal infusion rate of epinephrine was maintained at 0.05 μg/kg of body weight, while carefully monitoring possible arrhythmias.

Custom-made non-commercial software was used for analysis of MAPs. EADs were defined as low-amplitude afterdepolarizations that occur before the completion of repolarization, during phase 2 or 3 of the AP, and have a minimum amplitude of ≥3% of the preceding AP. DADs were defined as low amplitude afterdepolarizations occurring after completion of repolarization. To be included in the analyses, the minimum allowed amplitude of a DAD was 0.2 mV and 3% of the previous AP amplitude for at least five consecutive beats. DAD coupling interval was measured from the upslope of the previous AP to the peak of the DAD. The diastolic upslope of the DAD was calculated by measuring the mean rate of rise (dV/dt) of the ascending limb of the DAD, averaged over three consecutive beats.

For study II, data were available on three RyR2-P2328S patients and three healthy controls. In study III, these same six subjects' MAPs were evaluated for variability and alternans. APD was measured at 50% and 90% of repolarization (APD50 and APD90). STV during 30 consecutive beats was calculated with the formula $STV=\Sigma|Dn+1-Dn| / [30\times\sqrt{2}]$, where 'n' represents the beat number and 'D' represents APD50 and APD90. APD alternans was defined as an absolute difference ≥1ms with a beat-to-beat alternating pattern between consecutive odd and even numbered APDs that persisted for a minimum of ten consecutive beats.

1.2 24h ECG recordings (Studies II and III)

We recruited 19 patients from two Finnish families with known mutations in *RyR2*. The main clinical data on these patients have been published previously (Viitasalo et al. 2008). We studied thirteen patients from a family with a *RyR2*-P2328S mutation, of whom five had exercise-related syncope and three had cardiac arrest in their medical history. Six patients from another family with a *RyR2*-V4653F mutation were also studied. Three of them had a history of exercise-related syncope and two had suffered cardiac arrest. 24h ECGs were recorded off β-blockers, which were discontinued in 17 out of the 19 patients at least five drug half-lives before start of the ECG recording. Two asymptomatic CPVT patients were not receiving β-blocker therapy. After completion of the 24h ECG recording, all 17 patients continued β-blocker therapy. Seven

RyR2-P2328S (three with syncope, two with cardiac arrest) and five *RyR2*-V4653F (two with syncope, two with cardiac arrest) patients repeated a 24h ECG on β-blocker therapy. Five patients refused the second 24h ECG recording. Gender- and age-matched control subjects with available 24h ECGs were chosen from a database of genotyped healthy unaffected family members of long QT syndrome patients. None of the 19 control subjects were taking β-blockers.

All study subjects had normal echocardiography findings and serum electrolyte levels, and none were taking medications known to affect cardiac repolarization. All were in sinus rhythm without bundle-branch blocks. The study subjects were instructed on following normal daily activities during the recording. The study complies with the Declaration of Helsinki. The study was approved by the Ethics Review Committee of the Department of Medicine, University of Helsinki. All study subjects provided written informed consent.

Commercial tape recorders and software (Marquette Electronics Inc., USA) were used to record and perform initial analysis by labeling the QRS-complexes to normal, ventricular extrasystoles, or aberrant complexes. Further analysis of the 24h ECGs was performed with custom-made non-commercial software. Raw unsampled and unaveraged signal from the modified precordial lead V5 was used for all analyses. The baseline was corrected with a cubic spline baseline fitted to the PQ intervals of each beat. QRS onset was defined as the time instant where the signal amplitude of the envelope / hilbert transform of the high pass filtered signal exceeds the average of the predefined noise interval with five standard deviations. The T-wave apex was defined as the peak of the parabola fitted to the highest amplitude change after the QRS. The T-wave end was defined as the time instant when the steepest tangent after the T-wave apex crosses the baseline. To improve the accuracy of T-wave offset identification, low amplitude T waves (-0.1 – 0.1 mV) were excluded. The maximum allowed noise level was set to 0.05 mV and the minimum signal-to-noise ratio was set to 30. Premature beats were rejected according to Marquette software's criteria. Additionally, the maximum allowed RR interval difference between consecutive beats was set to 30%. Outliers were identified and excluded by plotting the QT interval values against the preceding respective RR intervals.

To assess non-alternating beat-to beat variability, STV during 30 consecutive beats was calculated with the formula $STV=\Sigma|Dn+1-Dn| / [30\times\sqrt{2}]$, where 'n'

represents the beat number and 'D' represents the duration of RR, QT-apex, QT-end etc. The QT variability index (QTVI) was calculated from consecutive 1000 second segments with the formula $QTVI=\log_{10}[(QT_v/QT_m^2)/(HR_v/HR_m^2)]$, where QT_v is the QT interval variance, QT_m is the QT interval mean, HR_v is the heart rate variance, and HR_m is the heart rate mean (Berger et al. 1997).

TWA was analyzed from a time window set to 100 – 400 ms from the trigger point and for U-wave alternans (UWA) to 0 – 200 ms after the end of the T-wave. Alternans in the latter window was interpreted as UWA without identifying the U-waves. TWA and UWA were calculated with two algorithms, a modified moving average (MMA) algorithm and a complex demodulation (CDM) algorithm. The MMA algorithm is based on finding the maximum amplitude difference between moving averages of even and odd beats (Nearing et al. 2002). The CDM algorithm is a modification of the spectral method (Smith et al. 1988, Rosenbaum et al. 1994). In CDM the alternans voltage is defined from the power spectra at a 0.5 1/beat frequency and corrected with a noise estimate from a 0.42 – 0.46 1/beat frequency range. In CDM the spectral method is modified by defining the spectral components by filtering demodulated beat-to-beat time-series with an infinite impulse response type low-pass filter (4th order Butterworth type IIR filter) instead of a finite impulse response type filter that is used as a window function in fast Fourier transform. All the other parts of the CDM and the spectral method algorithms are identical. To increase reliability of the CDM method, only beats with an alternans ratio over three, i.e. beats where the power of the alternans frequency was at least three standard deviations greater than the estimated mean noise, were included in the analyses. Data were calculated for all accepted beats and expressed at RR steps of 10 ms for RR intervals from 500 to 1200 ms.

For study II, T1-, T2-, and U-waves were defined as previously reported (Aizawa et al. 2006, Viitasalo et al. 2006, Viitasalo et al. 2008). T1-wave was defined as the first peak during repolarization. T2-wave was defined as such a second peak during repolarization that occasionally merges with the T1-wave. A U-wave was defined as a second or third peak during repolarization that never merges with the T1 wave.

1.3 The Mayo ADPKD database (Study IV)

The Mayo ADPKD Mutation Database (Rochester, Minnesota, USA) collects data on ADPKD patients (http://pkdb.mayo.edu). We examined the database in 2010, when it contained information on 2620 ADPKD patients, including 374 genotyped patients with identified *PKD* mutations (307 with *PKD1* and 67 with *PKD2* mutations). To investigate the association of ADPKD with heart failure, we decided to look for cases of idiopathic dilated cardiomyopathy (IDCM) among the patients in the database. The diagnosis of ADPKD in the presence of family history is based on Ravine's criteria, shown in table 2 (Ravine et al. 1994, Pei et al. 2009). In patients without a family history of ADPKD, diagnosis is based on at least 20 bilateral kidney cysts in the absence of clinical findings that would suggest a different cystic disease. A diagnosis of IDCM was based on left ventricular ejection fraction < 40%, exclusion of ≥ 50% obstruction in any coronary artery, exclusion of myocarditis, exclusion of a primary or a secondary heart muscle disease, and exclusion of stage 4 or 5 chronic kidney disease. Direct sequencing was used to screen for mutations in the coding and flanking intronic regions of *PKD1* and *PKD2*, as reported previously (Rossetti et al. 2007, Rossetti et al. 2009). The research protocol was approved by the Mayo Institutional Research Board as part of a study of genotype–phenotype correlations in PKD. All participants provided informed consent.

Table 2. Ravine's ultrasonographic diagnostic criteria for ADPKD.

Patients with a family history of ADPKD1	
Years of age	kidney cysts
< 30	≥ 2 cysts in 1 kidney or 1 cyst in each kidney
30 - 59	≥ 2 cysts in each kidney
≥ 60	≥ 4 cysts in each kidney
Patients with a family history of ADPKD of unknown genotype	
Years of age	kidney cysts
15 - 39	≥ 3 cysts (uni- or bilateral)
30 - 59	≥ 2 cysts in each kidney

2 Cell models

2.1 HEK 293 cells (Study I)

2.1.1 Site-directed mutagenesis and RyR2 expression

To study the effects of the *RyR2* mutations P2328S and V4653F on cellular Ca^{2+} handling, these point mutations were generated with a Chameleon Double-Stranded, Site-Directed Mutagenesis Kit (Stratagene, USA) in small fragments of *RYR2* cDNA. Fragments with these mutations were then subcloned back to their original positions in full length *RyR2* cDNA in expression vectors. For expression of RyR2, cultured HEK 293 cells were transfected with the *RyR2* cDNA with the Ca^{2+} phosphate precipitation method.

2.1.2 Calcium imaging

One day after transfection, the HEK 293 cells were imaged using confocal microscopy. The Ca^{2+} indicator dye Fluo-3 AM (Molecular Probes, The Netherlands) was used to load the cells for 30 minutes, followed by a 20 minute period of dye de-esterification, and imaging using an inverted microscope (Nikon Eclipse TE300, Japan) equipped with a confocal imaging system (Ultra View, PerkinElmer Life Sciences, UK). The images were recorded with a CCD-camera at 10 frames per second at room temperature in Tyrode's solution containing 1.8 mM Ca^{2+}.

For recording, a view with 10 – 20 cells was chosen. After a baseline recording, the cells were stimulated with 5 mM caffeine or a cAMP analoque (dioctanyol cAMP) by rapidly exchanging the bath solution. The data were analyzed offline and $[Ca^{2+}]_i$ was quantified as described previously (Lipp et al. 2000).

2.2 Induced pluripotent stem cell-derived cardiomyocytes (Studies II and III)

2.2.1 Generation of patient-specific iPSCs

The iPSC lines were generated as described previously (Takahashi et al. 2007). Fibroblasts harvested from a 25-year-old male with symptomatic CPVT due to a *RyR2*-P2328S point mutation were used to generate two iPSC lines. Two control cell lines were generated, one from foreskin fibroblasts, and the other from skin fibroblasts of a healthy 55-year-old female. The research protocol

was approved by the Ethics Committee of the Pirkanmaa Hospital District. All study subjects provided written informed consent.

2.2.2 Characterization of iPSC lines

Genomic sequencing to confirm the presence of the heterozygous *RyR2*-P2328S mutation in the CPVT iPSC lines, and its absence in the control iPSC lines, was performed with direct *RyR2* exon 46 sequencing of polymerase chain reaction (PCR)-amplified DNA. Karyotypes of the iPSC lines were determined with standard G-banding chromosome analysis. Reverse transcription PCR was used to determine endogenous and exogenous gene expression in the iPSC lines. For immunocytochemistry, fixed iPSCs were stained with primary antibodies for SOX2, NANOG, OCT3/4, stage-specific embryonic antigen (SSEA-4), and tumor-related antigens TRA-1-60 and TRA-1-81. IPSCs spontaneously form three-dimensional clusters of cells, termed embryoid bodies. Embryoid bodies were maintained for five weeks. The expression of markers characteristic for the three embryonic germ layers, ectoderm (Nestin), endoderm (AFP), and mesoderm (a-cardiactin) were identified in embryoid bodies with reverse transcription PCR. Finally, the pluripotency of the iPSC lines was assessed *in vivo* by studying teratoma formation. Nude mice were injected under the testis capsule with iPSCs and tumor samples were collected eight weeks later. Fixed sections were stained with hematoxylin and eosin.

2.2.3 Differentiation and characterization of cardiomyocytes

IPSCs were differentiated into cardiomyocytes in a co-culture with murine visceral endoderm-like (END-2) cells, as described previously (Mummery et al. 2003). Beating cell colonies were excised mechanically and dissociated with collagenase. Single spontaneously beating cardiomyocytes were stained with antibodies for the cardiac markers troponin T and connexin 43. RNA from cardiomyocytes was isolated, and used to quantify expression of troponin T, RyR2, SERCA2a, LTCC (Cav1.2), PLB, and NCX. GAPDH was used as a housekeeping gene.

2.2.4 Calcium imaging

In study II, dissociated cardiomyocytes were loaded with the ratiometric Ca^{2+} indicator dye Fura-2 AM (Invitrogen, Molecular Probes, USA) for 30 minutes, followed by 30-minute de-esterification. The coverslip containing the cells was transferred to a recording chamber equipped with pacing electrodes (Warner Instruments, USA). The cells were perfused with Tyrode's solution

(137 mmol/L NaCl, 5.0 mmol/L KCl, 0.44 mmol/L KH_2PO_4, 2.0 mmol/L $CaCl_2$, 1.2 mmol/L $MgCl_2$, 5.0 mmol/L glucose, 20 mmol/L HEPES, 4.2 mmol/L $NaHCO_3$, 1.0 mmol/L Na-puryvate. The pH was adjusted to 7.4 with NaOH). All steps were conducted at +37°C. Imaging was conducted on an inverted IX70 microscope (Olympus Corporation, Germany) equipped with an ANDOR iXon 885 CCD camera (Andor Technology, Northern Ireland). A UApo/340 x20 air objective (Olympus Corporation, Germany) was used to visualize the cells, and images were recorded at approximately 10 frames per second. The perfusate temperature was maintained with an inline heater connected to a control unit (Warner Instruments, USA). A Polychrome V light source (TILL Photonics, Germany) was used to excite the Fura-2 at wavelengths of 340 nm and 380 nm. Emission was recorded at 505 nm. The cells were electrically paced using a stimulator (Digitimer, USA) at a frequency slightly higher than their spontaneous beating frequency. The cells were stimulated with a perfusion of 1 μM epinephrine. The SR Ca^{2+} content was estimated by releasing SR Ca^{2+} with an instantaneous high concentration (40 mM) caffeine pulse. At the end of the experimental protocol, the viability of cells was confirmed by observing spontaneous beating. For fluorescence measurements, regions of interest were selected on spontaneously beating cells. Background noise was subtracted and changes in fluorescence intensity over time (ΔF) were normalized to resting fluorescence levels (F_0). The fluorescence values are presented as ratiometric values of F_{340}/F_{380} or as $\Delta F/F_0$. Analysis of data was performed, blinded to the genotype of the cells, with Clampfit software (Molecular Devices, USA).

In study III, coverslips containing the dissociated cardiomyocytes were loaded with the Ca^{2+} indicator dye Fluo-4 AM (Invitrogen, USA) for 30 minutes at +37°C in Tyrode's solution (136 mmol/L NaCl, 5.4 mmol/L KCl, 0.3 mmol/L NaH_2PO_4, 1.8 mmol/L $CaCl_2$, 1 mmol/L $MgCl_2$, 5 mmol/L glucose, 10 mmol/L HEPES, 2% BSA, pH adjusted to 7.4 with NaOH). After a 30-minute de-esterification at +37°C, the coverslips were transferred to a recording chamber equipped with electrodes for field stimulation (Warner Instruments, USA). Ca^{2+} imaging was conducted at +37°C on an inverted microscope using a UPlanSAPo x20 air objective (Olympus Corporation, Germany). The temperture inside a transparent plastic housing was controlled with a heater connected to a control unit (all Solent Scientific Limited, UK). The samples were excited with Polychrome IV (TILL Photonics, Germany) at a wavelength of 488 nm. Emitted light was filtered with a Chroma filter set (EM HQ535/50m, BS Q505LP, Chroma Technology Corporation, USA). Images were recorded

with a Hamamatsu ORCA-Flash 4.0 sCMOS camera (Hamamatsu Photonics K.K., Japan) at 50 – 67 frames per second. For electrical pacing, a stimulus isolation unit (Warner Instruments, USA) was used to give bipolar pulses of 10 ms duration at a rate approximately 20% higher than the intrinsic beating rate of the cells being visualized. For control of the Polychrome light source, the stimulator, and the camera, HCImage software was used (Hamamatsu Photonics K.K., Japan). Spontaneously beating cells to be analyzed were manually selected as regions of interest and the background was subtracted before quantifying the fluorescence in relation to baseline fluorescence (F/F_0). Ca^{2+} transients were recorded at baseline conditions as well as during electrical pacing and/or perfusion with 1 μM isoproterenol. Again, viability of cardiomyocytes was confirmed after the experimental protocol. Data acquisition and analysis were performed blinded to the genotype of the cardiomyocytes. Data were analyzed initially using the HCImage software and subsequently using Clampfit (Molecular devices, USA). STV of various Ca^{2+} transient parameters was calculated from 30 consecutive transients using the formula $STV=\Sigma|Dn+1-Dn| / [30\times\sqrt{2}]$, where 'D' represents the transient rise time, decay time, duration at half-amplitude, amplitude, or area. Ca^{2+} transient alternans was defined as a beat-to-beat alternation of over 10% in transient amplitude between consecutive even and odd transient oscillations persisting for a minimum of ten consecutive beats.

2.2.5 Patch-clamp measurements

APs were recorded in current-clamp mode with the perforated patch technique using Amphotericin B as the membrane perforating agent (Hamill et al. 1981). The extracellular solution contained 143 mmol/L NaCl, 5.0 mmol/L KCl, 1.8 mmol/L $CaCl_2$, 1.2 mmol/L $MgCl_2$, 5.0 mmol/L glucose, and 10 mmol/L HEPES. The pH was adjusted to 7.4 with NaOH and the osmolarity to 308 ± 2 mOsm with sucrose (Gonotec Osmomat 030, Labo Line Oy, Finland). The patch pipette (intracellular) solution consisted of 122 mmol/L $KMeSO_4$, 30 mmol/L KCl, 1.0 mmol/L $MgCl_2$, and 10 mmol/L HEPES. The pH was set to 7.15 with KOH and the osmolarity to 302 ± 2 mOsm. Spontaneously beating cardiomyocytes were patched under similar conditions as during Ca^{2+} imaging, 6 – 7 days after dissociation. The patch pipettes (Harvard Apparatus, UK) were pulled and flame polished (Narishige, UK) to a resistance of 3.0 – 3.5 MΩ. APs were recorded in gap-free mode using PClamp software, the signal was amplified with a patch-clamp amplifier, and digitized (all Molecular devices, USA). The current-clamp recordings were sampled at 20 kHz and filtered at 5 kHz with a low-pass Bessel filter.

APs were analyzed with Microcal Origin software for APD at 50% and 90% of repolarization (APD50 ad APD90), AP amplitude, maximum diastolic potential, and beating rate. dV/dT (V-max, maximal upslope velocity) was extracted from the differentiated time course traces as peak values corresponding to each single AP. Ventricular-like cardiomyocytes were defined by APD90/APD50 < 1.3 and AP amplitude > 95 mV, atrial-like by APD90/APD50 > 1.3 and AP amplitude > 95 mV and nodal-like by APD90/APD50 > 1.3 and AP amplitude < 95 mV.

3 Zebrafish (Study IV)

3.1 Zebrafish husbandry

Zebrafish embryos were maintained in a mixed population on a 14h light / 10h dark cycle. For experiments, we used Tu/AB wildtype (WT) lines and the insertional mutant line *pkd2/hi4166*, which lacks expression of the PC2 protein (Sun et al. 2004). Embryos were collected from the tank at "dawn" after lights came on, and were raised at 28°C in culture medium containing 0.25 mg/L methylene blue in deionized water. The homozygous *pkd2* mutant fish show dorsal body curvature, which makes them phenotypically easily distinguishable from WT/heterozygous fish, which have straight bodies. Zebrafish maintenance and experiments were performed in accordance with protocols approved by the Institutional Animal Care and Use Committee of Yale University School of Medicine and conform to the NIH Guide for the Care and Use of Laboratory Animals.

3.2 Immunohistochemistry

Zebrafish embryos aged 48 – 52 hours post fertilization (hpf) were fixed overnight and dehydrated for 24 hours. After rehydration, the embryos were washed and treated with trypsin-EDTA to dissociate tissues. Following three washes and blocking for 30 minutes, the samples were incubated in blocking buffer with primary antibodies for rabbit anti-zebrafish PKD2 (Obara et al. 2006), mouse anti-BiP (BD Bioscences, USA), and mouse anti-SERCA2a (Pierce, USA). After numerous washes, the samples were incubated for two hours with fluorescence-conjugated secondary antibodies (Jackson ImmunoResearch Laboratories, USA). Zebrafish hearts were excised manually and mounted on coverslips with Vectashield with DAPI (Vector Laboratories, USA). Images were acquired with a Nikon Eclipse upright microscope equipped with a Plan Apochromat 60x oil objective and NIS acquisition soft-

ware (all Nikon Instruments, Japan). Alternatively, the samples were counterstained with TOTO-3 (Molecular Probes, USA) and mounted in Vectashield medium (Vector Laboratories, USA). Fluorescence imaging was performed on a LSM 710 DUO laser confocal microscope (Zeiss, Germany) using a 40x C-Apochromat water objective and Zen 2010 software. Each fish heart was optically sectioned using a Z-stack with numerous 1 µm steps. Co-localization analysis and maximal Z-projections were performed in ImageJ (NIH, USA).

3.3 Morpholino antisense oligonucleotide injections

To silence the expression of PC2, WT eggs at the one-cell stage were injected with antisense morpholino oligonucleotides. MO3-*pkd2* (Gene Tools, USA) and Phenol Red in sterile water was injected using a microinjector (World Precision Instruments, USA). Morphant embryos showing the typical dorsal body curvature at 48 hpf were selected for the immunohistochemistry experiments.

3.4 Zebrafish real time PCR

Whole fish were used for mRNA extraction from *pkd2* mutants and siblings with normal phenotype using microRNeasy technology (Qiagen, USA). MultiScribe reverse transcriptase (Applied Biosystems, USA) was used to obtain cDNA, which was then amplified in duplicate using either TaqMan (PC2 and SERCA2a) or SYBR Green (RyR2a, RyR2b, IP3R1, IP3R2 and IP3R3) technology on a 7500 Fast real time machine (Applied Biosystems, USA). Elongation factor 1 was used as a housekeeping gene. Data were analyzed using the comparative CT method (Schmittgen et al. 2008), and presented as relative amounts (heterozygote / *pkd2* mutant).

3.5 Zebrafish *in vivo* cardiac physiology

3.5.1 Whole-fish image and heart video recordings

WT and *pkd2* mutant zebrafish embryos at 3, 6, and 9 dpf were anesthetized with tricaine and mounted in methylcellulose to assess for edema. Still images of the whole fish were captured under a dissecting microscope (Leica, Germany) using a SPOT digital camera and SPOT software (Sterling Heights, USA). Videos of the beating heart were captured at approximately 30 frames per second under DIC conditions using a microscope (Zeiss, Germany) equipped with a confocal imager (BD Bioscience, USA), a 20x plan-apochromat air objective (Zeiss, Germany), and Metamorph software (Molecular Devices, USA).

3.5.2 Heart rate measurement

Heart rates of embryonic zebrafish were counted during 20s intervals by directly observing ventricular contractions under a light microscope. After a 5 – 10 minute adaptation to the light, the counting was performed three times per fish and the mean heart rate calculated. As the heart rates were very stable, counting was subsequently performed during a single 20s interval. At ≥ 3 dpf, fish were moving actively and were therefore immobilized with low concentrations (75 – 125 mg/L) of tricaine that do not significantly interfere with heart rate (Craig et al. 2006, Denvir et al. 2008).

3.5.3 Cardiac output measurement

For cardiac output measurements, fish aged 74±2 hpf were placed into a recording chamber and given 5 – 10 minutes to adapt before imaging their heart and blood flow in the dorsal aorta with a NeuroCCD camera (Red Shirt Imaging, USA) at 125 frames per second. Due to a short recording time (4s), immobilization of the fish was not necessary. The blood flow was observed in the dorsal aorta just above the yolk, as shown in figure 18. Flow of erythrocytes was tracked with the "Manual Tracking" plug-in in Image J, allowing the distance travelled by an erythrocyte during one cardiac cycle to be determined.

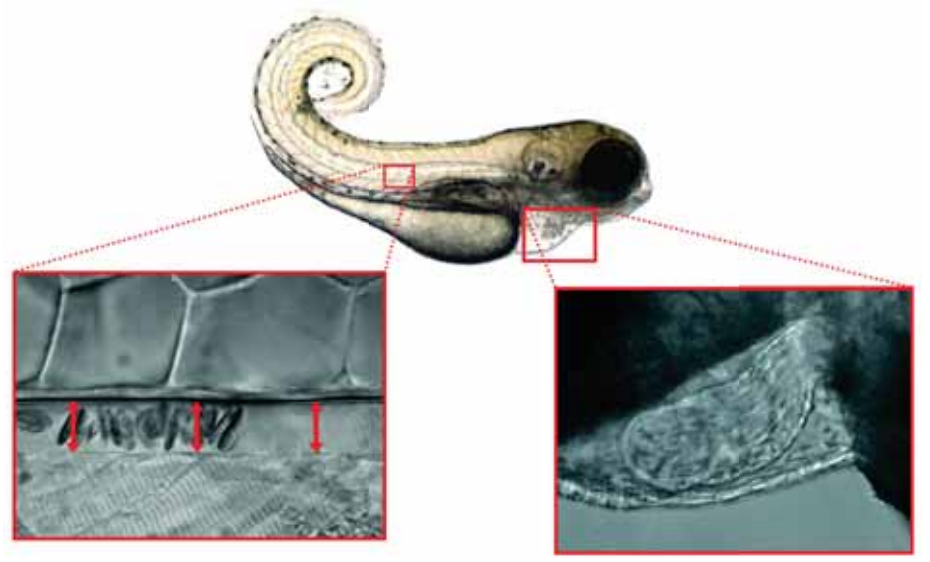

Figure 18. A *pkd2* mutant zebrafish at 3 dpf. Note the typical extensive dorsal curvature. The box on the left shows the location of blood flow measurement in the dorsal aorta. The close-up shows measurement of aortic diameter with red arrows. The box on the right shows the location of the heart, in the close-up the ventricle is clearly visible.

The heart rate was counted and the aortic diameter measured and averaged from multiple spots along the part of aorta used to track the erythrocytes. From these data, cardiac output was calculated as previously reported (Bagatto et al. 2006, Malone et al. 2007). Cardiac output (CO) = heart rate (HR) x stroke volume (SV), which can be calculated from the distance an erythrocyte travels (dx) within one cardiac cycle and the cross-sectional area of the aorta (A_{aorta}). Assuming a circular cross-section of the aorta, $A_{aorta} = (d_{aorta}/2)^2 \times \pi$, where d_{aorta} is the mean diameter of the aorta. It follows that stroke volume (SV) = A_{aorta} x dx.

3.6 Zebrafish *ex vivo* cardiac physiology

3.6.1 Calcium imaging

Under a dissection microscope, whole hearts from anesthetized zebrafish embryos aged 78±2 hpf were excised in Tyrode's solution (136 mmol/L NaCl, 5.4 mmol/L KCl, 0.3 mmol/L NaH_2PO_4, 1.8 mmol/L $CaCl_2$, 1 mmol/L $MgCl_2$, 5 mmol/L glucose, 10 mmol/L HEPES, 2% BSA). The hearts were immediately loaded for 30 minutes with a high concentration (50 µmol/L) of the Ca^{2+} indicator dye Fluo-4 AM (Molecular Probes, USA) together with 0.1% Pluronic F-127 (Molecular Probes, USA), followed by a 30-minute de-esterification. Unharmed, spontaneously normally beating hearts were chosen for experiments. To eliminate motion artifacts, 15 µmol/L blebbistatin was added to the imaging chamber equipped with field stimulation electrodes (Warner Instruments, USA) (Kovács et al. 2004, Jou et al. 2010). The hearts were visualized with an inverted microscope (Nikon, Japan) and illuminated with a 100W lamp (Nikon, Japan) connected to a DC power supply (Chiu Technical Corporation, USA). The light was filtered with a Chroma filter set (emission HQ535/50m, excitation HQ480/40x, and beamsplitter Q505LP). All stages of the experiments were performed at room temperature. Images were captured with a NeuroCCD camera at 125 frames per second (figure 19) and analyzed with Neuroplex Software (both Red Shirt Imaging, USA) and Clampfit (Molecular Devices, USA). Fluorescence was measured by manually drawing the region of interest separately for the atrium and the ventricle within the borders of the cardiac chamber in question. Background subtracted fluorescence was quantified in relation to baseline fluorescence (F/F_0). Averaged fluorescence values from multiple small regions of interest within a single cardiac chamber were found to be similar to each other, thus a single large region of interest was used per cardiac chamber. The hearts were paced with bipolar pulses at 60-240 beats per minute (bpm) using the Neuroplex software and an external stimulus isola-

tion unit (Warner Instruments, USA). Only hearts that were able to follow the pacing at the physiological rate of 140 bpm were included in the analyses. After the experimental protocol, viability of the hearts was confirmed by observing spontaneous beating.

To investigate Ca^{2+} transient alternans, hearts were paced at 120 bpm for 10s. Ca^{2+} alternans was defined as a minimum difference of 10% in peak transient amplitude between consecutive even and odd beats that persisted for a minimum of 10 consecutive beats.

To measure SR Ca^{2+} stores, embryonic zebrafish hearts were examined *ex vivo* at 48±3 hpf in modified Tyrode's solution lacking $CaCl_2$ and containing 1 mmol/L EGTA. The hearts lacked spontaneous beating in the absence of external Ca^{2+}. After 2 min of adaption, Ca^{2+} release from the SR stores was induced by adding caffeine (5 mmol/L) and thapsigargin (25 µmol/L) to the chamber.

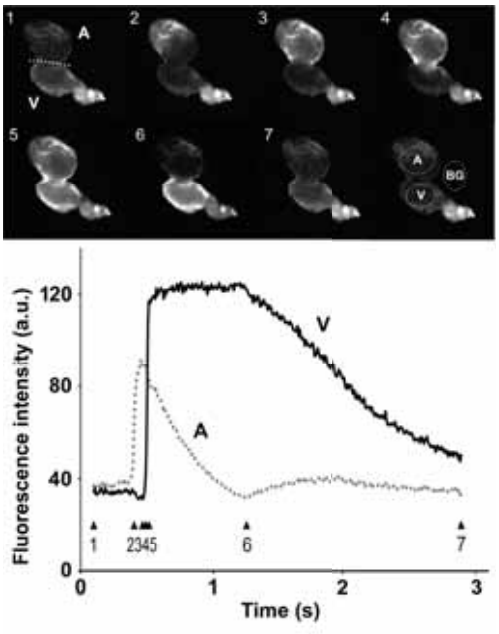

Figure 19. Fluorescent still images from a video of a Fluo-4 Ca^{2+} indicator loaded heart excised from a 2 dpf WT zebrafish. Ca^{2+} transients are imaged during spontaneous beating. Blebbistatin is used to prevent muscle contraction. A = atrium, V = ventricle, the AV junction is marked by a dotted line in image 1), which shows the heart during rest. 2) Ca^{2+} transient propagation initiates at the top of the atrium, indicated by the increase in fluorescence intensity. 3) The entire atrium is activated. 4) After a delay at the AV junction, the activation spreads to the ventricle. 5) The whole heart is now activated. 6) The atrium is quiet again, indicating complete decay of the intracellular Ca^{2+} transient. $[Ca^{2+}]_i$ remains high in the ventricle. 7) Also the ventricle is returning close to resting levels of $[Ca^{2+}]_i$. The chart shows the mean fluorescence intensity plotted over time in two regions of interest, the atrium (A) and the ventricle (V), as shown on the last still image. Background fluorescence values (BG) have been subtracted from the values of traces A and V in the chart. The numbered arrowheads below the traces indicate the timepoints shown in the seven still images on the montage.

3.6.2 Optical action potential recordings

APs were recorded with the same set-up that was used for Ca^{2+} imaging. Zebrafish whole hearts were excised at 4 – 6 dpf and stained with 5 µmol/L voltage-sensitive dye di-4-ANEPPS (Molecular Probes, USA) for 5 min and imaged immediately after. APD was measured from the time of maximal rise slope to the time at 90% repolarization. In each measurement, at least four consecutive APDs were averaged. Two immobilization agents, BDM and blebbistatin, were used at various concentrations. At the used concentrations, these agents had no apparent effect on the results.

4 Statistical analysis (Studies I – IV)

Continuous variables are shown as mean ± either standard deviation or standard error of the mean, as indicated. The significance of differences in normally distributed variables between two groups was calculated with the unpaired student's t-test. The significance of changes within a group was evaluated with the paired student's t-test. Between more than two normally distributed experiments the one-way ANOVA test was used, followed by Scheffe's test. The Wilcoxon signed-rank and Mann-Whitney U tests were used as nonparametric tests. Categorical variables were assessed with the Chi-Square test. No corrections were applied to account for potential inflation due to multiple testing. A P-value ≤ 0.05 was considered statistically significant.

Results

1 STUDY I

1.1 CPVT patients display DADs in MAP recordings

In study I, we examined MAP recordings in 15 CPVT patients with *RyR2* mutations (nine P2328S, five V4653F, and one Q4201R) and 12 healthy subjects. During a bicycle exercise test, all CPVT patients showed polymorphic PVCs or short runs of polymorphic VT. The mean threshold heart rate for ventricular bigeminy was 127±20 bpm. DADs were observed in 3/15 CPVT (two P2328S and one Q4201R) MAPs at baseline and 4/15 (three P2328S and one Q4201R) during epinephrine infusion. None of the five V4653F patients showed DADs. On the surface ECG, DADs coincided with U-waves. Epinephrine increased DAD amplitude, measured normalized to the previous AP amplitude, from 6 to 14%, and the rising slope from 6.7 to 11 mV/s. DADs occasionally triggered PVCs. No DADs were observed in the 12 control patients at baseline or during epinephrine infusion. The three CPVT patients that showed DADs already at baseline conditions had a significantly lower threshold for ventricular bigeminy during the stress test compared to those that showed no DADs (107±21 vs. 131±16 bpm, $P<0.05$). Additionally, one of these CPVT patients occasionally showed two- and three-peaked DADs.

1.2 Cells with mutant RyR2s show increased spontaneous Ca^{2+} release under cAMP stimulation

Expression of WT-, P2328S-, and V4653F-RyR2 in HEK 293 cells resulted in no significant difference in SR Ca^{2+} content (363±68, 299±59, and 274±33 nM), which was measured by high-dose caffeine-induced SR Ca^{2+} release. Under unstimulated baseline conditions, spontaneous Ca^{2+} release events were very rare, with no differences between the groups. Dioctanoyl-cAMP (cAMP analoque with 100-fold higher activity) in three concentrations was given to simulate sympathetic stimulation. Spontaneous Ca^{2+} waves increased in a dose-dependent manner, occurring significantly more in cells transfected with mutant RyR2s. This was observed without a concomitant increase in baseline $[Ca^{2+}]_i$.

2 STUDY II

2.1 Characterization of iPSC lines and cardiomyocytes

IPSC lines were generated from a CPVT patient and from a healthy control subject. The presence of the *RyR2*-P2328S mutation was confirmed in the two CPVT cell lines. All cell lines were morphologically and karyotypically normal. Endogenous pluripotency genes were turned on and expressed at the protein level, and the exogenous, retrovirally encoded reprogramming factors were silenced. Pluripotency of cell lines was further confirmed with teratoma formation *in vivo* and expression of markers from all three germ layers *in vitro*. IPSC lines were differentiated into cardiomyocytes in a co-culture with murine visceral endoderm-like cells. Spontaneously beating cells expressed the cardiac markers troponin T, connexin 43, and α-actinin at the protein level. CPVT and control cell lines showed similar expression levels of genes involved in cardiac Ca^{2+} cycling.

2.2 RyR2 mutant cells show irregular Ca^{2+} transients

Ca^{2+} imaging of spontaneously beating cells was performed. The cells were stimulated with electrical pacing, epinephrine perfusion, and high-dose pulses of caffeine. The observed Ca^{2+} transients were categorized into classes based on regularity of rhythm and transient amplitude (figure 20). In control cells, 8% showed irregular transients at baseline, and during epinephrine perfusion the proportion was 11%, although epinephrine tended to stabilize transient amplitude. Pacing completely abolished irregular rhythm and transient amplitude in control cells. In RyR2-P2328S cells, 14% of cells showed irregular Ca^{2+} release at baseline, and this proportion was slightly attenuated during pacing (10%). Perfusion with epinephrine provoked irregular transients in 29% of cells during spontaneous beating ($P<0.05$ vs. baseline) and in 32% during pacing.

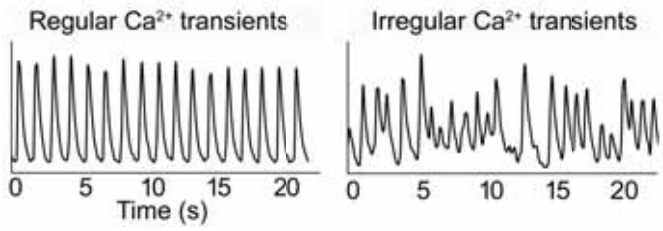

Figure 20. Representative example of regular Ca^{2+} transients in a single cardiomyocyte (left). Both frequency and amplitude are regular and stable. Representative example of irregular Ca^{2+} transients in a single cardiomyocyte (right). This cell is arrhythmic, displaying irregular rhythm and varying amplitude of transients.

2.3 Ca^{2+} cycling balance is altered in RyR2 mutant cells

At baseline, diastolic $[Ca^{2+}]_i$ levels were similar in control and RyR2-P2328S cells. Epinephrine raised the $[Ca^{2+}]_i$ to significantly higher levels in RyR2-P2328S cells than in control cells (1.20±0.11 vs. 0.84±0.03 Fura-2 ratio units, P=0.01). SR Ca^{2+} content, measured as transient amplitude of high-dose caffeine-induced Ca^{2+} release, was lower in RyR2-P2328S cells at baseline (1.00±0.08 vs. 1.62±0.18 Fura-2 ratio units, P=0.0003) and during pacing and simultaneous epinephrine perfusion (1.10±0.13 vs. 1.71±0.40 Fura-2 ratio units, P<0.05). Fractional Ca^{2+} release, referring to the amount of Ca^{2+} released from the SR during normal beating in proportion to the total SR Ca^{2+} store, was higher in RyR2-P2328S cells. This difference was clearest during pacing and simultaneous epinephrine perfusion, when fractional Ca^{2+} release in RyR2-P2328S cells was more than double of that in control cells (66.4±4.9% vs. 29.3±4.9%, P=0.000008).

2.4 In addition to DADs, RyR2 mutant cells display EADs

APs were measured in ventricular-like cells with the perforated patch technique. RyR2-P2328S and control cells showed similar AP morphologies. Three out of 16 control cells showed infrequent single DADs at baseline. No DADs were observed in five control cells during epinephrine perfusion. Six of 14 RyR2-P2328S cells showed occasional DADs at baseline. In 11 RyR2-P2328S cells exposed to epinephrine, six showed no afterdepolarizations, whereas five showed DADs and a subsequent decrease in beating rate. In three RyR2-P2328S cells that did not receive epinephrine, singular EADs were observed (figure 21). All EADs were initiated above -25mV and the maximum EAD amplitude was 45mV. One of these cells also showed DADs and a phase 3 burst episode lasting 20 beats. The EADs during the burst were initiated at -50 mV and were on average 95 mV in amplitude. No EADs or burst activity were observed in control cells.

Figure 21. Patch-clamp recording of membrane potential (V_m) in an iPSC -derived RyR2-P2328S cardiomyocyte. Among normal APs, occasional EADs were observed, as indicated by the arrow.

2.5 Changes corresponding to cellular abnormalities are observed in the clinical MAP and ECG recordings

The MAP recordings reported in study I were examined for changes corresponding to the findings in the iPSC-derived cardiomyocyte model. In addition to previously reported DADs, occasional EADs were observed in MAP recordings of CPVT patients, but not in MAP recordings of healthy controls. To avoid confusion between the second peak of a T-wave and a U-wave, 24h ECGs of 19 CPVT patients and 19 matched healthy controls were examined for the simultaneous occurrence of T1-, T2- (corresponding to EAD), and U-waves (corresponding to DAD). Such traces were found in ECGs of only CPVT patients.

3 STUDY III

3.1 Isoproterenol increases variability of Ca^{2+} transients in RyR2 mutant iPSC-derived cardiomyocytes

Ca^{2+} transients were measured in Fluo-4 loaded spontaneously beating cells. RyR2-P2328S cells had shorter transient durations during baseline and isoproterenol perfusion. STV of the Ca^{2+} transient rise time, decay time, duration at 50% amplitude, amplitude, and area were quantified from recordings of 30 consecutive transients during baseline and perfusion with isoproterenol. Isoproterenol failed to significantly increase STV of any of the Ca^{2+} transient parameters in control cells, whereas in RyR2-P2328S cells there was a significant increase in STV of Ca^{2+} transient duration at 50% amplitude, amplitude, and area, all of which approximately tripled compared to baseline values. STV of transient decay was similar in control and RyR2-P2328S cells, suggesting similar SERCA2a function. Alternans of Ca^{2+} transient amplitude was rare, occurring during isoproterenol perfusion in 3.2% of control cells and in 4.8% of RyR2-P2328S cells. This difference was not statistically significant. Taken together, β-adrenergic stimulation induces non-alternating variability of intracellular Ca^{2+} transients in RyR2-P2328S cells, which may affect membrane potential and be reflected on the surface ECG.

3.2 Epinephrine decreases the rate of depolarization in RyR2 mutant cardiomyocytes

APs in iPSC-derived cardiomyocytes were recorded using patch-clamp. STV of APD50 and APD90 showed large variation between cells. Values of STV

APD90 were similar in control and RyR2-P2328S cells (11.0 ± 2.6 ms vs. 18.0 ± 6.4 ms, *P*=NS, control N=4, RyR2-P2328S N=8), and showed similar responses to epinephrine. APD90 alternans was similar, observed during epinephrine in 1/4 of control and 2/8 of RyR2-P2328S cells. Epinephrine decreased maximal AP upslope velocity (dV/dt) (V-max) in RyR2-P2328S cells, whereas V-max remained unchanged in control cells (-19.6 ± 6.9% vs. +3.2 ± 1.3%, P<0.05).

3.3 Decreased rate of depolarization in response to epinephrine is reproduced in clinical MAP recordings of CPVT patients

MAPs recorded from the right ventricular septum in 13 CPVT patients with a *RyR2*-P2328S mutation and four healthy controls were evaluated. For assessing variability and alternans, sufficiently long MAP recordings with a stable cycling interval were available in three CPVT patients and three controls. STV of MAP duration (MAPD)90 was similar in control and CPVT patients at baseline and during epinephrine perfusion (control baseline 1.90 ± 0.37 ms, control epinephrine 2.99 ± 0.68 ms, CPVT baseline 2.45 ± 0.68 ms, CPVT epinephrine 3.22 ± 0.67 ms). MAPD alternans was observed during epinephrine perfusion in all three controls and in 2/3 of CPVT patients. In CPVT patients, epinephrine infusion decreased maximal MAP upslope velocity (V-max), whereas in controls MAP V-max increased compared to baseline (-30.4 ± 11.2% vs. +31.4 ± 27.7%, P<0.05).

3.4 CPVT patients show heart rate dependent changes in QT interval and age dependent changes in ECG R-upslope

24h ECGs of 19 CPVT patients (13 *RyR2*-P2328S and six *RyR2*-V4653F) and 19 age and gender-matched controls were studied. Mean 24h QT intervals were similar in CPVT patients and controls. CPVT patients tended to have shorter mean QT intervals at RR intervals 400 – 600 ms, and the difference reached significance at approximately half of measured timepoints, the maximal difference was 40 ms at RR interval 400ms (P<0.05). To examine whether the decreased rate of depolarization observed in cellular and MAP recordings is reflected on the surface ECG, we measured the QRS duration and determined the maximal R-spike upslope velocity (V-max). QRS durations were similar in controls and CPVT patients (91±11 vs. 95±14 ms, *P*=NS). Mean 24h values of R-upslope V-max were 4 – 7 mV/s lower in CPVT patients compared to controls at all RR intervals 500 – 1200 ms, but this trend remained

statistically insignificant. Interestingly, when the subjects were divided into two groups based on the median age of 30, those CPVT patients older than 30 years of age showed significantly reduced R-upslope V-max compared to matched controls (17 ± 2.5 mV/s vs. 28 ± 4.2 mV/s, $P<0.05$), as well as compared to CPVT patients younger than 30 years of age (17 ± 2.5 mV/s vs. 38 ± 3.7 mV/s, $P<0.001$). However, QRS durations remained similar in both age groups.

3.5 ECGs of CPVT patients show increased non-alternating variability of repolarization

Of these 19 CPVT patients, 13 had a history of exercise-related syncope or cardiac arrest and six were event-free. Using custom-made software, beat-to-beat variability of repolarization was quantified for each beat as STV of the QT-end interval (STV QTend) and of the QT-apex interval (STV QTapex) from 30 preceding consecutive beats. Automated detection of the T-wave apex was more reliable than that of T-wave end, which occasionally merged with a T2- or U-wave. Compared to controls, STV QTapex values were 1.4 – 2.0 ms higher in CPVT patients at all RR intervals 500 – 1200 ms (plotted every 100 ms), and this difference was significant at RR intervals 510 – 1180 ms. STV QTend values were 1.5 – 2.7 ms higher in CPVT patients, the difference being significant at 640 – 1110 ms. When CPVT patients were grouped according to history of arrhythmic events into symptomless, syncope, and VF/SCD groups, there was a trend of increasing mean STV QTapex and STV QTend with increasing severity of arrhythmic symptoms. CPVT patients with a history of VF/SCD had higher STV QTapex than healthy controls (6.7 ± 0.7 ms vs. 4.5 ± 0.3 ms, $P<0.01$). At higher heart rates, CPVT patients with a history of arrhythmic events showed a trend of higher mean STV QTapex than those without arrhythmic events. This difference increased from 0.6 ms at RR interval 1200 ms to 2.9 ms at RR interval 500 ms, but remained statistically insignificant. QTVI was similar in controls and CPVT patients.

3.6 CPVT patients show slightly lower alternans of repolarization

Alternans of repolarization was determined from the same 24h ECGs with the MMA method and the CDM method, which is a modification of the spectral method. Both methods gave lower values of TWA in CPVT patients at all RR intervals (500 – 1200 ms), the difference to controls was significant at RR intervals 510 – 680 ms (MMA) and 550 – 670 ms (CDM). The absolute differences in

TWA were 3.7 – 6.7 µV (MMA) and 1.7 – 4.5 µV (CDM). Neither method distinguished CPVT patients with a history of arrhythmic events from event-free patients at any RR interval (500 – 1200 ms). Interestingly, when CPVT patients were grouped according to history of arrhythmic events, an opposite trend to that in STV of QT was found. Mean TWA tended to decrease with increasing severity of arrhythmic symptoms, but the differences failed to reach statistical significance. UWA was lower in CPVT patients at RR intervals 500 – 600 ms with the MMA method and similar in controls and CPVT patients with the CDM method. Relevant results in 24h ECGs are summarized in table 3.

Table 3. Results of selected parameters from 24h ECGs.

Measure	Control (N=19)		CPVT (N=19)		P value
	mean	S.D.	mean	S.D.	
Mean RR interval (ms)	**802**	80	**842**	96	0,168
Mean QT-end interval (ms)	**393**	21	**394**	28	0,896
Mean QT-apex interval (ms)	**308**	20	**309**	22	0,919
Mean STV QTend (ms)	**5,5**	1,6	**6,9**	2,3	*0,031*
Max STV QTend (ms)	**13**	5,4	**15**	5,5	0,427
Mean STV QTapex (ms)	**4,5**	1,2	**5,9**	2,2	*0,024*
Max STV QTapex (ms)	**8,6**	3,5	**11**	4,3	*0,049*
QTVI (T-end)	**-0,91**	0,25	**-0,86**	0,33	0,609
Mean T-wave alternans (MMA) (µV)	**31**	8,9	**25**	6,2	*0,020*
Max T-wave alternans (MMA) (µV)	**48**	14	**40**	8,6	*0,037*
Mean T-wave alternans (CDM) (µV)	**10**	4,8	**8,3**	3,4	0,116
Max T-wave alternans (CDM) (µV)	**17**	6,8	**14**	4,8	0,151
Mean U-wave alternans (MMA) (µV)	**27**	6,7	**24**	6,9	0,120
Max U-wave alternans (MMA) (µV)	**41**	9,4	**37**	8,5	0,153
Mean U-wave alternans (CDM) (µV)	**5,4**	1,7	**5,0**	1,5	0,553
Max U-wave alternans (CDM) (µV)	**8,7**	2,3	**8,4**	4,3	0,793

4 STUDY IV

4.1 Polycystin-2 is expressed in the heart

WT zebrafish express the PC2 protein throughout their hearts, where it co-localizes with SERCA2a and Binding immunoglobulin Protein (BiP) predominantly to the SR. *Pkd2* mutants lack expression of PC2, as do 2 dpf WT fish injected with a morholino to silence *pkd2*.

4.2 Cardiac function is weakened in *pkd2* mutant zebrafish

Pkd2 mutant embryos showed lower heart rates than WT fish, and this difference increased with time. We quantified stroke volume by examining aortic blood flow at 3 dpf, and found significantly lower stroke volumes in *pkd2* mutant fish. The resulting cardiac output was nearly halved in *pkd2* mutants compared to WT fish (9.8±0.7 nL/min vs. 16.7±1.1 nL/min, $P<0.001$). However, peak systolic velocities of erythrocytes in the proximal aorta were similar in WTs and *pkd2* mutants (1.94±0.05 mm/s vs. 1.71±0.09 mm/s, $P>0.05$).

The fish were observed until 9 dpf. *Pkd2* mutant fish showed increasing edema that concentrated to the abdomen and pericardium. By 9 dpf, 77% of *pkd2* mutants showed edema. After 3 dpf, *pkd2* mutant fish started developing AV block, where approximately 1/3 of atrial impulses failed to induce ventricular contraction. By 9 dpf, 28% of *pkd2* mutants showed AV block. The AV block did not develop secondary to the edema, as some arrhythmic fish lacked edema. No edema or arrhythmias were observed in WT fish. *Pkd2* mutants and WT fish had similar delays in propagation of the Ca^{2+} wave from atrium to ventricle. Heart sizes were also similar. We did not observe significant AV valve defects or regurgitation.

4.3 *Pkd2* mutant zebrafish hearts display impaired Ca^{2+} cycling

We performed Ca^{2+} imaging on Fluo-4 loaded excised whole hearts at 3 dpf. The duration of ventricular Ca^{2+} transients in *pkd2* mutant fish was longer than in WT fish (1.40±0.19s vs. 1.03±0.09s, $P<0.05$). Transient rise time was doubled in the ventricles (179±15ms vs. 82±15ms, $P<0.001$), and also transient decay was significantly prolonged (567±60 ms vs. 378±25ms, $P<0.01$). Upon electrical pacing at 120 bpm, *pkd2* mutant hearts were prone to develop Ca^{2+} transient amplitude alternans. 15% of *pkd2* mutant hearts had alternans, whereas no alternans was observed in WT hearts. In *pkd2* mutant ventricles, pacing increased diastolic Ca^{2+} levels in the cytosol (+74±20%, $P<0.01$ vs.

baseline), whereas in WT ventricles diastolic Ca^{2+} levels were unchanged by pacing (+22±10%, P>0.05 vs. baseline). These responses to pacing were significantly different between *pkd2* mutant and WT fish (P<0.05). Also ventricular SR Ca^{2+} stores, measured as transient amplitude of caffeine-induced Ca^{2+} release, were found to be reduced in *pkd2* mutants compared to WT fish (F/F_0: 2.47±0.54 vs. 4.42±0.91, P<0.05). Quantitative reverse transcription PCR was performed to quantify mRNA levels of Ca^{2+} cycling proteins that might explain the observed functional differences between *pkd2* mutants and WT fish. We found no differences in the mRNA levels of RyR2a, RyR2b, SERCA2a, IP3R1, IP3R2, and IP3R3 that are likely to explain the functional differences. The results indicate that PC2 is necessary for normal Ca^{2+} cycling in the heart.

4.4 Ventricular APD is shortened in *pkd2* mutants

Optical AP measurements were performed in di-4-ANEPPS loaded excised whole hearts of 4 – 6 dpf fish. Compared to WT fish, *pkd2* mutants showed shorter APD during spontaneous beating (in ms: 272±8 vs. 233±8, P<0.01) and consistently during all frequencies of pacing, faster AV conduction (in ms: 83±4 vs. 65±4, P<0.01), and capture at a higher maximum frequency of pacing (in bpm: 161±12 vs. 207±3, P<0.01).

4.5 Prevalence of dilated cardiomyopathy is high in ADPKD patients

We examined the Mayo ADPKD Mutation Database for an association between ADPKD and IDCM. We focused on genotyped ADPKD patients with known *PKD* mutations. Of the 307 PKD1 patients, seven patients from seven different families had a diagnosis of IDCM. There were 67 PKD2 patients, of whom six patients from four families had a diagnosis of IDCM. All *PKD2* mutations in these four families are predicted to lead to truncation of the PC2 protein. Additionally, two other PKD2 patients from the same families had subclinical or stress-induced DCM. One family member had a diagnosis of IDCM in the absence of ADPKD. Of the six PKD2 IDCM patients, at the time of IDCM diagnosis four were normotensive, five had serum creatinine values 80 – 115 µmol/L indicating preserved kidney function, four had conduction abnormalities, and five had ventricular extrasystoles. One patient received a heart transplant due to IDCM. Among these six patients, the mean age at diagnosis was 52 for ADPKD, 56 for IDCM , and 60 for hypertension.

Discussion

1 Main findings

In study I we recorded right ventricular MAPs in CPVT patients carrying *RyR2* mutations, and in control subjects. CPVT patients displayed DADs that increased in magnitude in response to epinephrine infusion. These DADs were reflected as U-waves on the surface ECG, and occasionally triggered APs and PVCs. No DADs were observed in MAP recordings of control patients. Intracellular Ca^{2+} handling was studied in HEK cells, which had been transfected with WT or mutant RyR2s. No spontaneous Ca^{2+} release events were observed under baseline conditions. Sympathetic stimulation, which was mimicked by bathing the cells in a cAMP-analoque, resulted in increased spontaneous Ca^{2+} release events in cells expressing mutant RyR2s compared to cells expressing WT RyR2.

In study II we generated iPSC lines from skin fibroblasts of a CPVT patient carrying a *RyR2*-P2328S mutation, and from a healthy control. We then investigated cellular electrophysiology and intracellular Ca^{2+} handling in cardiomyocytes differentiated from these iPSC lines. In patch-clamp studies RyR2-P2328S cells exhibited DADs, as well as EADs. Corresponding changes were present in clinical MAP recordings of CPVT patients. Control cells displayed rare single DADs and no EADs. No EADs or DADs were observed in MAP recordings of control subjects. At baseline Ca^{2+} transients were similar in WT and RyR2-P2328S cells. Stimulation with epinephrine increased irregularity of rhythm and amplitude of Ca^{2+} transients in RyR2-P2328S cells, and resulted in elevation of diastolic $[Ca^{2+}]_i$. SR Ca^{2+} stores were lower in RyR2-P2328S cells, and the proportion of SR Ca^{2+} released per beat was higher in RyR2-P2328S cells, most notably during pacing under epinephrine perfusion.

In study III we quantified the variability of Ca^{2+} release by calculating STV of Ca^{2+} transients in iPSC-derived cardiomyocytes, using the same cell lines as in study II. Ca^{2+} transients were measured during baseline and isoproterenol perfusion. β-agonists increased STV of Ca^{2+} transients in RyR2-P2328S. In patch-clamp measurements, β-agonists decreased the rate of depolarization in RyR2-P2328S cells, but not in control cells. Clinical MAP recordings reproduced the depolarization changes observed in the cell model, with decreased rates of depolarization in response to β-agonists only in CPVT patients. In 24h ECG recordings of CPVT patients and matched controls, the rate of depolarization was evaluated by examining maximal R-upslope velocity. CPVT patients had a trend toward lower maximal R-upslope velocity, which failed to reach statis-

tical significance. However, the maximal R-upslope velocity decreased notably in older CPVT patients compared to young CPVT patients and to age-matched controls. To assess variability in 24h ECGs, STV of the QT interval was calculated. STV of QT was higher in CPVT patients compared to controls, and highest in those CPVT patients that had a history of severe arrhythmic symptoms. In contrast, TWA was higher in control subjects than in CPVT patients. The difference in TWA was clearest at high heart rates.

Based on the findings in studies I – III, various potential arrhythmia mechanisms of CPVT were identified. They are summarized in figure 22.

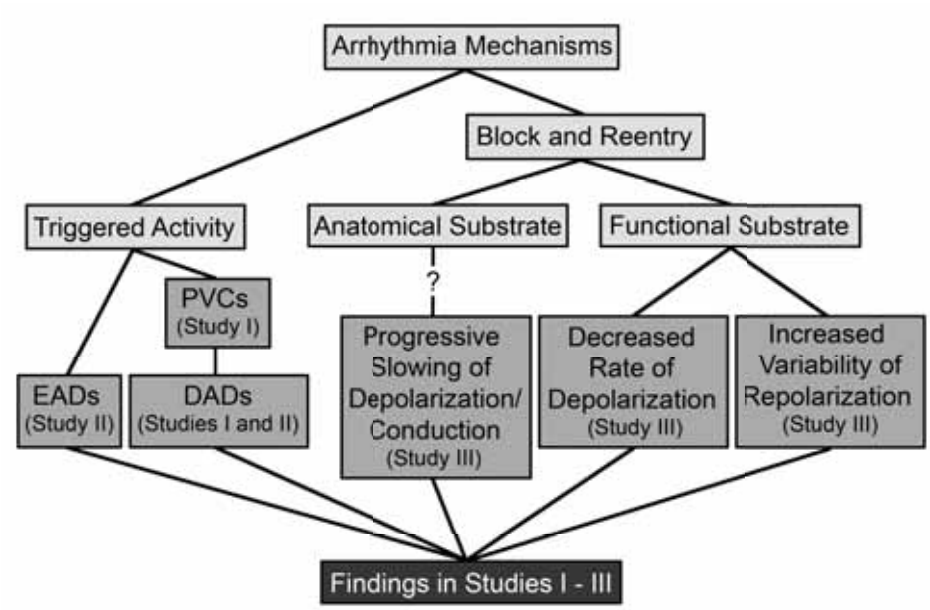

Figure 22. Discovered potential arrhythmia mechanisms of CPVT. The '?' refers to a hypothecial anatomical substrate, for example fibrosis, which needs to be investigared further.

In study IV, cardiac function was investigated in a zebrafish model of PKD that lacks expression of the PC2 protein. *In vivo* studies revealed reduced cardiac output, edema, and arrhythmias in the *pkd2* mutant fish, indicating heart failure. *Ex vivo* Ca^{2+} imaging of zebrafish hearts showed impaired Ca^{2+} cycling in the *pkd2* mutant fish, characterized by slow transients, Ca^{2+} alternans, and poor tolerance when stressed with pacing. Examination of the Mayo ADPKD Mutation Database for an association between ADPKD and IDCM showed that IDCM is common among ADPKD patients, especially those patients with *PKD2* mutations.

2 Relation to previous studies

2.1 Study I

Study I was the first to show DADs in CPVT patients with *RyR2* mutations. A case report published a decade earlier, when the genetic background of CPVT was unknown, showed similar findings in a 14-year-old male (Nakajima et al. 1997). In our study CPVT patients displayed DADs with concomitant U-waves and occasional PVCs. Cells expressing two mutant RyR2s showed spontaneous Ca^{2+} release events during low-dose cAMP stimulation. Our results suggest mutant RyR2s induce DADs and triggered activity by spontaneous SR Ca^{2+} release under conditions of sympathetic stimulation. In unstimulated baseline conditions, spontaneous Ca^{2+} release events were rare. This differs from a previous report where a gain-of-function mutation in *RyR2* led to frequent spontaneous Ca^{2+} waves (Jiang et al. 2002b). This contrasting result may be due to differences in experimental protocol, e.g. expression levels of transfected RyR2 channels, or sensitivity and duration of Ca^{2+} imaging. Alternatively, the result might be explained by a mutation-specific difference in basal Ca^{2+} activity. Diastolic $[Ca^{2+}]_i$ levels remained essentially constant during cAMP stimulation, indicating that $[Ca^{2+}]_i$ alone is unlikely to account for the increase in spontaneous Ca^{2+} release. Our results suggest that the increased propensity to Ca^{2+} waves in the RyR2 mutants is explained by lowering of the Ca^{2+} release threshold due to increased sensitivity to cytosolic or luminal (SR) Ca^{2+}.

Marks and colleaques have found that the RyR2-calstabin2 interaction is a mechanistically important regulator of RyR2 Ca^{2+} release (Lehnart et al. 2004b, Wehrens et al. 2005). Interestingly, the same three *RyR2* mutations as in our study (P2328S, V4653F, and Q4201R) showed decreased calstabin2 binding and the experimental drug JTV519 normalized RyR2 channel function by binding calstabin2 to RyR2 (Lehnart et al. 2004a). We transfected HEK293 cells with mutant and WT RyR2, but not with calstabin2. These cells lack expression of calstabin2 (Gaburjakova et al. 2001, Zissimopoulos et al. 2005, Xiao et al. 2007). Thus, in our model the increased propensity of mutant RyR2 for spontaneous Ca^{2+} release was independent of calstabin2. While we did not study the role of calstabin2, many others have addressed these questions. Compared to WT RyR2, several RyR2 mutants showed similar or increased binding to calstabin2 under baseline and oxidized conditions (Zissimopoulos et al. 2009). In separate work, β-adrenergic induced hyperphosphorylation of

RyR2 led to increased SR Ca^{2+} release in cells with mutant RyR2, despite equivalent dissociation of calstabin2 from RyR2 as in cells with WT RyR2 (George et al. 2003). Furthermore, stimulation with caffeine, which also increased Ca^{2+} release in cells with mutant RyR2, had no effect on the extent of the RyR2-calstabin2 interaction. The authors concluded that altered regulation of RyR2 by calstabin2 is unlikely to explain the functional defect in mutant RyR2. Studies using various models have given contrasting results. Thus the role of calstabin2 in RyR2 Ca^{2+} release remains incompletely understood.

Because the MAP catheter records electrical activity from a region of a few millimeters in its vicinity, our MAP recording from a single site per patient will likely have missed the majority of DADs generated further away in the ventricles (Franz 1999). This is likely to explain the lack of an increase in DAD amplitude associated with a premature ventricular beat. DADs were observed in three CPVT patients consistently even at baseline. The magnitude of DADs increased with epinephrine stimulation, increasing the likelihood for reaching threshold voltage for triggering ectopic beats. This is supported by the finding that patients who showed DADs at baseline developed ventricular extrasystoles at a significantly lower heart rate than those with no DADs at baseline. Under conditions of Ca^{2+} overload, polymorphic VT may be caused by DAD-mediated triggered activity arising from multiple locations in the ventricles (Katra et al. 2005). Although frequent DAD-mediated triggered activity may explain slow PVT, its degeneration to hemodynamically unstable rapid VT and VF is likely to involve additional mechanisms. Epicardial myocytes are the last to depolarize but the first to repolarize. Therefore, triggered beats in the epicardium most clearly increase spatial heterogeneity of repolarization, forming a functional substrate that predisposes to conduction block and reentry, which underlie the transition from slow to rapid VT that may degenerate further into VF (Nam et al. 2005).

2.2 Study II

The recent discovery of iPSCs derived from human adult somatic cells, and their differentiation into cardiomyocytes *in vitro*, has opened novel possibilities to investigate the mechanisms of CPVT in a patient-specific manner. This avenue has been enthusiastically pursued, as evidenced by the flood of reports using iPSCs to model CPVT in recent years (Fatima et al. 2011, Itzhaki et al. 2012, Jung et al. 2012, Novak et al. 2012, Di Pasquale et al. 2013, Zhang et al. 2013a).

The strength of study II is the identification of EADs as a novel manifestation in CPVT. Furthermore, the results of Ca^{2+} imaging experiments suggest Ca^{2+}-mediated mechanisms behind the EAD-formation. Importantly, corresponding changes in electrical instability are also manifested in clinical MAP and ECG recordings.

As discussed above, diastolic release of Ca^{2+} from the SR underlies DADs, which may generate triggered arrhythmias (Schlotthauer et al. 2000). We observed disturbances in intracellular Ca^{2+} release in RyR2-P2328S cells upon stimulation with epinephrine, correlating with the clinical manifestation of arrhythmias under conditions of physical or mental stress. Epinephrine perfusion transferred the balance of Ca^{2+} cycling more toward Ca^{2+} release, as indicated by increased diastolic $[Ca^{2+}]_i$, decreased SR Ca^{2+} content, and increased fractional Ca^{2+} release. It must be acknowledged that the measurement of diastolic $[Ca^{2+}]_i$ is technically challenging, therefore these results between different cells have to be interpreted with caution. Overall, our results demonstrate increased sensitivity of Ca^{2+} release in mutant RyR2. This finding is essential in explaining the phenotypic changes observed in CPVT.

The long established view was that EADs develop under conditions of APD prolongation, such as LQT2, when the LTCCs have sufficient time to recover from inactivation and reactivate while the membrane is still depolarized enough (January et al. 1992). However, recent findings highlight the roles of cytoplasmic Ca^{2+} overload and spontaneous Ca^{2+} release in EAD formation (Volders et al. 2000, Xie et al. 2009). The result of this "excess" Ca^{2+} in the cytosol is the activation of NCX, resulting in inward currents manifesting as afterdepolarizations. Viewed in this light, the mechanistic distinction between EADs and DADs is not necessarily great. Thus, the observation of EADs in RyR2-P2328S cells, though novel, cannot be considered surprising. Indeed, previous findings in ECG recordings of CPVT patients suggested the possibility of EAD-mediated triggered activity (Viitasalo et al. 2008).

Overall, the iPSC-derived cardiomyocyte model of CPVT recapitulated the arrhythmic changes observed clinically. This confirms the usefulness of the model in pathomechanistic studies, and suggests its applicability to screening and optimization of drugs.

2.3 Study III

In the third study we investigated depolarization, and repolarization variability and alternans in CPVT using *in vivo* and *in vitro* methods. IPSC-derived RyR2 mutant cardiomyocytes showed increased variability of Ca^{2+} transients upon β-agonist stimulation. Results of clinical MAP recordings were in line with the *in vitro* findings. Importantly, these results were consistent in 24h ECGs, which showed increased variability of the QT interval but decreased repolarization alternans in CPVT patients.

STV of APD failed to distinguish iPSC-derived CPVT cardiomyocytes from control cardiomyocytes. Similarly, STV of MAPD failed to distinguish CPVT patients from healthy controls. Nevertheless, there was a consistent trend of higher STV of APD and MAPD in CPVT cardiomyocytes and patients compared to controls. However, the small number of cells and patients precludes drawing definite conclusions based on these data alone.

As was reported in study II, during epinephrine perfusion irregular Ca^{2+} transients were observed in approximately 29% of RyR2 mutant cells and 11% of control cells. On the other hand, Ca^{2+} transient amplitude alternans was comparatively rare, observed in less than 5% of cells during epinephrine perfusion. Based on the findings of abundant irregular non-alternating Ca^{2+} release in the cell model of CPVT, we hypothesized that this variability might be reflected on the ECG in CPVT patients. Beat-to-beat variability measured over periods of 30 beats was chosen to quantify such variability. STV measures rapid changes, occurring from one beat to another, whereas QTVI measures slower changes that do not consider the beat-to-beat order of these changes (Oosterhoff et al. 2011). STV QTapex and STV QTend were high in CPVT patients, whereas QTVI was similar to control patients, suggesting that the changes in QTapex and QTend in CPVT patients are rapid irregular events. This is in line with the changes observed in the cell model. Consistently, transient QT prolongation after rapid pacing has been associated with arrhythmia induction in CPVT patients (Nof et al. 2011).

To our knowledge, non-alternating beat-to-beat variability of repolarization is previously uninvestigated in CPVT patients. It has recently been linked to ventricular arrhythmia in patients with LTQ2 (Nemec et al. 2010) and in a mouse model lacking CASQ2 (Mezu et al. 2012). These studies suggest aberrant intracellular Ca^{2+} handling as a central pathomechanism, indicating poten-

tial mechanistic similarities with *RyR2* mutations (Antoons et al. 2010, Brette 2010). Additionally, mice harboring *RyR2* mutations showed increased non-alternating variability of Ca^{2+} transients at the organ level (*ex vivo*) in response to adrenergic stimulation (Chen et al. 2012). This was associated with corresponding changes in AP morphology. More supportive evidence comes from a recent study that found increased isoproterenol-induced spontaneous Ca^{2+} release by RyR2s to underlie increased beat-to-beat variability of repolarization that could be rescued by inhibiting spontaneous SR Ca^{2+} release (Johnson et al. 2013). These changes were independent of APD. Likewise, a study in DCM patients with moderate heart failure found STV of the QT interval to be higher than in controls, and to be the strongest indicator of a history of VT, independent of QT interval prolongation (Hinterseer et al. 2010). Indeed, such non-alternating variability or repolarization may reflect different underlying phenomena than TWA. For example, beat-to-beat variability of repolarization increased, but TWA remained negative in a pig model of myocardial infarction (Flore et al. 2011). Pacing induced TWA similarly in pigs with myocardial infarction and sham pigs, whereas VF was inducible in 25% of pigs with myocardial infarction and none of the sham-operated pigs.

In the past decade, microvolt TWA has been studied in numerous patient groups. Although TWA on the surface ECG has been found to predict ventricular arrhythmias, consensus on its clinical applicability remains unestablished (Calo et al. 2011, Gupta et al. 2012). Until now TWA remains poorly investigated in CPVT patients. One study found UWA in one CPVT patient following rapid pacing, and in another following an exercise stress test (Aizawa et al. 2006). Murine hearts hetero- and homozygous for the RyR2-P2328S mutation were evaluated *ex vivo* for MAPD alternans during rapid pacing and epinephrine (Sabir et al. 2010). The authors saw higher MAPD alternans in homozygous mice during epinephrine infusion and pacing at short cycling intervals, and conclude that their findings confirm an alternans phenotype in the RyR2-P2328S murine heart. However, it remains unclear why the group with the highest proportion of observed arrhythmias was WT mouse hearts receiving epinephrine + propranolol or why in homozygous RyR2-P2328S mouse hearts receiving propranolol, the epinephrine stress test increased observed arrhythmias, but approximately halved the alternans magnitude at the fastest cycling interval. The conclusion reached by the authors contradicts our findings. In addition to interpretation of data, this opposing result may be explained by differences in pacing and drug protocols, and by differences between mice and

humans, exemplified by heart rates that in mice are 6-fold compared to humans.

At slow and moderate heart rates TWA was similar in CPVT patients and controls. At higher heart rates, TWA was higher in controls, measured with both MMA and CDM methods. This may be related to shortened and reduced refractoriness of mutant RyR2s (Györke 2009). Alternans is caused by an imbalance in Ca^{2+} cycling, due to abnormal release and/or reuptake of Ca^{2+} (Laurita et al. 2008a). Gain-of-function mutations in RyR2, the main Ca^{2+} release channel, may thus enable faster cycling of Ca^{2+} and decrease the likelihood of developing alternans. Most available evidence supports this hypothesis. Drugs that render the SR leaky by increasing RyR2 open probability decrease alternans in normal and failing rat hearts (Dumitrescu et al. 2002). In rat ventricular myocytes, decreasing RyR2 open probability promotes the development of alternans (Diaz et al. 2002). This is associated with prolongation of Ca^{2+} transient rise and decay times. Consistent with this finding, compared to control cells we saw significantly faster rise and decay times of Ca^{2+} transients in RyR2 mutant cells. In line with this, mice lacking CASQ2 show faster Ca^{2+} transient rise times, shortened RyR2 refractoriness, reduced Ca^{2+} alternans, and lower TWA (Kornyeyev et al. 2012). Also modeling studies find a causal relationship between increased RyR2 refractoriness and Ca^{2+} alternans (Alvarez-Lacalle et al. 2013). Furthermore, upon rapid pacing, canine transmural ventricular wedge preparations show spontaneous Ca^{2+} release and DADs most often endocardially, but the observed Ca^{2+} alternans does not correlate with these sites of spontaneous Ca^{2+} release (Katra et al. 2005). However, also contrasting findings have been reported. Calstabin2-deficient mice showed MAP alternans that closely associated with bidirectional VT, suggesting that both increased and decreased RyR2 activity may result in alternans (Lehnart et al. 2006). In addition to the findings discussed above, the lower TWA observed in the CPVT patients at high heart rates may be explained by interference to the alternating pattern by increased non-alternating beat-to-beat variability of repolarization, which might have reduced the occurrence and/or decreased the magnitude of alternans.

Upon examining depolarization, we found that stimulation with epinephrine decreased AP upslope velocity (V-max) significantly in RyR2 mutant cells and MAP recordings of CPVT patients, whereas in control cells and patients V-max remained unchanged. A similar finding was recently reported in homozygous RyR2-P2328S mouse hearts (Zhang et al. 2013b). Additionally, the au-

thors found decreased epicardial conduction velocity that associated with arrhythmia. QRS duration was similar in control and RyR2 mutant mice at baseline and in response to isoproterenol+caffeine. This is consistent with our finding of similar QRS durations in controls and CPVT patients.

We found the reduction of V-max in single mutant RyR2 cells in response to epinephrine to be relatively smaller than that observed in the clinical MAP recordings. As the MAP catheter records activity from a region of a few millimeters, this greater reduction in V-max may be due to decreased conduction velocity within the recording area. At the cellular level V-max is decreased by the inhibitory effect of high $[Ca^{2+}]_i$ on I_{Na} (Casini et al. 2009). In study II, we found higher $[Ca^{2+}]_i$ in RyR2 mutant cells during adrenaline perfusion, suggesting this may have contributed to the observed decrease in V-max at the level of the single cardiomyocyte, and perhaps also indirectly to conduction between cells. However, because we did not measure I_{Na} directly, only cautious interpretations can be made based on these results alone. Additionally, high $[Ca^{2+}]_i$ is known to promote closure of gap juctions and thus impair cell-to-cell conduction (Kurebayashi et al. 2008). Importantly, the authors found that this propagation delay caused beat-to-beat variability in conduction and Ca^{2+} transients. Therefore it is reasonable to hypothesize that conduction delay under conditions of high $[Ca^{2+}]_i$ may provide an arrhythmogenic substrate for block and reentry in CPVT, possibly contributing to degeneration of slow VT to rapid VT and VF.

On the ECG, R-upslope V-max was similar in controls and CPVT patients, though the trend toward lower R-upslope V-max in CPVT patients is consistent with the findings of decreased AP and MAP upslope V-max observed in CPVT cells and patients, respectively. Interestingly, there was a marked reduction in R-upslope V-max in older CPVT patients, suggesting potential disease progression. Such reduction in conduction velocity may involve fibrosis following the death of cardiomyocytes. As discussed, intracellular Ca^{2+} overload can lead to cell death and fibrosis. In addition to the high $[Ca^{2+}]_i$ observed *in vitro* in CPVT cardiomyocytes, the shortened QT interval observed in CPVT patients at high heart rates is a finding indirectly suggesting the possibility of high $[Ca^{2+}]_i$ *in vivo*. High $[Ca^{2+}]_i$ may lead to shortened QT interval by more rapid LTCC inactivation resulting in shortening of APD. Furthermore, leaky RyR2s are also known to contribute to myocardial remodelling and fibrosis (Fauconnier et al. 2011, Sedej et al. 2013). Additionally, the lack of CASQ2, which leads to a CPVT phenotype, has recently been associated with

increased fibrosis (Glukhov et al. 2013). Such fibrosis may increase the likelihood of sustained arrhythmias by forming an anatomical substrate for reentry.

2.4 Study IV

In study IV, the focus on the role of Ca^{2+} is shifted from arrhythmias to heart failure. Using a zebrafish model lacking the PC2 protein, we described weakened cardiac function and showed underlying impairment in intracellular Ca^{2+} cycling. The clinical significance of these findings is supported by the high prevalence of IDCM among patients with *PKD2* mutations.

Young normotensive ADPKD patients with preserved renal function show diastolic ventricular dysfunction (Oflaz et al. 2005). Our findings are in agreement with this, as most PKD2 patients had normal blood pressure and kidney function at the time of IDCM diagnosis. Diastolic dysfunction was also hypothesized as a possible mechanism behind heart failure in *pkd2* knockout mice, which die before parturition (Wu et al. 2000). Altered Ca^{2+} handling is implicated in diastolic dysfunction, which is characterized by reduced cardiac output and prolonged relaxation (Periasamy et al. 2008). Several findings in the zebrafish model indicate a predominantly diastolic mechanism of heart failure. Peak systolic flow velocity in the aorta was maintained in *pkd2* mutant fish, although cardiac output was almost halved compared to WT fish. The prolongation of ventricular Ca^{2+} transients in the *pkd2* mutants was mainly due to slow transient decay (approximately +200 ms in *pkd2* mutants), i.e. slow relaxation. Furthermore, preservation of normal heart size, but poor ability to cycle Ca^{2+} when stressed with pacing, point towards diastolic dysfunction in the *pkd2* mutant fish (Chatterjee et al. 2007).

Defects in intracellular Ca^{2+} handling are known to underlie development of DCM. Impaired reuptake of cytosolic Ca^{2+} to the SR and therefore prolongation of Ca^{2+} transient decay have been shown to cause DCM and heart failure (Schmitt et al. 2003). Also abnormal release of Ca^{2+} from the SR is implicated in DCM. *RyR2* mutations that reduce the threshold concentration of luminal SR Ca^{2+} at which RyR2 terminates Ca^{2+} release, are associated with increased fractional Ca^{2+} release and DCM (Tang et al. 2012). Interestingly, *RyR2* mutations that increase the threshold concentration of luminal SR Ca^{2+} release termination and reduce fractional Ca^{2+} release associate with hypertrophic cardiomyopathy and not DCM. Previous findings in murine cardiomyocytes have shown that PC2 binds to RyR2, keeping it closed during diastole (Anyatonwu et al. 2007). We suggest that loss of PC2 function may lead to prolonged RyR2

openings and promote the development of DCM in a similar manner. Supporting this hypothesis are the prolonged Ca^{2+} transients, increased diastolic $[Ca^{2+}]_i$, and decreased SR Ca^{2+} stores observed in the *pkd2* mutant hearts.

We observed occasional Ca^{2+} transient amplitude alternans in *pkd2* mutant hearts. Ca^{2+} alternans manifests on the ECG as TWA, which is a common finding in patients with IDCM and heart failure, and a known predictor of SCD due to ventricular tachyarrhythmias (Pruvot et al. 2004, Narayan 2006, Salerno-Uriarte et al. 2007). Ca^{2+} alternans is caused by an imbalance in Ca^{2+} cycling due to abnormal release or reuptake of Ca^{2+} (Laurita et al. 2008a). Abnormal RyR2 function can cause Ca^{2+} alternans. As discussed above, most evidence implicates depressed RyR2 activity with Ca^{2+} alternans (Diaz et al. 2002, Pieske et al. 2002, Kornyeyev et al. 2012, Alvarez-Lacalle et al. 2013), but also increased RyR2 activity might cause it (Lehnart et al. 2006). It is therefore possible that increased RyR2 activity due to loss of inhibition by PC2 might lead to Ca^{2+} alternans. However, PC2 is known to interact with multiple proteins involved in intracellular Ca^{2+} cycling, as reviewed above. These interactions require further studies to pinpoint the exact molecular mechanisms of the discovered cardiac dysfunction.

The *pkd2* mutant hearts showed regular prolonged Ca^{2+} transients. Despite elevated diastolic $[Ca^{2+}]_i$ levels, no spontaneous diastolic Ca^{2+} release events were observed. Similarly, triggered beats and even afterdepolarizations were absent in the optical AP measurements. This indicates NCX activity remained below threshold for detecting observable diastolic inward currents (Langenbacher et al. 2005). This is expected, because in zebrafish SR Ca^{2+} release contributes to contraction less than in mammals, thus making aftertransients and DADs less likely (Xie et al. 2008b, Zhang et al. 2011). $I_{Ca,L}$ through LTCCs contributes importantly to APD (Brette et al. 2008, Nemtsas et al. 2010) and $[Ca^{2+}]_i$-dependent inactivation of LTCCs is an important regulator of APD in zebrafish hearts (Zhang et al. 2011). The relative contribution of LTCC and NCX to APD is species-specific. In zebrafish and other species with long APD, an increase in $[Ca^{2+}]_i$ will decrease APD by faster inactivation of LTCCs (Han et al. 2002). Therefore, faster inactivation of LTCCs due to high $[Ca^{2+}]_i$ may explain the shorter APD and capture at faster rates of pacing observed in the *pkd2* mutant ventricles. However, additional sarcolemmal Ca^{2+} currents may have contributed to the observed difference in APD between *pkd2* mutant and WT fish.

Two out of six PKD2 IDCM patients and approximately 28% of *pkd2* mutant fish had AV block. Prolonged Ca^{2+} transients in the *pkd2* mutant hearts lower the maximum frequency with which they are able to cycle Ca^{2+} and maintain a normal contraction-relaxation cycle. As a critical threshold rate is reached, the ventricle fails to contract. This is preceded by the development of Ca^{2+} alternans as an indication of the Ca^{2+} cycling capacity nearing its limits, as observed in the *pkd2* mutant hearts already at a physiological rate of pacing (120 bpm). Additionally, faster AV conduction in *pkd2* mutant hearts may have contributed to the occasional inability of the atrial AP to induce ventricular contraction, as the arriving impulse may have met a ventricular Ca^{2+} cycling machinery that was still refractory. On the other hand, faster AV conduction may in part have decreased cardiac output in *pkd2* mutants by reducing the time available for ventricular filling.

In the Mayo ADPKD Mutation Database, approximately 9% of genotyped PKD2 patients had a diagnosis of IDCM. Additionally two PKD2 patients had subclinical or stress-induced DCM. In genotyped PKD1 patients, the prevalence of IDCM was approximately 2%. PC2 forms a Ca^{2+} channel and interacts with multiple Ca^{2+} cycling proteins, whereas PC1 interacts closely with PC2 (Casuscelli et al. 2009). In this light the result of increased IDCM prevalence in PKD patients is logical, with PKD2 patients being more often affected than PKD1 patients. The association between ADPKD and IDCM seems true, as the prevalence of IDCM among ADPKD patients is 86-fold higher than among the general population. However, examining patients in the ADPKD Mutation Database probably introduces a bias, as symptomatic patients with a more severe disease phenotype are more likely to be included in the analysis and to undergo thorough cardiac evaluation. On the other hand, this bias should favor inclusion of PKD1 patients, who develop symptoms and progress to end-stage renal disease earlier than PKD2 patients. It is therefore interesting to note that of the 11 families with identified PKD mutations, four (36%) had *PKD2* mutations. This is a higher proportion than the 10 – 15% usually identified in clinical studies, where PKD2 patients may be under-represented due to a milder disease phenotype (Rossetti 2007). It is therefore also possible that cases of early or mild IDCM may have gone undiagnosed, especially in PKD2 patients with a mild kidney disease phenotype. Still, ADPKD does not fully explain the cases of IDCM in these families, as one family member had IDCM but no *PKD* mutations or clinical PKD. We hypothesize that ADPKD increases the risk of developing cardiomyopathy, and requires additional genetic or environmental factors to cause symptomatic disease.

In summary, in study IV we found a novel association between ADPKD and IDCM. Based on the zebrafish model lacking PC2 we suggest impaired Ca^{2+} cycling as a potential mechanism leading to prolonged Ca^{2+} transients, elevated diastolic $[Ca^{2+}]_i$, Ca^{2+} alternans, AV block, and reduced cardiac output due to mainly diastolic dysfunction. While many questions about the molecular pathomechanisms and the nature of the relationship between ADPKD and IDCM remain, we recommend considering ADPKD as a disease that may predispose to IDCM.

3 Study limitations

3.1 Monophasic action potential recordings

The dose of epinephrine infused during MAP recording was low, resulting in an average heart rate of 87 bpm in CPVT patients and 90 bpm in control subjects. These heart rates are well below the threshold for development of ventricular arrhythmias, partly explaining why most CPVT patients failed to show DADs. MAPs were recorded at a single endocardial site in the right ventricular septum. As the MAP catheter records electrical area only from its vicinity, the ventricular extrasystoles coinciding with DADs of low amplitude may have been initiated at sites further in the ventricles. Furthermore, MAPs record extracellular activity, and therefore provide only limited information on events taking place across the cell membranes.

3.2 Studies in HEK 293 cells

HEK 293 cells are morphologically different from cardiomyocytes. In cardiomyocytes, RyR2s are located on the SR membrane in the immediate proximity of T-tubules, whereas HEK 293 cells lack T-tubules. Ca^{2+} release events in HEK 293 cells are notably slower than in cardiomyocytes, indicative of underlying differences in the Ca^{2+} cycling machinery. Cardiomyocytes might therefore provide a more optimal model for functional studies.

3.3 ECG recordings

Noise and acquisition frequency of the ECG signal are limiting factors in the 24h recordings. Although noisy signal is excluded using automated and manual methods, signal qualities between and within recordings remain variable to some extent. The data acquisition frequency of 128Hz limits the accurate analysis of changes especially of short intervals/segments such as QRS duration,

when using raw unsampled data. Higher data acquisition frequency and improvement of signal-to-noise ratio will increase the accuracy of ECG analyses.

3.4 Studies in iPSC-derived cardiomyocytes

The studies were limited to studying two cell lines generated from a single CPVT patient, and two cell lines from a single healthy control. We cannot therefore conclude whether the changes we saw are specific to this mutation, this patient, or even only these cell lines. Future studies will need to examine identical and different mutations in multiple cell lines derived from multiple patients. A weakness of the Ca^{2+} imaging method is not being able to distinguish between the varipus types of cardiomyocytes (atrial, nodal, or ventricular). Therefore, although based on patch-clamp experiments the vast majority of beating cells are ventricular-like cardiomyocytes, also other cardiomyocyte-types may have been included in the Ca^{2+} imaging studies. One solution to this problem will be to measure APs and Ca^{2+} transients simultaneously. Importantly, simultaneous recording will give important mechanistic information on the interplay between Ca^{2+} cycling and membrane potential. Another weakness of this novel model is the immature phenotype of the differentiated cardiomyocytes. As discussed above, improvement of differentiation and purification protocols looks likely to yield more homogenous populations of more mature cardiomyocytes in the future. Methodologically, measurement of Ca^{2+} sparks would have been useful to quantify Ca^{2+} leak and assess the impact of different interventions on Ca^{2+} leak, strengthening the studies mechanistically.

3.5 Studies in the zebrafish model

Findings in the zebrafish heart should be extrapolated to humans very cautiously, especially regarding Ca^{2+} cycling, as some of the the ion channel properties are different (Zhang et al. 2011). Interesting findings should be studied further in mammalian models and e.g. human cell models such as iPSC – derived cells.

3.6 Comparison of models

Electrophysiological and Ca^{2+} handling characteristics of the different models highlighting their weaknesses and differences are provided in tables 4 – 6. On several occasions, the results of different studies are contradictory. For comparison, characteristics of human adult ventricular myocytes are listed in table 7.

Table 4. Electrophysiological characteristics of HEK 293 cells	
AP amplitude (mV)	No
APD90 (ms)	No
Ca^{2+} signaling	Endogenous mediators of store-operated Ca^{2+} entry > may affect Ca^{2+} signaling (Babnigg et al. 2000)
Calsequestrin	Absent (Itzhaki et al. 2011b)
dV/dt max (V/s)	No
EC-coupling	No
Funny current	Unknown
Junctin and triadin	Unknown
K^+ channels / currents	Some results contradictory. Outward-rectifying delayed K^+ current, no I_{to} (Yu et al. 1998). Delayed rectifying K^+ current and I_{to} present (Jiang et al. 2002a). Voltage-gated and calcium-activated K^+ channel proteins present (Thomas et al. 2005)
L-type Ca^{2+} channels / current	Channel absent (Itzhaki et al. 2011b)
Morphology	Pyramidal or rhombic, small hair-like filopodia at membrane periphery
Na^+ channels / current	Channel subunits present (Thomas et al. 2005)
NCX	Absent (Cross et al. 2012)
Phospholamban	Absent (Itzhaki et al. 2011b)
Resting membrane potential (mV)	-20 – -40 (Thomas et al. 2005)(Thomas 2005)
RyR2	Absent (Itzhaki et al. 2011b)
SERCA2a	Absent (Itzhaki et al. 2011b)
SR	ER
T-tubules	Absent
T-type Ca^{2+} channels / current	Unknown
Summary	**Useful as a plasma membrane enclosed "test tube" to express and study recombinant proteins in relative isolation**

Table 5. Electrophysiological characteristics of human iPSC ventricular cardiomyocytes	
AP amplitude (mV)	90 – 120 (Zhang et al. 2009a, Moretti et al. 2010, Itzhaki et al. 2011a, Ma et al. 2011, Doss et al. 2012, Itzhaki et al. 2012, Kujala et al. 2012, Lahti et al. 2012, Novak et al. 2012)
APD90 (ms)	310 – 500 (Zhang et al. 2009a, Moretti et al. 2010, Itzhaki et al. 2011a, Ma et al. 2011, Itzhaki et al. 2012, Kujala et al. 2012, Lahti et al. 2012)(Doss et al. 2012)
Ca^{2+} signaling	Large IP3 sensitive Ca^{2+} stores (Itzhaki et al. 2011b)
Calsequestrin	Some results contradictory. Absent (not there to buffer SR Ca^{2+}), but calreticulin is expressed (Li et al. 2013b). Present (Itzhaki et al. 2011b, Lee et al. 2011). CASQ2 mRNA levels low compared to levels in adult heart, but protein levels similar (Jung et al. 2012). CASQ2 mRNA (Germanguz et al. 2011) and also protein present (Novak et al. 2012)
dV/dt max (V/s)	5 – 40 (Zhang et al. 2009a, Moretti et al. 2010, Itzhaki et al. 2011a, Ma et al. 2011, Doss et al. 2012, Itzhaki et al. 2012, Lahti et al. 2012, Novak et al. 2012)
EC-coupling	Poor EC-coupling due to lack of T-tubules (Lee et al. 2011)
Funny current	Higher funny current density than in adult CMs* > may promote spontaneous beating (Hoekstra et al. 2012)
Junctin and triadin	Some results contradictory. Absent (not there to facilitate RyR2 function) (Li et al. 2013b). Present less than in hESC d-CMs* (Lee et al. 2011). mRNA levels high compared to levels in adult heart, but protein levels similar (Jung et al. 2012). Junctin mRNA, triadin mRNA and protein present (Novak et al. 2012)
K^+ channels / currents	Large variation in peak currents of various K^+ channels. I_{Kr} density similar to adult CMs*, I_{Ks} density may be higher than in adult CMs*, peak I_{K1} one fourth of that in adult CMs* (Ma et al. 2011). Resting membrane potential less negative than in adult CMs*, may contribute to spontaneous beating. I_{K1} density increases and spontaneous activity decreases as cells mature (Hoekstra et al. 2012). I_{Kr}, I_{to}, I_{Ks}: channel subunit mRNA levels high, I_{K1}: channel subunit mRNA levels variable compared to adult heart levels (Jung et al. 2012). Very small I_{K1}, robust I_{Kr} (Doss et al. 2012), channel subunit mRNA present (Di Pasquale et al. 2013)
L-type Ca^{2+} channels / current	Peak current similar to adult CMs*, but highly variable in both groups (Hoekstra et al. 2012). Channel subunit mRNA levels similar, but variable compared to adult heart levels (Jung et al. 2012). Channel subunit mRNA present (Kujala et al. 2012, Di Pasquale et al. 2013)
Morphology	Multiangular, disorganized sarcomeres (Dick et al. 2010). Small cell size (Knollmann 2013)
Na^+ channels / current	Similar to adult CMs*, but peak current data for comparison lacking – Lower dV/dt max due to lower functional availability of channels because of higher resting membrane potential (Hoekstra et al. 2012). I_{Na}: channel subunit mRNA levels similar to adult heart levels (Jung et al. 2012), Channel subunit mRNA present (Di Pasquale et al. 2013)
NCX	Protein expression shown (less than in hESC d-CMs**), but function not studied (Lee et al. 2011). I_{NCX}: channel subunit mRNA levels similar compared to adult heart levels (Jung et al. 2012). Peak I_{NCX} 2-3 pA/pF, similar function as in adult mammalian CMs* (Zhang et al. 2013a). Channel

	subunit mRNA present (Kujala et al. 2012, Novak et al. 2012)
Phospholamban	Some results contradictory. Absent (Li et al. 2013b). Present (Itzhaki et al. 2011b). mRNA levels high compared to levels in adult heart, but protein levels similar (Jung et al. 2012). mRNA present (Kujala et al. 2012)
Resting membrane potential (mV)	-60 – -80 (Zhang et al. 2009a, Moretti et al. 2010, Itzhaki et al. 2011a, Ma et al. 2011, Doss et al. 2012, Itzhaki et al. 2012, Kujala et al. 2012, Lahti et al. 2012, Novak et al. 2012)
RyR2	Present (Itzhaki et al. 2011b). Lower expression than in hESC d-CMs** (Lee et al. 2011, Li et al. 2013b). mRNA levels low compared to levels in adult heart, but protein levels similar (Jung et al. 2012). mRNA (Kujala et al. 2012, Novak et al. 2012) and protein present (Germanguz et al. 2011, Itzhaki et al. 2012, Di Pasquale et al. 2013)
SERCA2a	Present (Itzhaki et al. 2011b). Lower expression than in hESC d-CMs** (Lee et al. 2011, Li et al. 2013b). mRNA and protein levels similar to levels in adult heart (Jung et al. 2012). mRNA present (Kujala et al. 2012, Novak et al. 2012)
SR	Immature (Lee et al. 2011)
T-tubules	Immature ultrastructure, no T-tubules (Novak et al. 2012, Li et al. 2013b)
T-type Ca^{2+} channels / current	No functional presence (Ma et al. 2011)
Summary	**Resemble neonatal cardiomyocytes with small cell size, lack of T-tubules, and immature EC-coupling. However, slow maturation does occur (Lundy et al. 2013)**

*CM = cardiomyocyte, **hESC d-CMs = human embryonic stem cell -derived cardiomyocyte.

Table 6. Electrophysiological characteristics of adult zebrafish ventricular cardiomyocytes	
AP amplitude (mV)	99 (Nemtsas et al. 2010)
APD90 (ms)	150 (Brette et al. 2008), 132 (Nemtsas et al. 2010), 275 in 2 dpf embryos at RT* (Jou et al. 2010)
Ca^{2+} signaling	Sarcolemmal Ca^{2+} currents, including $I_{Ca,T}$, are more robust than in humans (Nemtsas et al. 2010)
Calsequestrin	Unknown
dV/dt max (V/s)	92 (Nemtsas et al. 2010), 6 in 2 dpf embryos at RT* (Jou et al. 2010)
EC-coupling	$I_{Ca,L}$ important, but SR less important to EC-coupling (Zhang et al. 2011)
Funny current	Present, but much less than in atria (Warren et al. 2001), present also in embryos (Baker et al. 1997)
Junctin and triadin	Unknown
K^+ channels / currents	I_{Kr} present, I_{K1} robustly present, I_{Ks} Absent, I_{to} Absent (Nemtsas et al. 2010). In embryos I_{Kr} present (Baker et al. 1997). I_{Kr} and I_{Ks} present (Tsai et al. 2011)
L-type Ca^{2+} channels / current	Fivefold larger current density than in human CMs**. Ca^{2+} dependent inactivation similar to that in mammals (Zhang et al. 2011). Current density similar to that in mammals (Brette et al. 2008). Robust presence (Nemtsas et al. 2010), also in embryos (Baker et al. 1997)
Morphology	Rod-shaped, sarcomeres present (Brette et al. 2008). Striated, but smaller than mammalian CMs** (Nemtsas et al. 2010)
Na^+ channels / current	Current density 4 times smaller than in mammals (Brette et al. 2008) present (Nemtsas et al. 2010) also in embryos (Baker et al. 1997)
NCX	Contributes to membrane potential and contraction at positive membrane potentials (Zhang et al. 2011)
Phospholamban	Present (Little et al. 2013)
Resting membrane potential (mV)	-72 (Nemtsas et al. 2010), -68 in 2 dpf embryos at RT* (Jou et al. 2010)
RyR2	Present as the most highly expressed RyR isoform (Darbandi et al. 2009)
SERCA2a	Present (Little et al. 2013)
SR	SR Ca^{2+} release contributes to contraction less than in mammals (Zhang et al. 2011), also in embryos (Xie et al. 2008b)
T-tubules	Absent (Brette et al. 2008). But smaller cell size allows rapid Ca^{2+} wave propagation
T-type Ca^{2+} channels / current	Robust presence, suggesting an immature phenotype compared to mammalian CMs** (Nemtsas et al. 2010), also in embryos (Baker et al. 1997). Essential for EC-coupling in embryos (Xie et al. 2008b)
Summary	**Small cells that lack T-tubules, sarcolemmal currents are more important for contractile function than in mammals, SR of less importance for EC-coupling. Thus Ca^{2+} aftertransients and DADs are less likely to occur**

*RT = room temperature, **CM = cardiomyocyte.

Table 7. Electrophysiological characteristics of human adult ventricular cardiomyocytes	
AP amplitude (mV)	100 – 110 (Drouin et al. 1998, Magyar et al. 2000, Nemtsas et al. 2010)
APD90 (ms)	210 – 350 (Drouin et al. 1998, Magyar et al. 2000, Nemtsas et al. 2010)
Ca^{2+} signaling	Rapid and synchronous
Calsequestrin	Present (Zhang et al. 1997)
dV/dt max (V/s)	180 – 230 (Drouin et al. 1998, Magyar et al. 2000, Nemtsas et al. 2010)
EC-coupling	Essential contribution of SR (Bers 2002)
Funny current	During heart failure (Hoppe et al. 1998)
Junctin and triadin	Present (Zhang et al. 1997)
K^+ channels / currents	Peak Ito 5-16 pA/pF (Näbauer et al. 1996). Peak I_{K1} 3.6 pA/pF (Magyar et al. 2000). Peak I_{Kr} 0.30 pA/pF (Iost et al. 1998, Magyar et al. 2000). Peak I_{Ks} 0.20 pA/pF (Virág et al. 2001). I_{to} and I_{K1} decreased in heart failure (Beuckelmann et al. 1993)
L-type Ca^{2+} Channels / current	Peak current -10 pA/pF (Magyar et al. 2000)
Morphology	Rod-shaped, sarcomeres present
Na^+ channels / current	Robust, as indicated by high dV/dt max.
NCX	Expression increased in heart failure (Hasenfuss et al. 1999)
Phospholamban	Inhibitory effect on SERCA2a increased in heart failure (Frank et al. 2000)
Resting membrane potential (mV)	-80 – -90 (Drouin et al. 1998, Magyar et al. 2000, Nemtsas et al. 2010)
RyR2	Present (Zhang et al. 1997)
SERCA2a	Expression decreased in heart failure (Hasenfuss et al. 1994, Hasenfuss et al. 2002)
SR	Essential for EC-coupling (Bers 2002)
T-tubules	Extensive
T-type Ca^{2+} channels / current	Present under pathological conditions (hypertrophy, heart failure) (Ono et al. 2010)
Summary	**Mature cardiomyocytes with extensive T-tubules and robust EC-coupling, where SR Ca^{2+} plays an essential role**

Conclusions

The research works included in this thesis were designed as translational studies, aimed at tackling clinically relevant problems in the lab. Our goal was to improve understanding and eventually take this knowledge back to the clinic in order to help those, for whom this work is done for in the first place, the patients.

Studies I-III investigated CPVT. MAP recordings in the right ventricles displayed afterdepolarizations and concomitant U-waves were observed in the ECG. These afterdepolarizations increased upon β-agonist stimulation, and occasionally triggered APs and ventricular extrasystoles. Cell studies revealed an increased propensity to spontaneous SR Ca^{2+} release by the mutant RyR2 channels. More detailed studies of mutant RyR2s in iPSC-derived cardiomyocytes showed increased and irregular spontaneous Ca^{2+} release that upon β-agonist stimulation resulted in decreased SR Ca^{2+} and increased cytosolic Ca^{2+} concentrations. Interestingly, in addition to DADs, mutant cells also showed occasional EADs. Based on the observed variability of Ca^{2+} cycling in the mutant cells, the CPVT patients' clinical ECG and MAP recordings were examined for corresponding phenomena. Increased non-alternating variability of repolarization was found in the ECG recordings, recapitulating the cell-level findings.

Cellular and *in vivo* AP recordings revealed prolonged depolarization upon β-agonist stimulation in CPVT. Older CPVT patient showed notably reduced R-spike upslope velocity on 24h ECG recordings. These findings suggest that progressively reduced conduction velocity may contribute to an arrhythmic substrate in these patients.

The novel iPSC technology is a promising tool for mechanistic studies of arrhythmic disorders. The discovered ECG changes in CPVT patients raise questions that should be addressed in further studies. Do increased variability of the QT interval and prolonged depolarization have value in arrhythmia risk prediction? Can they guide pharmacologic therapy? Or help in choosing the optimal treatment strategy (drugs, ICD, sympathetic denervation)? These questions are relevant not only for CPVT patients, but all patients at risk of ventricular arrhythmias.

Study IV investigated cardiac function in a zebrafish model of polycystic kidney disease. These fish showed signs of heart failure, including reduced cardiac output, edema, and arrhythmias. Detailed studies on excised whole hearts showed markedly impaired Ca^{2+} cycling, indicating that PC2 is necessary for maintaining normal Ca^{2+} handling and cardiac function. Importantly, a database search found that the prevalence of IDCM is high among ADPKD patients, especially those with *PKD2* mutations.

These findings suggest impaired Ca^{2+} cycling as an essential mechanism of cardiac dysfunction in these patients. Furthermore, they encourage future studies to investigate the mechanism of the association between ADPKD and IDCM in more detail. It remains unclear whether screening for early signs of cardiac dysfunction in ADPKD patients would result in better cardiac outcomes. Additionally, the zebrafish proved an attractive model organism for studies on cardiac physiology. Its booming popularity in biomedical research is likely to continue.

What next?

Models

I believe efforts to develop stem cell technologies should continue. The field is developing rapidly, and new promising methodologies are introduced frequently (Obokata et al. 2014). The potential benefits are huge. Identification of genotype-phenotype correlations and disease mechanisms will progress *in vitro*. On the other hand, physiological experiments will allow scientists to optimize treatment in a patient-specific manner, even before possessing detailed knowledge of the complex interplay of modifying genetic factors in that individual. This is crucial because a disease such as CPVT may arise from hundreds of different mutations, and optimal therapy is likely to be mutation-, and even individual patient-, dependent. Additional applications of stem cell technologies include toxicology screening, and further down the line, the potential for cell therapy to mend hearts following devastating injuries, such as myocardial infarction.

I think that also zebrafish can be a valuable model organism in high throughput drug discovery, toxicological studies, and as a first-line *in vivo* model for physiological studies involving drugs, genes, or other molecules of interest. When its limits are kept in mind, it can also provide meaningful mechanistic insights.

CPVT and other arrhythmias

Although studying molecular and cell-level mechanisms related to arrhythmias is important and stem cell-derived cardiomyocytes open exciting possibilities to do this, clinical cardiac electrophysiology will remain the cornerstone. Arrhythmias are complex phenomena, which need to be studied and understood at the organ and organism levels. Arrhythmia risk prediction and treatment have a long way to improve. As prevention is the best treatment, effort needs to be put on risk stratification to learn whom to treat and how, to prevent adverse outcomes. Once we know what signs of risk to look for, I'm confident the technology will be there to enable the timely detection of these red flags. The focus need to be on ventricular tachyarrhythmias, which remain incompletely understood, especially polymorphic VT in a structurally healthy heart (Josephson 2007). Regarding risk stratification and treatment of CPVT, what is needed now is a shift from studies on animal models to randomized prospective placebo controlled clinical trials, which due to the rarity of the condition will require a concerted international multi-center approach. If well designed

and implemented, such studies will teach us the signs of danger to look for, and the usefulness of different therapies.

Technology will change the game

I envision that the development of portable monitoring devices and applications, such as simple ECG recordings taken by devices like smart phones, will allow follow-up of selected high risk patients and reduce the frequency of physical visits to the clinic. ECG readouts sent to the treating physician, perhaps among other parameters containing data on variability of repolarization and alternans, may allow interventions such as changes in pharmacotherapy to be taken as preventive measures before adverse events would occur. This applies not just to patients with inherited arrhythmias, but to all patients at high risk of SCD, and even more broadly when readings on weight changes, blood glucose, blood pressure etc. are included.

ADPKD

Studies on the mechanisms of cardiac dysfunction in ADPKD need to take the logical next step from zebrafish to mammalian models, as is currently happening. Once this relationship is understood in more detail, studies on human ADPKD patients will hopefully bring benefits in the form of reduced cardiac morbidity and mortality to the millions of ADPKD patients world-wide.

It is therefore my humble hope that opportunities are given for translational cardiac research and training that will deepen our understanding and most importantly, eventually benefit the patients.

Acknowledgements

The clinical work for studies I – III was carried out at the Department of Cardiology, Helsinki University Central Hospital. The basic research work for studies I (2002 – 2004) and III (2013) was carried out at the Unit of Cardiovascular Research, Minerva Foundation Institute for Medical Research, Biomedicum, Helsinki. The basic research work for study II (2010 – 2012) was conducted at the Institute of Biomedical Technology, University of Tampere and BioMediTech, Tampere. For study IV (2008 – 2011), the zebrafish work was done at the Departments of Pharmacology and Genetics, Yale University School of Medicine, New Haven, CT. Clinical data for study IV came from the Division of Nephrology and Hypertension, Mayo Clinic, Rochester, MN.

I have been financially supported by research grants from the Finnish Medical Foundation/The Finnish Medical Society Duodecim, the Emil Aaltonen Foundation, the Finnish Foundation for Cardiovascular Research, the Maud Kuistila Memorial Foundation, the Paavo Nurmi Foundation, the Aarne Koskelo Foundation, the Biomedicum Helsinki Foundation, the Ida Montin Foundation, the Orion-Farmos Research Foundation, and the Oskar Öflund Foundation. The support of the funders is sincerely acknowledged.

I am truly grateful to **Mika Laine,** my PhD supervisor and **Ilkka "Success comes before Work only in the dictionary" Tikkanen**, the head of the Cardiovascular Research Unit in Minerva, for opening the door (and keeping it open!) when a young oblivious 2nd year medical student came knocking on it in 2002. I was hooked by Ilkka offering me a small stipend for the summer, and by Mika taking the time and effort to teach me the cool flashy stuff that's calcium imaging (while he was at the same time specializing, raising small sons, and building a house!). Ilkka, you have always supported and shown trust in me, and given me opportunities to participte in international meetings. Mika's enthusiasm and support have been crucial along the way, exemplified by the time when I went to give my first talk, at the AHA meeting in 2004 in New Orleans, and the first reaction of the staff on seeing me at the meeting's presenter center was: "What are you – 16?!" Mika and Ilkka, thank you for all your help and support!

Matti Viitasalo, my PhD supervisor, I thank you with all my heart for being my Mentor! I feel truly lucky to have you as my supervisor, you have been nothing but encouraging. Your door has always been open for me, and you have put a tremendous amount of patience, time, and effort into guiding and teaching me throughout the years. Your selfless support also gave me the chance to visit Yale. You possess the kind of expertise, wisdom, and humble dignity that commends my deepest respect.

Barbara Ehrlich, my supervisor and head of the Laboratory of Molecular Hermeneutics at Yale School of Medicine. Thank you for all your support, starting from giving me a chance to work in your lab based on an email and a phone conversation. You trusted me and gave me free hands to pursue what I wanted, and with your vast contact network always found somebody to answer my questions, provide equipment etc. You make science fun and have found what looks like the optimal balance in life! We are grateful for the many memorable moments, from taking us to your family Thanksgiv-

ing Dinners and charity running events, to just chilling on the sofa drinking beer and watching the Super Bowl (commercials). I can still taste the wasabi ice cream on my tongue!

Katriina Aalto-Setälä, the head of the Heart Group at the University of Tampere, thank you for giving me an important role in your exciting projects. Collaboration with you has been smooth and fruitful, and I really hope we can continue to work together.

I would like to acknowledge **Markku S. Nieminen**, the Custos and Head of Cardiology, for being so supportive of my research ambitions and for his active help and support in organizing the PhD defense.

Kari Ylitalo and **Pasi Tavi**, the reviewers of my dissertation, thank you for taking the time and effort to provide valuable comments on how to improve the dissertation on such a tight schedule during the holiday season. Your contribution has greatly improved this work! I would especially like to thank Pasi for our interesting and inspiring phone conversation on intracellular calcium cycling as well as for earlier phone consultations.

I would like to thank the following coauthors. From the Department of Cardiology and Medicine in Helsinki, **Kimmo Kontula**, **Lauri Toivonen**, and **Heikki Swan**. Your thorough examination of the CPVT patients, willingness to include me in the research work, and invaluable contributions to studies I – III have made them possible, thank you. **Heikki Väänänen** from the Aalto University. Thank you for designing and explaining the intricacies of the ECG analysis software, without which study III would not have been possible. From the University of Tampere, I am thankful to **Kirsi Kujala** for the fun calcium imaging experiments in study II and to **Kim Larsson** for the patch-clamp experiments in studies II and III. From Yale I thank **Simon Schliffke** and **Ivana Kuo** from Barbara's lab. I am especially grateful to Simon, his effort in study IV was essential, and he is also a true friend with whom we have enjoyed many great discussions and fun times outside the lab from ice climbing in New Hampshire to sailing in Germany. I acknowledge **Zhaoxia Sun** and **Shiaulou Yuan** from the zebrafish lab at Yale for their valuable contributions to study IV. Also, a huge thank you to all the little Nemos of study IV. I would also like to thank our collaborators at the Mayo Clinic, **Vicente Torres**, **Peter Harris**, and **Sandro Rossetti**. E-mail correspondence and data transfer with you was as fast and smooth as you would have been sitting in the next room, thank you for your great effort!

From Minerva, I want to say a special thank you to **Vesa Olkkonen**, the Director of Minerva Institute. Vesa, thank you for always supporting me and for being such an inclusionist. It is hard to see how study III would have been possible without your effort in helping me get the high-speed camera system for calcium imaging. You show genuine passion towards science and lead with enthusiasm and example. Thanks also to **Cia Olsson**, the Laboratory Chief of Minerva. Cia, it is a great feeling to know you are always there to help with whatever is needed in the lab. With the two of you, Minerva is in good hands. From Ilkka's group, I want to thank **Katariina Immonen** and **Riikka Kosonen**, our technicians, and post-doc **Päivi Lakkisto**, for always being there and forming the core of our Team. Thank you for your help in all the smaller and larger things I have needed help with during these years.

PS. Thank you also to Teemu and the Lions for the inspiration and example, by demonstrating that with Teamwork and Sisu, anything is possible.

I want to thank the understanding and supportive staff and chief physicians **Jouni Silvo** at the Töölö Occupational Health Center of the City of Helsinki, and **Janne Soveri** at the Leppävaara Health Center of the City of Espoo, where I worked as a part time physician 2010 – 2013. Thank you for being so flexible and allowing me to adjust my clinical work schedules according to the needs of my research work.

Aaah, my friends! You are all dear to me and I thank you for all the times spent together, for all your support and encouragement, for being you! First I want to thank the Best of Men: **Jussi** (also for providing food and shelter on my visits to Tampere during study II), **Lauri K**, **Panu**, and **Tuomas,** you guys are the best friends one can hope to have - you mean a lot to me. My warmest thanks to my friends **Alex**, **Altti**, **cK**, **Elina F**, **Elina K**, **Erkko**, **Hanna I**, **Hanna K**, **Ina**, **Japa**, **Jari**, **Jaro**, **Jenny**, **Jesse**, **Johanna**, **Kata**, **Katja H**, **Katja K**, **Kimmo**, **Laura**, **Lauri P**, **Manna**, **Mara**, **Markku**, **Mikko K**, **Mikko M**, **Niina**, **Pimppis**, **Sami**, **Samuel**, **Sini**, **Suski**, **Taina**, **and Tuukka.** And many others! Wow – just writing your names out like this fills me with warmth and gratitude!

I want to express my sincere gratitude to my in-laws, **Sebestyén Ibolya** and **Gaál Aladár**, who have welcomed me to the family from the beginning and supported me all this time. And all this despite the fact that my Hungarian has hardly improved! You are very dear to me.

I want to thank my dear Family. Thank you **Äiti**, you have taught me the meaning of perseverance, tolerance, understanding, forgiveness, and unconditional love. You have always believed in me and given me your unconditional support. The world would be a much colder place without people like you. Thank you **Isi**, you have taught me confidence and trust in my ability to boldly go out and reach for my goals, while at the same time "keeping my antennas out" and staying sensitive to my surroundings. You have also taught me the great strength and harmony that Mother Nature can give us. Thank you **Taru**, you have enthusiastically joined in your big brother's fishing and other adventures, and given me many happy memories and proud moments. You have a bright mind with huge potentials to unlock, and I hope you will find the right channel to pour all that intelligence into.

Emili, the Love of my life, meeting You is the best thing that has happened to me. I am a lucky man. I want to thank You for all that You are. You combine wisdom and intelligence, faith and reason, as well as pushing the limits and having fun, in a unique way that I had no idea can exist. You are a remarkable Woman, and I feel so blessed for having the chance to journey through life side-by-side with You. ILU my Butterfly!

In Espoo, February 5th 2014

References

Abdul-Majeed S and Nauli SM (2011). Calcium-mediated mechanisms of cystic expansion. Biochim Biophys Acta 1812(10): 1281-1290.

Abi-Gerges N, Valentin JP and Pollard CE (2010). Dog left ventricular midmyocardial myocytes for assessment of drug-induced delayed repolarization: short-term variability and proarrhythmic potential. Br J Pharmacol 159(1): 77-92.

Ackerman MJ, Priori SG, Willems S, Berul C, Brugada R, Calkins H, Camm AJ, Ellinor PT, Gollob M, Hamilton R, Hershberger RE, Judge DP, Le Marec H, McKenna WJ, Schulze-Bahr E, Semsarian C, Towbin JA, Watkins H, Wilde A, Wolpert C and Zipes DP (2011). HRS/EHRA expert consensus statement on the state of genetic testing for the channelopathies and cardiomyopathies this document was developed as a partnership between the Heart Rhythm Society (HRS) and the European Heart Rhythm Association (EHRA). Heart Rhythm 8(8): 1308-1339.

Adam DR, Smith JM, Akselrod S, Nyberg S, Powell AO and Cohen RJ (1984). Fluctuations in T-wave morphology and susceptibility to ventricular fibrillation. J Electrocardiol 17(3): 209-218.

Adams SR (2010). How calcium indicators work. Cold Spring Harb Protoc 2010(3): pdb top70.

Addis RC and Epstein JA (2013). Induced regeneration--the progress and promise of direct reprogramming for heart repair. Nat Med 19(7): 829-836.

Aistrup GL, Balke CW and Wasserstrom JA (2011). Arrhythmia triggers in heart failure: the smoking gun of [Ca2+]i dysregulation. Heart Rhythm 8(11): 1804-1808.

Aizawa Y, Komura S, Okada S, Chinushi M, Morita H and Ohe T (2006). Distinct U wave changes in patients with catecholaminergic polymorphic ventricular tachycardia (CPVT). Int Heart J 47(3): 381-389.

Al-Khatib SM and Pritchett EL (1999). Clinical features of Wolff-Parkinson-White syndrome. Am Heart J 138(3 Pt 1): 403-413.

Alvarez-Lacalle E, Cantalapiedra IR, Penaranda A, Cinca J, Hove-Madsen L and Echebarria B (2013). Dependency of calcium alternans on ryanodine receptor refractoriness. PLoS One 8(2): e55042.

Amin AS, Tan HL and Wilde AA (2010). Cardiac ion channels in health and disease. Heart Rhythm 7(1): 117-126.

Amsterdam A, Burgess S, Golling G, Chen W, Sun Z, Townsend K, Farrington S, Haldi M and Hopkins N (1999). A large-scale insertional mutagenesis screen in zebrafish. Genes Dev 13(20): 2713-2724.

Antoons G and Thomsen MB (2010). Repolarization variability and early afterdepolarizations in long QT syndrome type 2: is labile calcium the common denominator? Heart Rhythm 7(11): 1695-1696.

Antzelevitch C (2006). Cellular basis for the repolarization waves of the ECG. Ann N Y Acad Sci 1080: 268-281.

Antzelevitch C, Burashnikov A and Di Diego JM (2008). Mechanisms of Cardiac Arrhythmia. In: Electrical Diseases of the Heart. Gussak I and Antzelevitch C. London, Springer-Verlag. Pages 65-132.

Anyatonwu GI and Ehrlich BE (2004). Calcium signaling and polycystin-2. Biochem Biophys Res Commun 322(4): 1364-1373.

Anyatonwu GI, Estrada M, Tian X, Somlo S and Ehrlich BE (2007). Regulation of ryanodine receptor-dependent calcium signaling by polycystin-2. Proc Natl Acad Sci U S A 104(15): 6454-6459.

Arnaout R, Ferrer T, Huisken J, Spitzer K, Stainier DY, Tristani-Firouzi M and Chi NC (2007). Zebrafish model for human long QT syndrome. Proc Natl Acad Sci U S A 104(27): 11316-11321.

Babnigg G, Heller B and Villereal ML (2000). Cell-to-cell variation in store-operated calcium entry in HEK-293 cells and its impact on the interpretation of data from stable clones expressing exogenous calcium channels. Cell Calcium 27(2): 61-73.

Bagatto B and Burggren W (2006). A three-dimensional functional assessment of heart and vessel development in the larva of the zebrafish (Danio rerio). Physiol Biochem Zool 79(1): 194-201.

Bajwa ZH, Sial KA, Malik AB and Steinman TI (2004). Pain patterns in patients with polycystic kidney disease. Kidney Int 66(4): 1561-1569.

Baker K, Warren KS, Yellen G and Fishman MC (1997). Defective "pacemaker" current (Ih) in a zebrafish mutant with a slow heart rate. Proc Natl Acad Sci U S A 94(9): 4554-4559.

Bakkers J (2011). Zebrafish as a model to study cardiac development and human cardiac disease. Cardiovasc Res 91(2): 279-288.

Bardaji A, Vea AM, Gutierrez C, Ridao C, Richart C and Oliver JA (1998). Left ventricular mass and diastolic function in normotensive young adults with autosomal dominant polycystic kidney disease. Am J Kidney Dis 32(6): 970-975.

Bassani JW, Yuan W and Bers DM (1995). Fractional SR Ca release is regulated by trigger Ca and SR Ca content in cardiac myocytes. Am J Physiol 268(5 Pt 1): C1313-1319.

Bayer JD, Narayan SM, Lalani GG and Trayanova NA (2010). Rate-dependent action potential alternans in human heart failure implicates abnormal intracellular calcium handling. Heart Rhythm 7(8): 1093-1101.

Berg KJ (1960). Multifocal ventricular extrasystoles with Adams-Stokes syndrome in siblings. Am Heart J 60: 965-970.

Berger RD, Kasper EK, Baughman KL, Marban E, Calkins H and Tomaselli GF (1997). Beat-to-beat QT interval variability: novel evidence for repolarization lability in ischemic and nonischemic dilated cardiomyopathy. Circulation 96(5): 1557-1565.

Bers DM (2002). Cardiac excitation-contraction coupling. Nature 415(6868): 198-205.

Bers DM (2008). Calcium cycling and signaling in cardiac myocytes. Annu Rev Physiol 70: 23-49.

Bers DM, Eisner DA and Valdivia HH (2003). Sarcoplasmic reticulum Ca2+ and heart failure: roles of diastolic leak and Ca2+ transport. Circ Res 93(6): 487-490.

Bers DM and Grandi E (2009). Calcium/calmodulin-dependent kinase II regulation of cardiac ion channels. J Cardiovasc Pharmacol 54(3): 180-187.

Beuckelmann DJ, Nabauer M and Erdmann E (1992). Intracellular calcium handling in isolated ventricular myocytes from patients with terminal heart failure. Circulation 85(3): 1046-1055.

Beuckelmann DJ, Nabauer M and Erdmann E (1993). Alterations of K+ currents in isolated human ventricular myocytes from patients with terminal heart failure. Circ Res 73(2): 379-385.

Bhuiyan ZA, Hamdan MA, Shamsi ET, Postma AV, Mannens MM, Wilde AA and Al-Gazali L (2007). A novel early onset lethal form of catecholaminergic polymorphic ventricular tachycardia maps to chromosome 7p14-p22. J Cardiovasc Electrophysiol 18(10): 1060-1066.

Boca M, D'Amato L, Distefano G, Polishchuk RS, Germino GG and Boletta A (2007). Polycystin-1 induces cell migration by regulating phosphatidylinositol 3-kinase-dependent cytoskeletal rearrangements and GSK3beta-dependent cell cell mechanical adhesion. Mol Biol Cell 18(10): 4050-4061.

Brette F (2010). Calcium polymorphic ventricular tachycardia: a new name for CPVT? Cardiovasc Res 87(1): 10-11.

Brette F, Luxan G, Cros C, Dixey H, Wilson C and Shiels HA (2008). Characterization of isolated ventricular myocytes from adult zebrafish (Danio rerio). Biochem Biophys Res Commun 374(1): 143-146.

Brini M (2008). Calcium-sensitive photoproteins. Methods 46(3): 160-166.

Burashnikov A and Antzelevitch C (2006). Late-phase 3 EAD. A unique mechanism contributing to initiation of atrial fibrillation. Pacing Clin Electrophysiol 29(3): 290-295.

Burdon-Sanderson J (1884). On the Electrical Phenomena of the Excitatory Process in the Heart of the Frog and of the Tortoise, as investigated Photographically. J Physiol 4(6): 327-386 315.

Calo L, De Santo T, Nuccio F, Sciarra L, De Luca L, Stefano LM, Piroli E, Zuccaro L, Rebecchi M, de Ruvo E and Lioy E (2011). Predictive value of microvolt T-wave alternans for cardiac death or ventricular tachyarrhythmic events in ischemic and nonischemic cardiomyopathy patients: a meta-analysis. Ann Noninvasive Electrocardiol 16(4): 388-402.

Casini S, Verkerk AO, van Borren MM, van Ginneken AC, Veldkamp MW, de Bakker JM and Tan HL (2009). Intracellular calcium modulation of voltage-gated sodium channels in ventricular myocytes. Cardiovasc Res 81(1): 72-81.

Casuscelli J, Schmidt S, DeGray B, Petri ET, Celic A, Folta-Stogniew E, Ehrlich BE and Boggon TJ (2009). Analysis of the cytoplasmic interaction between polycystin-1 and polycystin-2. Am J Physiol Renal Physiol 297(5): F1310-1315.

Cerrone M, Colombi B, Santoro M, di Barletta MR, Scelsi M, Villani L, Napolitano C and Priori SG (2005). Bidirectional ventricular tachycardia and fibrillation elicited in a knock-in mouse model carrier of a mutation in the cardiac ryanodine receptor. Circ Res 96(10): e77-82.

Cerrone M, Napolitano C and Priori SG (2009). Catecholaminergic polymorphic ventricular tachycardia: A paradigm to understand mechanisms of arrhythmias associated to impaired Ca(2+) regulation. Heart Rhythm 6(11): 1652-1659.

Cerrone MC, B.; Bloise, R.; Memmi, M.; Moncalvo, C.; Potenza, D.; Drago, F.; Napolitano, C.; Bradley, D.J.; Priori, S.G. (2004). Clinical and molecular characterization of a large cohort of patients affected with catecholaminergic polymorphic ventricular tachycardia (abstr). Circulation 110(Suppl II): 552.

Chablais F, Veit J, Rainer G and Jazwinska A (2011). The zebrafish heart regenerates after cryoinjury-induced myocardial infarction. BMC Dev Biol 11: 21.

Chang MY and Ong AC (2012). Mechanism-based therapeutics for autosomal dominant polycystic kidney disease: recent progress and future prospects. Nephron Clin Pract 120(1): c25-34; discussion c35.

Chapman AB, Johnson AM, Rainguet S, Hossack K, Gabow P and Schrier RW (1997). Left ventricular hypertrophy in autosomal dominant polycystic kidney disease. J Am Soc Nephrol 8(8): 1292-1297.

Chatterjee K and Massie B (2007). Systolic and diastolic heart failure: differences and similarities. J Card Fail 13(7): 569-576.

Chen B, Guo A, Gao Z, Wei S, Xie Y-P, Chen SRW, Anderson ME and Song L-S (2012). In Situ Confocal Imaging in Intact Heart Reveals Stress-Induced Ca2+ Release Variability in a Murine CPVT Model of RyR2R4496C+/- Mutation. Circulation. Arrhythmia and electrophysiology.

Chen W, Wang R, Chen B, Zhong X, Kong H, Bai Y, Zhou Q, Xie C, Zhang J, Guo A, Tian X, Jones PP, O'Mara ML, Liu Y, Mi T, Zhang L, Bolstad J, Semeniuk L, Cheng H, Zhang J, Chen J, Tieleman DP, Gillis AM, Duff HJ, Fill M, Song LS and Chen SR (2014). The ryanodine receptor store-sensing gate controls Ca waves and Ca-triggered arrhythmias. Nat Med.

Chen X, Zhang X, Kubo H, Harris DM, Mills GD, Moyer J, Berretta R, Potts ST, Marsh JD and Houser SR (2005). Ca2+ influx-induced sarcoplasmic reticulum Ca2+ overload causes mitochondrial-dependent apoptosis in ventricular myocytes. Circ Res 97(10): 1009-1017.

Chico TJ, Ingham PW and Crossman DC (2008). Modeling cardiovascular disease in the zebrafish. Trends Cardiovasc Med 18(4): 150-155.

Choi BR, Burton F and Salama G (2002). Cytosolic Ca2+ triggers early afterdepolarizations and Torsade de Pointes in rabbit hearts with type 2 long QT syndrome. J Physiol 543(Pt 2): 615-631.

Chudin E, Goldhaber J, Garfinkel A, Weiss J and Kogan B (1999). Intracellular Ca(2+) dynamics and the stability of ventricular tachycardia. Biophys J 77(6): 2930-2941.

Cohen LB and Salzberg BM (1978). Optical measurement of membrane potential. Rev Physiol Biochem Pharmacol 83: 35-88.

Cohn JN, Johnson G, Ziesche S, Cobb F, Francis G, Tristani F, Smith R, Dunkman WB, Loeb H, Wong M and et al. (1991). A comparison of enalapril with hydralazine-isosorbide dinitrate in the treatment of chronic congestive heart failure. N Engl J Med 325(5): 303-310.

Cohn JN, Levine TB, Olivari MT, Garberg V, Lura D, Francis GS, Simon AB and Rector T (1984). Plasma norepinephrine as a guide to prognosis in patients with chronic congestive heart failure. N Engl J Med 311(13): 819-823.

Collura CA, Johnson JN, Moir C and Ackerman MJ (2009). Left cardiac sympathetic denervation for the treatment of long QT syndrome and catecholaminergic polymorphic ventricular tachycardia using video-assisted thoracic surgery. Heart Rhythm 6(6): 752-759.

Consortium TIPKD (1995). Polycystic kidney disease: the complete structure of the PKD1 gene and its protein. Cell 81(2): 289-298.

Coumel P, Fidelle, J., Lucet, V., Attuel, P., Bouvrain, Y. (1978). Catecholaminergic-induced severe ventricular arrhythmias with Adams-Stokes syndrome in children: report of four cases. Brit Heart J 40: 28-37.

Craig MP, Gilday SD and Hove JR (2006). Dose-dependent effects of chemical immobilization on the heart rate of embryonic zebrafish. Lab Anim (NY) 35(9): 41-47.

Cross JL, Boulos S, Shepherd KL, Craig AJ, Lee S, Bakker AJ, Knuckey NW and Meloni BP (2012). High level over-expression of different NCX isoforms in HEK293 cell lines and primary neuronal cultures is protective following oxygen glucose deprivation. Neurosci Res 73(3): 191-198.

Dahme T, Katus HA and Rottbauer W (2009). Fishing for the genetic basis of cardiovascular disease. Dis Model Mech 2(1-2): 18-22.

Dalgaard OZ (1957). Bilateral polycystic disease of the kidneys; a follow-up of two hundred and eighty-four patients and their families. Acta Med Scand Suppl 328: 1-255.

Darbandi S and Franck JP (2009). A comparative study of ryanodine receptor (RyR) gene expression levels in a basal ray-finned fish, bichir (Polypterus ornatipinnis) and the derived euteleost zebrafish (Danio rerio). Comp Biochem Physiol B Biochem Mol Biol 154(4): 443-448.

Davidenko JM (1993). Spiral wave activity: a possible common mechanism for polymorphic and monomorphic ventricular tachycardias. J Cardiovasc Electrophysiol 4(6): 730-746.

Del Monte F and Hajjar RJ (2008). Intracellular devastation in heart failure. Heart Fail Rev 13(2): 151-162.

Demaurex N and Distelhorst C (2003). Cell biology. Apoptosis--the calcium connection. Science 300(5616): 65-67.

Denvir MA, Tucker CS and Mullins JJ (2008). Systolic and diastolic ventricular function in zebrafish embryos: influence of norepenephrine, MS-222 and temperature. BMC Biotechnol 8: 21.

Di Pasquale E, Lodola F, Miragoli M, Denegri M, Avelino-Cruz JE, Buonocore M, Nakahama H, Portararo P, Bloise R, Napolitano C, Condorelli G and Priori SG (2013). CaMKII inhibition rectifies arrhythmic phenotype in a patient-specific model of catecholaminergic polymorphic ventricular tachycardia. Cell Death Dis 4: e843.

Diaz ME, Eisner DA and O'Neill SC (2002). Depressed ryanodine receptor activity increases variability and duration of the systolic Ca2+ transient in rat ventricular myocytes. Circ Res 91(7): 585-593.

Diaz ME, O'Neill SC and Eisner DA (2004). Sarcoplasmic reticulum calcium content fluctuation is the key to cardiac alternans. Circ Res 94(5): 650-656.

Dick E, Rajamohan D, Ronksley J and Denning C (2010). Evaluating the utility of cardiomyocytes from human pluripotent stem cells for drug screening. Biochem Soc Trans 38(4): 1037-1045.

Dorn GW, 2nd (2009). Apoptotic and non-apoptotic programmed cardiomyocyte death in ventricular remodelling. Cardiovasc Res 81(3): 465-473.

Doss MX, Di Diego JM, Goodrow RJ, Wu Y, Cordeiro JM, Nesterenko VV, Barajas-Martinez H, Hu D, Urrutia J, Desai M, Treat JA, Sachinidis A and Antzelevitch C (2012). Maximum diastolic potential of human induced pluripotent stem cell-derived cardiomyocytes depends critically on I(Kr). PLoS One 7(7): e40288.

Draper MH and Weidmann S (1951). Cardiac resting and action potentials recorded with an intracellular electrode. J Physiol 115(1): 74-94.

Drouin E, Lande G and Charpentier F (1998). Amiodarone reduces transmural heterogeneity of repolarization in the human heart. J Am Coll Cardiol 32(4): 1063-1067.

Dumitrescu C, Narayan P, Efimov IR, Cheng Y, Radin MJ, McCune SA and Altschuld RA (2002). Mechanical alternans and restitution in failing SHHF rat left ventricles. Am J Physiol Heart Circ Physiol 282(4): H1320-1326.

Ecder T (2013). Cardiovascular complications in autosomal dominant polycystic kidney disease. Curr Hypertens Rev 9(1): 2-11.

Einthoven W (1903). Die galvanometrische Registerung des menschlichen Elektrokardiogram: Zugleich eine Beurtheilung der Anwendung des Capillar Elektrometers in der Physiologie. Pflugers Arch ges Physiol 99: 472-480.

Eisen JS and Smith JC (2008). Controlling morpholino experiments: don't stop making antisense. Development 135(10): 1735-1743.

Eisner D, Bode E, Venetucci L and Trafford A (2013). Calcium flux balance in the heart. J Mol Cell Cardiol 58: 110-117.

Epstein AE, DiMarco JP, Ellenbogen KA, Estes NA, 3rd, Freedman RA, Gettes LS, Gillinov AM, Gregoratos G, Hammill SC, Hayes DL, Hlatky MA, Newby LK, Page RL, Schoenfeld MH, Silka MJ, Stevenson LW, Sweeney MO, Tracy CM, Epstein AE, Darbar D, DiMarco JP, Dunbar SB, Estes NA, 3rd, Ferguson TB, Jr., Hammill SC, Karasik PE, Link MS, Marine JE, Schoenfeld MH, Shanker AJ, Silka MJ, Stevenson LW, Stevenson WG, Varosy PD, American College of Cardiology F, American Heart Association Task Force on Practice G and Heart Rhythm S (2013). 2012 ACCF/AHA/HRS focused update incorporated into the ACCF/AHA/HRS 2008 guidelines for device-based therapy of cardiac rhythm abnormalities: a report of the American College of Cardiology Foundation/American Heart Association Task Force on Practice Guidelines and the Heart Rhythm Society. J Am Coll Cardiol 61(3): e6-75.

Faggioni M, Kryshtal DO and Knollmann BC (2012). Calsequestrin mutations and catecholaminergic polymorphic ventricular tachycardia. Pediatr Cardiol 33(6): 959-967.

Fatima A, Xu G, Shao K, Papadopoulos S, Lehmann M, Arnaiz-Cot JJ, Rosa AO, Nguemo F, Matzkies M, Dittmann S, Stone SL, Linke M, Zechner U, Beyer V, Hennies HC, Rosenkranz S, Klauke B, Parwani AS, Haverkamp W, Pfitzer G, Farr M, Cleemann L, Morad M, Milting H,

Hescheler J and Saric T (2011). In vitro modeling of ryanodine receptor 2 dysfunction using human induced pluripotent stem cells. Cell Physiol Biochem 28(4): 579-592.

Fauconnier J, Meli AC, Thireau J, Roberge S, Shan J, Sassi Y, Reiken SR, Rauzier JM, Marchand A, Chauvier D, Cassan C, Crozier C, Bideaux P, Lompre AM, Jacotot E, Marks AR and Lacampagne A (2011). Ryanodine receptor leak mediated by caspase-8 activation leads to left ventricular injury after myocardial ischemia-reperfusion. Proc Natl Acad Sci U S A 108(32): 13258-13263.

Ferrantini C, Crocini C, Coppini R, Vanzi F, Tesi C, Cerbai E, Poggesi C, Pavone FS and Sacconi L (2013). The transverse-axial tubular system of cardiomyocytes. Cell Mol Life Sci 70(24): 4695-4710.

Fick GM, Johnson AM, Hammond WS and Gabow PA (1995). Causes of death in autosomal dominant polycystic kidney disease. J Am Soc Nephrol 5(12): 2048-2056.

Fischer TH, Herting J, Tirilomis T, Renner A, Neef S, Toischer K, Ellenberger D, Forster A, Schmitto JD, Gummert J, Schondube FA, Hasenfuss G, Maier LS and Sossalla S (2013). Ca2+/Calmodulin-Dependent Protein Kinase II and Protein Kinase A Differentially Regulate Sarcoplasmic Reticulum Ca2+ Leak in Human Cardiac Pathology. Circulation 128(9): 970-981.

Flore V, Claus P, Antoons G, Oosterhoff P, Holemans P, Vos MA, Sipido KR and Willems R (2011). Microvolt T-wave alternans and beat-to-beat variability of repolarization during early postischemic remodeling in a pig heart. Heart Rhythm 8(7): 1050-1057.

Frank K and Kranias EG (2000). Phospholamban and cardiac contractility. Ann Med 32(8): 572-578.

Franz MR (1983). Long-term recording of monophasic action potentials from human endocardium. Am J Cardiol 51(10): 1629-1634.

Franz MR (1991). Method and theory of monophasic action potential recording. Prog Cardiovasc Dis 33(6): 347-368.

Franz MR (1999). Current status of monophasic action potential recording: theories, measurements and interpretations. Cardiovasc Res 41(1): 25-40.

Gabow PA (1993). Autosomal dominant polycystic kidney disease. N Engl J Med 329(5): 332-342.

Gaburjakova M, Gaburjakova J, Reiken S, Huang F, Marx SO, Rosemblit N and Marks AR (2001). FKBP12 binding modulates ryanodine receptor channel gating. J Biol Chem 276(20): 16931-16935.

Gaeta SA and Christini DJ (2012). Non-linear dynamics of cardiac alternans: subcellular to tissue-level mechanisms of arrhythmia. Front Physiol 3: 157.

Gallagher AR, Cedzich A, Gretz N, Somlo S and Witzgall R (2000). The polycystic kidney disease protein PKD2 interacts with Hax-1, a protein associated with the actin cytoskeleton. Proc Natl Acad Sci U S A 97(8): 4017-4022.

Garratt CJ, Elliott P, Behr E, Camm AJ, Cowan C, Cruickshank S, Grace A, Griffith MJ, Jolly A, Lambiase P, McKeown P, O'Callagan P, Stuart G, Watkins H and Heart Rhythm UKFSCDSSDG (2010). Heart Rhythm UK position statement on clinical indications for implantable cardioverter defibrillators in adult patients with familial sudden cardiac death syndromes. Europace 12(8): 1156-1175.

Gattone VH, 2nd, Wang X, Harris PC and Torres VE (2003). Inhibition of renal cystic disease development and progression by a vasopressin V2 receptor antagonist. Nat Med 9(10): 1323-1326.

Geberth S, Ritz E, Zeier M and Stier E (1995). Anticipation of age at renal death in autosomal dominant polycystic kidney disease (ADPKD)? Nephrol Dial Transplant 10(9): 1603-1606.

Geng L, Boehmerle W, Maeda Y, Okuhara DY, Tian X, Yu Z, Choe CU, Anyatonwu GI, Ehrlich BE and Somlo S (2008). Syntaxin 5 regulates the endoplasmic reticulum channel-release properties of polycystin-2. Proc Natl Acad Sci U S A 105(41): 15920-15925.

Geng L, Okuhara D, Yu Z, Tian X, Cai Y, Shibazaki S and Somlo S (2006). Polycystin-2 traffics to cilia independently of polycystin-1 by using an N-terminal RVxP motif. J Cell Sci 119(Pt 7): 1383-1395.

Geng L, Segal Y, Pavlova A, Barros EJ, Lohning C, Lu W, Nigam SK, Frischauf AM, Reeders ST and Zhou J (1997). Distribution and developmentally regulated expression of murine polycystin. Am J Physiol 272(4 Pt 2): F451-459.

George CH, Higgs GV and Lai FA (2003). Ryanodine receptor mutations associated with stress-induced ventricular tachycardia mediate increased calcium release in stimulated cardiomyocytes. Circ Res 93(6): 531-540.

George CH, Jundi H, Walters N, Thomas NL, West RR and Lai FA (2006). Arrhythmogenic mutation-linked defects in ryanodine receptor autoregulation reveal a novel mechanism of Ca2+ release channel dysfunction. Circ Res 98(1): 88-97.

Germanguz I, Sedan O, Zeevi-Levin N, Shtrichman R, Barak E, Ziskind A, Eliyahu S, Meiry G, Amit M, Itskovitz-Eldor J and Binah O (2011). Molecular characterization and functional properties of cardiomyocytes derived from human inducible pluripotent stem cells. J Cell Mol Med 15(1): 38-51.

Glukhov AV, Kalyanasundaram A, Lou Q, Hage LT, Hansen BJ, Belevych AE, Mohler PJ, Knollmann BC, Periasamy M, Györke S and Fedorov VV (2013). Calsequestrin 2 deletion causes sinoatrial node dysfunction and atrial arrhythmias associated with altered sarcoplasmic reticulum calcium cycling and degenerative fibrosis within the mouse atrial pacemaker complex. Eur Heart J.

Gonzalez-Rosa JM, Martin V, Peralta M, Torres M and Mercader N (2011). Extensive scar formation and regression during heart regeneration after cryoinjury in zebrafish. Development 138(9): 1663-1674.

Gout AM, Martin NC, Brown AF and Ravine D (2007). PKDB: Polycystic Kidney Disease Mutation Database--a gene variant database for autosomal dominant polycystic kidney disease. Hum Mutat 28(7): 654-659.

Grant AO (2009). Cardiac ion channels. Circ Arrhythm Electrophysiol 2(2): 185-194.

Grantham JJ (2008). Clinical practice. Autosomal dominant polycystic kidney disease. N Engl J Med 359(14): 1477-1485.

Grantham JJ, Torres VE, Chapman AB, Guay-Woodford LM, Bae KT, King BF, Jr., Wetzel LH, Baumgarten DA, Kenney PJ, Harris PC, Klahr S, Bennett WM, Hirschman GN, Meyers CM, Zhang X, Zhu F, Miller JP and Investigators C (2006). Volume progression in polycystic kidney disease. N Engl J Med 354(20): 2122-2130.

Grynkiewicz G, Poenie M and Tsien RY (1985). A new generation of Ca2+ indicators with greatly improved fluorescence properties. J Biol Chem 260(6): 3440-3450.

Guo W and Campbell KP (1995). Association of triadin with the ryanodine receptor and calsequestrin in the lumen of the sarcoplasmic reticulum. J Biol Chem 270(16): 9027-9030.

Gupta A, Hoang DD, Karliner L, Tice JA, Heidenreich P, Wang PJ and Turakhia MP (2012). Ability of microvolt T-wave alternans to modify risk assessment of ventricular tachyarrhythmic events: a meta-analysis. Am Heart J 163(3): 354-364.

Gwathmey JK, Copelas L, MacKinnon R, Schoen FJ, Feldman MD, Grossman W and Morgan JP (1987). Abnormal intracellular calcium handling in myocardium from patients with end-stage heart failure. Circ Res 61(1): 70-76.

Györke I, Hester N, Jones LR and Györke S (2004). The role of calsequestrin, triadin, and junctin in conferring cardiac ryanodine receptor responsiveness to luminal calcium. Biophys J 86(4): 2121-2128.

Györke S (2009). Molecular basis of catecholaminergic polymorphic ventricular tachycardia. Heart Rhythm 6(1): 123-129.

Györke S and Terentyev D (2008). Modulation of ryanodine receptor by luminal calcium and accessory proteins in health and cardiac disease. Cardiovasc Res 77(2): 245-255.

Hain J, Onoue H, Mayrleitner M, Fleischer S and Schindler H (1995). Phosphorylation modulates the function of the calcium release channel of sarcoplasmic reticulum from cardiac muscle. Journal of Biological Chemistry 270(5): 2074-2081.

Hamill OP, Marty A, Neher E, Sakmann B and Sigworth FJ (1981). Improved patch-clamp techniques for high-resolution current recording from cells and cell-free membrane patches. Pflugers Arch 391(2): 85-100.

Han C, Tavi P and Weckstrom M (2002). Modulation of action potential by [Ca2+]i in modeled rat atrial and guinea pig ventricular myocytes. Am J Physiol Heart Circ Physiol 282(3): H1047-1054.

Harris PC, Bae KT, Rossetti S, Torres VE, Grantham JJ, Chapman AB, Guay-Woodford LM, King BF, Wetzel LH, Baumgarten DA, Kenney PJ, Consugar M, Klahr S, Bennett WM, Meyers CM, Zhang QJ, Thompson PA, Zhu F and Miller JP (2006). Cyst number but not the rate of cystic growth is associated with the mutated gene in autosomal dominant polycystic kidney disease. J Am Soc Nephrol 17(11): 3013-3019.

Hasenfuss G and Pieske B (2002). Calcium cycling in congestive heart failure. J Mol Cell Cardiol 34(8): 951-969.

Hasenfuss G, Reinecke H, Studer R, Meyer M, Pieske B, Holtz J, Holubarsch C, Posival H, Just H and Drexler H (1994). Relation between myocardial function and expression of sarcoplasmic reticulum Ca(2+)-ATPase in failing and nonfailing human myocardium. Circ Res 75(3): 434-442.

Hasenfuss G, Schillinger W, Lehnart SE, Preuss M, Pieske B, Maier LS, Prestle J, Minami K and Just H (1999). Relationship between Na+-Ca2+-exchanger protein levels and diastolic function of failing human myocardium. Circulation 99(5): 641-648.

Hassel D, Dahme T, Erdmann J, Meder B, Huge A, Stoll M, Just S, Hess A, Ehlermann P, Weichenhan D, Grimmler M, Liptau H, Hetzer R, Regitz-Zagrosek V, Fischer C, Nurnberg P, Schunkert H, Katus HA and Rottbauer W (2009). Nexilin mutations destabilize cardiac Z-disks and lead to dilated cardiomyopathy. Nat Med 15(11): 1281-1288.

Hassel D, Scholz EP, Trano N, Friedrich O, Just S, Meder B, Weiss DL, Zitron E, Marquart S, Vogel B, Karle CA, Seemann G, Fishman MC, Katus HA and Rottbauer W (2008). Deficient zebrafish ether-a-go-go-related gene channel gating causes short-QT syndrome in zebrafish reggae mutants. Circulation 117(7): 866-875.

Hateboer N, v Dijk MA, Bogdanova N, Coto E, Saggar-Malik AK, San Millan JL, Torra R, Breuning M and Ravine D (1999). Comparison of phenotypes of polycystic kidney disease types 1 and 2. European PKD1-PKD2 Study Group. Lancet 353(9147): 103-107.

Hayashi M, Denjoy I, Extramiana F, Maltret A, Buisson NR, Lupoglazoff JM, Klug D, Takatsuki S, Villain E, Kamblock J, Messali A, Guicheney P, Lunardi J and Leenhardt A (2009). Incidence and risk factors of arrhythmic events in catecholaminergic polymorphic ventricular tachycardia. Circulation 119(18): 2426-2434.

Hayashi T, Mochizuki T, Reynolds DM, Wu G, Cai Y and Somlo S (1997). Characterization of the exon structure of the polycystic kidney disease 2 gene (PKD2). Genomics 44(1): 131-136.

Heideman W, Antkiewicz DS, Carney SA and Peterson RE (2005). Zebrafish and cardiac toxicology. Cardiovasc Toxicol 5(2): 203-214.

Herron TJ, Lee P and Jalife J (2012). Optical imaging of voltage and calcium in cardiac cells & tissues. Circ Res 110(4): 609-623.

Hinterseer M, Beckmann BM, Thomsen MB, Pfeufer A, Ulbrich M, Sinner MF, Perz S, Wichmann HE, Lengyel C, Schimpf R, Maier SK, Varro A, Vos MA, Steinbeck G and Kaab S (2010). Usefulness of short-term variability of QT intervals as a predictor for electrical remodeling and proarrhythmia in patients with nonischemic heart failure. Am J Cardiol 106(2): 216-220.

Hinterseer M, Thomsen MB, Beckmann BM, Pfeufer A, Schimpf R, Wichmann HE, Steinbeck G, Vos MA and Kaab S (2008). Beat-to-beat variability of QT intervals is increased in patients with drug-induced long-QT syndrome: a case control pilot study. Eur Heart J 29(2): 185-190.

Hoekstra M, Mummery CL, Wilde AA, Bezzina CR and Verkerk AO (2012). Induced pluripotent stem cell derived cardiomyocytes as models for cardiac arrhythmias. Front Physiol 3: 346.

Hohendanner F, Ljubojevic S, Macquaide N, Sacherer M, Sedej S, Biesmans L, Wakula P, Platzer D, Sokolow S, Herchuelz A, Antoons G, Sipido K, Pieske B and Heinzel FR (2013). Intracellular dyssynchrony of diastolic cytosolic [Ca2+] decay in ventricular cardiomyocytes in cardiac remodeling and human heart failure. Circ Res 113(5): 527-538.

Hoppe UC, Jansen E, Sudkamp M and Beuckelmann DJ (1998). Hyperpolarization-activated inward current in ventricular myocytes from normal and failing human hearts. Circulation 97(1): 55-65.

Hossack KF, Leddy CL, Johnson AM, Schrier RW and Gabow PA (1988). Echocardiographic findings in autosomal dominant polycystic kidney disease. N Engl J Med 319(14): 907-912.

Hughes J, Ward CJ, Peral B, Aspinwall R, Clark K, San Millan JL, Gamble V and Harris PC (1995). The polycystic kidney disease 1 (PKD1) gene encodes a novel protein with multiple cell recognition domains. Nat Genet 10(2): 151-160.

Hunt DJ, Jones PP, Wang R, Chen W, Bolstad J, Chen K, Shimoni Y and Chen SR (2007). K201 (JTV519) suppresses spontaneous Ca2+ release and [3H]ryanodine binding to RyR2 irrespective of FKBP12.6 association. Biochem J 404(3): 431-438.

Hwang HS, Hasdemir C, Laver D, Mehra D, Turhan K, Faggioni M, Yin H and Knollmann BC (2011). Inhibition of cardiac Ca2+ release channels (RyR2) determines efficacy of class I antiarrhythmic drugs in catecholaminergic polymorphic ventricular tachycardia. Circ Arrhythm Electrophysiol 4(2): 128-135.

Ikemoto N and Yamamoto T (2002). Regulation of calcium release by interdomain interaction within ryanodine receptors. Front Biosci 7: d671-683.

Iost N, Virág L, Opincariu M, Szécsi J, Varró A and Papp JG (1998). Delayed rectifier potassium current in undiseased human ventricular myocytes. Cardiovasc Res 40(3): 508-515.

Issa ZF, Miller JM and Zipes DP (2012). Chapter 3 - Electrophysiological Mechanisms of Cardiac Arrhythmias. In: Clinical Arrhythmology and Electrophysiology: A Companion to Braunwald's Heart Disease (Second Edition). Issa ZF, Miller JM and Zipes DP. Philadelphia, W.B. Saunders. 36-61.

Itzhaki I, Maizels L, Huber I, Gepstein A, Arbel G, Caspi O, Miller L, Belhassen B, Nof E, Glikson M and Gepstein L (2012). Modeling of catecholaminergic polymorphic ventricular tachycardia with patient-specific human-induced pluripotent stem cells. J Am Coll Cardiol 60(11): 990-1000.

Itzhaki I, Maizels L, Huber I, Zwi-Dantsis L, Caspi O, Winterstern A, Feldman O, Gepstein A, Arbel G, Hammerman H, Boulos M and Gepstein L (2011a). Modelling the long QT syndrome with induced pluripotent stem cells. Nature 471(7337): 225-229.

Itzhaki I, Rapoport S, Huber I, Mizrahi I, Zwi-Dantsis L, Arbel G, Schiller J and Gepstein L (2011b). Calcium handling in human induced pluripotent stem cell derived cardiomyocytes. PLoS One 6(4): e18037.

January CT and Moscucci A (1992). Cellular mechanisms of early afterdepolarizations. Ann N Y Acad Sci 644: 23-32.

Jiang B, Sun X, Cao K and Wang R (2002a). Endogenous Kv channels in human embryonic kidney (HEK-293) cells. Mol Cell Biochem 238(1-2): 69-79.

Jiang D, Wang R, Xiao B, Kong H, Hunt DJ, Choi P, Zhang L and Chen SR (2005). Enhanced store overload-induced Ca2+ release and channel sensitivity to luminal Ca2+ activation are common defects of RyR2 mutations linked to ventricular tachycardia and sudden death. Circ Res 97(11): 1173-1181.

Jiang D, Xiao B, Yang D, Wang R, Choi P, Zhang L, Cheng H and Chen SR (2004). RyR2 mutations linked to ventricular tachycardia and sudden death reduce the threshold for store-overload-induced Ca2+ release (SOICR). Proc Natl Acad Sci U S A 101(35): 13062-13067.

Jiang D, Xiao B, Zhang L and Chen SR (2002b). Enhanced basal activity of a cardiac Ca2+ release channel (ryanodine receptor) mutant associated with ventricular tachycardia and sudden death. Circ Res 91(3): 218-225.

Jochim K, Katz LN and Mayne W (1935). The monophasic electrogram obtained from the mammalian heart. Am J Physiol(111): 177-186.

Johnson DM, Heijman J, Bode EF, Greensmith DJ, van der Linde H, Abi-Gerges N, Eisner DA, Trafford AW and Volders PG (2013). Diastolic spontaneous calcium release from the sarcoplasmic reticulum increases beat-to-beat variability of repolarization in canine ventricular myocytes after beta-adrenergic stimulation. Circ Res 112(2): 246-256.

Josephson ME (2007). Electrophysiology at a crossroads. Heart Rhythm 4(5): 658-661.

Jou CJ, Spitzer KW and Tristani-Firouzi M (2010). Blebbistatin effectively uncouples the excitation-contraction process in zebrafish embryonic heart. Cell Physiol Biochem 25(4-5): 419-424.

Jung CB, Moretti A, Mederos y Schnitzler M, Iop L, Storch U, Bellin M, Dorn T, Ruppenthal S, Pfeiffer S, Goedel A, Dirschinger RJ, Seyfarth M, Lam JT, Sinnecker D, Gudermann T, Lipp P and Laugwitz KL (2012). Dantrolene rescues arrhythmogenic RYR2 defect in a patient-specific stem cell model of catecholaminergic polymorphic ventricular tachycardia. EMBO Mol Med 4(3): 180-191.

Kannankeril PJ, Mitchell BM, Goonasekera SA, Chelu MG, Zhang W, Sood S, Kearney DL, Danila CI, De Biasi M, Wehrens XH, Pautler RG, Roden DM, Taffet GE, Dirksen RT, Anderson ME and Hamilton SL (2006). Mice with the R176Q cardiac ryanodine receptor mutation exhibit catecholamine-induced ventricular tachycardia and cardiomyopathy. Proc Natl Acad Sci U S A 103(32): 12179-12184.

Katra RP and Laurita KR (2005). Cellular mechanism of calcium-mediated triggered activity in the heart. Circ Res 96(5): 535-542.

Kelleher CL, McFann KK, Johnson AM and Schrier RW (2004). Characteristics of hypertension in young adults with autosomal dominant polycystic kidney disease compared with the general U.S. population. Am J Hypertens 17(11 Pt 1): 1029-1034.

Kimberling WJ, Fain PR, Kenyon JB, Goldgar D, Sujansky E and Gabow PA (1988). Linkage heterogeneity of autosomal dominant polycystic kidney disease. N Engl J Med 319(14): 913-918.

Klahr S, Breyer JA, Beck GJ, Dennis VW, Hartman JA, Roth D, Steinman TI, Wang SR and Yamamoto ME (1995). Dietary protein restriction, blood pressure control, and the progression of polycystic kidney disease. Modification of Diet in Renal Disease Study Group. J Am Soc Nephrol 5(12): 2037-2047.

Knollmann BC (2013). Induced pluripotent stem cell-derived cardiomyocytes: boutique science or valuable arrhythmia model? Circ Res 112(6): 969-976; discussion 976.

Knollmann BC, Chopra N, Hlaing T, Akin B, Yang T, Ettensohn K, Knollmann BE, Horton KD, Weissman NJ, Holinstat I, Zhang W, Roden DM, Jones LR, Franzini-Armstrong C and Pfeifer K (2006). Casq2 deletion causes sarcoplasmic reticulum volume increase, premature Ca2+ release, and catecholaminergic polymorphic ventricular tachycardia. J Clin Invest 116(9): 2510-2520.

Kockskamper J, Zima AV, Roderick HL, Pieske B, Blatter LA and Bootman MD (2008). Emerging roles of inositol 1,4,5-trisphosphate signaling in cardiac myocytes. J Mol Cell Cardiol 45(2): 128-147.

Koller ML, Riccio ML and Gilmour RF, Jr. (1998). Dynamic restitution of action potential duration during electrical alternans and ventricular fibrillation. Am J Physiol 275(5 Pt 2): H1635-1642.

Kornyeyev D, Petrosky AD, Zepeda B, Ferreiro M, Knollmann B and Escobar AL (2012). Calsequestrin 2 deletion shortens the refractoriness of Ca(2)(+) release and reduces rate-dependent Ca(2)(+)-alternans in intact mouse hearts. J Mol Cell Cardiol 52(1): 21-31.

Korsgren M, Leskinen E, Sjostrand U and Varnauskas E (1966). Intracardiac recording of monophasic action potentials in the human heart. Scand J Clin Lab Invest 18(5): 561-564.

Koulen P, Cai Y, Geng L, Maeda Y, Nishimura S, Witzgall R, Ehrlich BE and Somlo S (2002). Polycystin-2 is an intracellular calcium release channel. Nat Cell Biol 4(3): 191-197.

Kovács M, Tóth J, Hetényi C, Málnási-Csizmadia A and Sellers JR (2004). Mechanism of blebbistatin inhibition of myosin II. J Biol Chem 279(34): 35557-35563.

Krebs EG (1989). The Albert Lasker Medical Awards. Role of the cyclic AMP-dependent protein kinase in signal transduction. JAMA 262(13): 1815-1818.

Kujala K, Paavola J, Lahti A, Larsson K, Pekkanen-Mattila M, Viitasalo M, Lahtinen AM, Toivonen L, Kontula K, Swan H, Laine M, Silvennoinen O and Aalto-Setala K (2012). Cell model of catecholaminergic polymorphic ventricular tachycardia reveals early and delayed afterdepolarizations. PLoS One 7(9): e44660.

Kurebayashi N, Nishizawa H, Nakazato Y, Kurihara H, Matsushita S, Daida H and Ogawa Y (2008). Aberrant cell-to-cell coupling in Ca2+-overloaded guinea pig ventricular muscles. Am J Physiol Cell Physiol 294(6): C1419-1429.

Lahat H, Eldar M, Levy-Nissenbaum E, Bahan T, Friedman E, Khoury A, Lorber A, Kastner DL, Goldman B and Pras E (2001a). Autosomal recessive catecholamine- or exercise-induced polymorphic ventricular tachycardia: clinical features and assignment of the disease gene to chromosome 1p13-21. Circulation 103(23): 2822-2827.

Lahat H, Pras E, Olender T, Avidan N, Ben-Asher E, Man O, Levy-Nissenbaum E, Khoury A, Lorber A, Goldman B, Lancet D and Eldar M (2001b). A missense mutation in a highly conserved region of CASQ2 is associated with autosomal recessive catecholamine-induced polymorphic ventricular tachycardia in Bedouin families from Israel. Am J Hum Genet 69(6): 1378-1384.

Lahti AL, Kujala VJ, Chapman H, Koivisto AP, Pekkanen-Mattila M, Kerkela E, Hyttinen J, Kontula K, Swan H, Conklin BR, Yamanaka S, Silvennoinen O and Aalto-Setala K (2012).

Model for long QT syndrome type 2 using human iPS cells demonstrates arrhythmogenic characteristics in cell culture. Dis Model Mech 5(2): 220-230.

Laitinen PJ, Brown KM, Piippo K, Swan H, Devaney JM, Brahmbhatt B, Donarum EA, Marino M, Tiso N, Viitasalo M, Toivonen L, Stephan DA and Kontula K (2001). Mutations of the cardiac ryanodine receptor (RyR2) gene in familial polymorphic ventricular tachycardia. Circulation 103(4): 485-490.

Langenbacher AD, Dong Y, Shu X, Choi J, Nicoll DA, Goldhaber JI, Philipson KD and Chen JN (2005). Mutation in sodium-calcium exchanger 1 (NCX1) causes cardiac fibrillation in zebrafish. Proc Natl Acad Sci U S A 102(49): 17699-17704.

Laurita KR and Rosenbaum DS (2008a). Cellular mechanisms of arrhythmogenic cardiac alternans. Prog Biophys Mol Biol 97(2-3): 332-347.

Laurita KR and Rosenbaum DS (2008b). Mechanisms and potential therapeutic targets for ventricular arrhythmias associated with impaired cardiac calcium cycling. J Mol Cell Cardiol 44(1): 31-43.

Lee YK, Ng KM, Lai WH, Chan YC, Lau YM, Lian Q, Tse HF and Siu CW (2011). Calcium homeostasis in human induced pluripotent stem cell-derived cardiomyocytes. Stem Cell Rev 7(4): 976-986.

Leenhardt A, Denjoy I and Guicheney P (2012). Catecholaminergic polymorphic ventricular tachycardia. Circ Arrhythm Electrophysiol 5(5): 1044-1052.

Leenhardt A, Lucet V, Denjoy I, Grau F, Ngoc DD and Coumel P (1995). Catecholaminergic polymorphic ventricular tachycardia in children. A 7-year follow-up of 21 patients. Circulation 91(5): 1512-1519.

Lehnart SE, Mongillo M, Bellinger A, Lindegger N, Chen BX, Hsueh W, Reiken S, Wronska A, Drew LJ, Ward CW, Lederer WJ, Kass RS, Morley G and Marks AR (2008). Leaky Ca2+ release channel/ryanodine receptor 2 causes seizures and sudden cardiac death in mice. J Clin Invest 118(6): 2230-2245.

Lehnart SE, Terrenoire C, Reiken S, Wehrens XH, Song LS, Tillman EJ, Mancarella S, Coromilas J, Lederer WJ, Kass RS and Marks AR (2006). Stabilization of cardiac ryanodine receptor prevents intracellular calcium leak and arrhythmias. Proc Natl Acad Sci U S A 103(20): 7906-7910.

Lehnart SE, Wehrens XH, Laitinen PJ, Reiken SR, Deng SX, Cheng Z, Landry DW, Kontula K, Swan H and Marks AR (2004a). Sudden death in familial polymorphic ventricular tachycardia associated with calcium release channel (ryanodine receptor) leak. Circulation 109(25): 3208-3214.

Lehnart SE, Wehrens XH and Marks AR (2004b). Calstabin deficiency, ryanodine receptors, and sudden cardiac death. Biochem Biophys Res Commun 322(4): 1267-1279.

Lewis T (1911). Notes upon alternation of the heart. the Quarterly Journal of Medicine 4(14): 141-144.

Li L, Desantiago J, Chu G, Kranias EG and Bers DM (2000). Phosphorylation of phospholamban and troponin I in beta-adrenergic-induced acceleration of cardiac relaxation. Am J Physiol Heart Circ Physiol 278(3): H769-779.

Li Q, Dai Y, Guo L, Liu Y, Hao C, Wu G, Basora N, Michalak M and Chen XZ (2003a). Polycystin-2 associates with tropomyosin-1, an actin microfilament component. J Mol Biol 325(5): 949-962.

Li Q, Shen PY, Wu G and Chen XZ (2003b). Polycystin-2 interacts with troponin I, an angiogenesis inhibitor. Biochemistry 42(2): 450-457.

Li S, Chen G and Li RA (2013a). Calcium Signaling of Human Pluripotent Stem Cell-Derived Cardiomyocytes. J Physiol.

Li S, Chen G and Li RA (2013b). Calcium signalling of human pluripotent stem cell-derived cardiomyocytes. J Physiol 591(Pt 21): 5279-5290.

Lipp P, Laine M, Tovey SC, Burrell KM, Berridge MJ, Li W and Bootman MD (2000). Functional InsP3 receptors that may modulate excitation-contraction coupling in the heart. Curr Biol 10(15): 939-942.

Little AG and Seebacher F (2013). Thyroid hormone regulates cardiac performance during cold acclimation in Zebrafish (Danio rerio). J Exp Biol.

Liu B, Ho HT, Velez-Cortes F, Lou Q, Valdivia C, Knollmann B, Valdivia H and Gyorke S (2014). Genetic ablation of ryanodine receptor 2 phosphorylation at Ser-2808 aggravates Ca2+-dependent cardiomyopathy by exacerbating diastolic Ca2+ release. J Physiol.

Liu N, Colombi B, Memmi M, Zissimopoulos S, Rizzi N, Negri S, Imbriani M, Napolitano C, Lai FA and Priori SG (2006). Arrhythmogenesis in catecholaminergic polymorphic ventricular tachycardia: insights from a RyR2 R4496C knock-in mouse model. Circ Res 99(3): 292-298.

Liu N, Ruan Y, Denegri M, Bachetti T, Li Y, Colombi B, Napolitano C, Coetzee WA and Priori SG (2011). Calmodulin kinase II inhibition prevents arrhythmias in RyR2(R4496C+/-) mice with catecholaminergic polymorphic ventricular tachycardia. J Mol Cell Cardiol 50(1): 214-222.

Liu N, Ruan Y and Priori SG (2008). Catecholaminergic polymorphic ventricular tachycardia. Prog Cardiovasc Dis 51(1): 23-30.

Lozano R, Naghavi M, Foreman K, Lim S, Shibuya K, Aboyans V, Abraham J, Adair T, Aggarwal R, Ahn SY, Alvarado M, Anderson HR, Anderson LM, Andrews KG, Atkinson C, Baddour LM, Barker-Collo S, Bartels DH, Bell ML, Benjamin EJ, Bennett D, Bhalla K, Bikbov B, Bin Abdulhak A, Birbeck G, Blyth F, Bolliger I, Boufous S, Bucello C, Burch M, Burney P,

Carapetis J, Chen H, Chou D, Chugh SS, Coffeng LE, Colan SD, Colquhoun S, Colson KE, Condon J, Connor MD, Cooper LT, Corriere M, Cortinovis M, de Vaccaro KC, Couser W, Cowie BC, Criqui MH, Cross M, Dabhadkar KC, Dahodwala N, De Leo D, Degenhardt L, Delossantos A, Denenberg J, Des Jarlais DC, Dharmaratne SD, Dorsey ER, Driscoll T, Duber H, Ebel B, Erwin PJ, Espindola P, Ezzati M, Feigin V, Flaxman AD, Forouzanfar MH, Fowkes FG, Franklin R, Fransen M, Freeman MK, Gabriel SE, Gakidou E, Gaspari F, Gillum RF, Gonzalez-Medina D, Halasa YA, Haring D, Harrison JE, Havmoeller R, Hay RJ, Hoen B, Hotez PJ, Hoy D, Jacobsen KH, James SL, Jasrasaria R, Jayaraman S, Johns N, Karthikeyan G, Kassebaum N, Keren A, Khoo JP, Knowlton LM, Kobusingye O, Koranteng A, Krishnamurthi R, Lipnick M, Lipshultz SE, Ohno SL, Mabweijano J, MacIntyre MF, Mallinger L, March L, Marks GB, Marks R, Matsumori A, Matzopoulos R, Mayosi BM, McAnulty JH, McDermott MM, McGrath J, Mensah GA, Merriman TR, Michaud C, Miller M, Miller TR, Mock C, Mocumbi AO, Mokdad AA, Moran A, Mulholland K, Nair MN, Naldi L, Narayan KM, Nasseri K, Norman P, O'Donnell M, Omer SB, Ortblad K, Osborne R, Ozgediz D, Pahari B, Pandian JD, Rivero AP, Padilla RP, Perez-Ruiz F, Perico N, Phillips D, Pierce K, Pope CA, 3rd, Porrini E, Pourmalek F, Raju M, Ranganathan D, Rehm JT, Rein DB, Remuzzi G, Rivara FP, Roberts T, De Leon FR, Rosenfeld LC, Rushton L, Sacco RL, Salomon JA, Sampson U, Sanman E, Schwebel DC, Segui-Gomez M, Shepard DS, Singh D, Singleton J, Sliwa K, Smith E, Steer A, Taylor JA, Thomas B, Tleyjeh IM, Towbin JA, Truelsen T, Undurraga EA, Venketasubramanian N, Vijayakumar L, Vos T, Wagner GR, Wang M, Wang W, Watt K, Weinstock MA, Weintraub R, Wilkinson JD, Woolf AD, Wulf S, Yeh PH, Yip P, Zabetian A, Zheng ZJ, Lopez AD, Murray CJ, AlMazroa MA and Memish ZA (2012). Global and regional mortality from 235 causes of death for 20 age groups in 1990 and 2010: a systematic analysis for the Global Burden of Disease Study 2010. Lancet 380(9859): 2095-2128.

Lumiaho A, Ikaheimo R, Miettinen R, Niemitukia L, Laitinen T, Rantala A, Lampainen E, Laakso M and Hartikainen J (2001). Mitral valve prolapse and mitral regurgitation are common in patients with polycystic kidney disease type 1. Am J Kidney Dis 38(6): 1208-1216.

Lundy SD, Zhu WZ, Regnier M and Laflamme MA (2013). Structural and functional maturation of cardiomyocytes derived from human pluripotent stem cells. Stem Cells Dev 22(14): 1991-2002.

Luo M and Anderson ME (2013). Mechanisms of altered Ca2+ handling in heart failure. Circ Res 113(6): 690-708.

Ma J, Guo L, Fiene SJ, Anson BD, Thomson JA, Kamp TJ, Kolaja KL, Swanson BJ and January CT (2011). High purity human-induced pluripotent stem cell-derived cardiomyocytes: electrophysiological properties of action potentials and ionic currents. Am J Physiol Heart Circ Physiol 301(5): H2006-2017.

MacRae CA (2013). Recent advances in in vivo screening for antiarrhythmic drugs. Expert Opin Drug Discov 8(2): 131-141.

Magyar J, Iost N, Kortvély A, Bányász T, Virág L, Szigligeti P, Varró A, Opincariu M, Szécsi J, Papp JG and Nánási PP (2000). Effects of endothelin-1 on calcium and potassium currents in undiseased human ventricular myocytes. Pflugers Arch 441(1): 144-149.

Maier LS and Bers DM (2007). Role of Ca2+/calmodulin-dependent protein kinase (CaMK) in excitation-contraction coupling in the heart. Cardiovasc Res 73(4): 631-640.

Malone MH, Sciaky N, Stalheim L, Hahn KM, Linney E and Johnson GL (2007). Laser-scanning velocimetry: a confocal microscopy method for quantitative measurement of cardiovascular performance in zebrafish embryos and larvae. BMC Biotechnol 7: 40.

Markoff A, Bogdanova N, Knop M, Ruffer C, Kenis H, Lux P, Reutelingsperger C, Todorov V, Dworniczak B, Horst J and Gerke V (2007). Annexin A5 interacts with polycystin-1 and interferes with the polycystin-1 stimulated recruitment of E-cadherin into adherens junctions. J Mol Biol 369(4): 954-966.

Marx SO, Reiken S, Hisamatsu Y, Jayaraman T, Burkhoff D, Rosemblit N and Marks AR (2000). PKA phosphorylation dissociates FKBP12.6 from the calcium release channel (ryanodine receptor): defective regulation in failing hearts. Cell 101(4): 365-376.

McCombs JE and Palmer AE (2008). Measuring calcium dynamics in living cells with genetically encodable calcium indicators. Methods 46(3): 152-159.

McMurray JJ and Pfeffer MA (2005). Heart failure. Lancet 365(9474): 1877-1889.

Medeiros-Domingo A, Bhuiyan ZA, Tester DJ, Hofman N, Bikker H, van Tintelen JP, Mannens MM, Wilde AA and Ackerman MJ (2009). The RYR2-encoded ryanodine receptor/calcium release channel in patients diagnosed previously with either catecholaminergic polymorphic ventricular tachycardia or genotype negative, exercise-induced long QT syndrome: a comprehensive open reading frame mutational analysis. J Am Coll Cardiol 54(22): 2065-2074.

Mekahli D, Parys JB, Bultynck G, Missiaen L and De Smedt H (2013). Polycystins and cellular Ca2+ signaling. Cell Mol Life Sci 70(15): 2697-2712.

Mekahli D, Sammels E, Luyten T, Welkenhuyzen K, van den Heuvel LP, Levtchenko EN, Gijsbers R, Bultynck G, Parys JB, De Smedt H and Missiaen L (2012). Polycystin-1 and polycystin-2 are both required to amplify inositol-trisphosphate-induced Ca2+ release. Cell Calcium 51(6): 452-458.

Menke AL, Spitsbergen JM, Wolterbeek AP and Woutersen RA (2011). Normal anatomy and histology of the adult zebrafish. Toxicol Pathol 39(5): 759-775.

Mezu UL, Singh P, Shusterman V, Hwang HS, Knollmann BC and Nemec J (2012). Accelerated Junctional Rhythm and Nonalternans Repolarization Lability Precede Ventricular Tachycardia in Casq2-/- Mice. J Cardiovasc Electrophysiol.

Milan DJ and Macrae CA (2008). Zebrafish genetic models for arrhythmia. Prog Biophys Mol Biol 98(2-3): 301-308.

Milan DJ, Peterson TA, Ruskin JN, Peterson RT and MacRae CA (2003). Drugs that induce repolarization abnormalities cause bradycardia in zebrafish. Circulation 107(10): 1355-1358.

Mochizuki T, Wu G, Hayashi T, Xenophontos SL, Veldhuisen B, Saris JJ, Reynolds DM, Cai Y, Gabow PA, Pierides A, Kimberling WJ, Breuning MH, Deltas CC, Peters DJ and Somlo S (1996). PKD2, a gene for polycystic kidney disease that encodes an integral membrane protein. Science 272(5266): 1339-1342.

Mohamed U, Gollob MH, Gow RM and Krahn AD (2006). Sudden cardiac death despite an implantable cardioverter-defibrillator in a young female with catecholaminergic ventricular tachycardia. Heart Rhythm 3(12): 1486-1489.

Moore HJ and Franz MR (2007). Monophasic action potential recordings in humans. J Cardiovasc Electrophysiol 18(7): 787-790.

Mordwinkin NM, Burridge PW and Wu JC (2013). A review of human pluripotent stem cell-derived cardiomyocytes for high-throughput drug discovery, cardiotoxicity screening, and publication standards. J Cardiovasc Transl Res 6(1): 22-30.

Moretti A, Bellin M, Welling A, Jung CB, Lam JT, Bott-Flugel L, Dorn T, Goedel A, Hohnke C, Hofmann F, Seyfarth M, Sinnecker D, Schomig A and Laugwitz KL (2010). Patient-specific induced pluripotent stem-cell models for long-QT syndrome. N Engl J Med 363(15): 1397-1409.

Mummery C, Ward-van Oostwaard D, Doevendans P, Spijker R, van den Brink S, Hassink R, van der Heyden M, Opthof T, Pera M, de la Riviere AB, Passier R and Tertoolen L (2003). Differentiation of human embryonic stem cells to cardiomyocytes: role of coculture with visceral endoderm-like cells. Circulation 107(21): 2733-2740.

Mummery CL, Zhang J, Ng ES, Elliott DA, Elefanty AG and Kamp TJ (2012). Differentiation of human embryonic stem cells and induced pluripotent stem cells to cardiomyocytes: a methods overview. Circ Res 111(3): 344-358.

Näbauer M, Beuckelmann DJ, Uberfuhr P and Steinbeck G (1996). Regional differences in current density and rate-dependent properties of the transient outward current in subepicardial and subendocardial myocytes of human left ventricle. Circulation 93(1): 168-177.

Nakajima T, Kaneko Y, Taniguchi Y, Hayashi K, Takizawa T, Suzuki T and Nagai R (1997). The mechanism of catecholaminergic polymorphic ventricular tachycardia may be triggered activity due to delayed afterdepolarization. Eur Heart J 18(3): 530-531.

Nakayama H, Chen X, Baines CP, Klevitsky R, Zhang X, Zhang H, Jaleel N, Chua BH, Hewett TE, Robbins J, Houser SR and Molkentin JD (2007). Ca2+- and mitochondrial-dependent cardiomyocyte necrosis as a primary mediator of heart failure. J Clin Invest 117(9): 2431-2444.

Nam GB, Burashnikov A and Antzelevitch C (2005). Cellular mechanisms underlying the development of catecholaminergic ventricular tachycardia. Circulation 111(21): 2727-2733.

Narayan SM (2006). T-wave alternans and the susceptibility to ventricular arrhythmias. J Am Coll Cardiol 47(2): 269-281.

Narayan SM, Bayer JD, Lalani G and Trayanova NA (2008). Action potential dynamics explain arrhythmic vulnerability in human heart failure: a clinical and modeling study implicating abnormal calcium handling. J Am Coll Cardiol 52(22): 1782-1792.

Nasevicius A and Ekker SC (2000). Effective targeted gene 'knockdown' in zebrafish. Nat Genet 26(2): 216-220.

Nearing BD and Verrier RL (2002). Modified moving average analysis of T-wave alternans to predict ventricular fibrillation with high accuracy. J Appl Physiol 92(2): 541-549.

Neher E, Sakmann B and Steinbach JH (1978). The extracellular patch clamp: a method for resolving currents through individual open channels in biological membranes. Pflugers Arch 375(2): 219-228.

Nemec J, Kim JJ, Gabris B and Salama G (2010). Calcium oscillations and T-wave lability precede ventricular arrhythmias in acquired long QT type 2. Heart Rhythm 7(11): 1686-1694.

Nemtsas P, Wettwer E, Christ T, Weidinger G and Ravens U (2010). Adult zebrafish heart as a model for human heart? An electrophysiological study. J Mol Cell Cardiol 48(1): 161-171.

Nerbonne JM and Kass RS (2005). Molecular physiology of cardiac repolarization. Physiol Rev 85(4): 1205-1253.

Neumann HP, Jilg C, Bacher J, Nabulsi Z, Malinoc A, Hummel B, Hoffmann MM, Ortiz-Bruechle N, Glasker S, Pisarski P, Neeff H, Kramer-Guth A, Cybulla M, Hornberger M, Wilpert J, Funk L, Baumert J, Paatz D, Baumann D, Lahl M, Felten H, Hausberg M, Zerres K, Eng C and Else Kroener Fresenius AR (2013). Epidemiology of autosomal-dominant polycystic kidney disease: an in-depth clinical study for south-western Germany. Nephrol Dial Transplant 28(6): 1472-1487.

Nivala M and Qu Z (2012). Calcium alternans in a couplon network model of ventricular myocytes: role of sarcoplasmic reticulum load. Am J Physiol Heart Circ Physiol 303(3): H341-352.

Nof E, Belhassen B, Arad M, Bhuiyan ZA, Antzelevitch C, Rosso R, Fogelman R, Luria D, El-Ani D, Mannens MM, Viskin S, Eldar M, Wilde AA and Glikson M (2011). Postpacing abnormal repolarization in catecholaminergic polymorphic ventricular tachycardia associated with a mutation in the cardiac ryanodine receptor gene. Heart Rhythm 8(10): 1546-1552.

Novak A, Barad L, Zeevi-Levin N, Shick R, Shtrichman R, Lorber A, Itskovitz-Eldor J and Binah O (2012). Cardiomyocytes generated from CPVTD307H patients are arrhythmogenic in response to beta-adrenergic stimulation. J Cell Mol Med 16(3): 468-482.

Obara T, Mangos S, Liu Y, Zhao J, Wiessner S, Kramer-Zucker AG, Olale F, Schier AF and Drummond IA (2006). Polycystin-2 immunolocalization and function in zebrafish. J Am Soc Nephrol 17(10): 2706-2718.

Obokata H, Wakayama T, Sasai Y, Kojima K, Vacanti MP, Niwa H, Yamato M and Vacanti CA (2014). Stimulus-triggered fate conversion of somatic cells into pluripotency. Nature 505(7485): 641-647.

Odero A, Bozzani A, De Ferrari GM and Schwartz PJ (2010). Left cardiac sympathetic denervation for the prevention of life-threatening arrhythmias: the surgical supraclavicular approach to cervicothoracic sympathectomy. Heart Rhythm 7(8): 1161-1165.

Oflaz H, Alisir S, Buyukaydin B, Kocaman O, Turgut F, Namli S, Pamukcu B, Oncul A and Ecder T (2005). Biventricular diastolic dysfunction in patients with autosomal-dominant polycystic kidney disease. Kidney Int 68(5): 2244-2249.

Okano H, Nakamura M, Yoshida K, Okada Y, Tsuji O, Nori S, Ikeda E, Yamanaka S and Miura K (2013). Steps toward safe cell therapy using induced pluripotent stem cells. Circ Res 112(3): 523-533.

Omichi C, Lamp ST, Lin SF, Yang J, Baher A, Zhou S, Attin M, Lee MH, Karagueuzian HS, Kogan B, Qu Z, Garfinkel A, Chen PS and Weiss JN (2004). Intracellular Ca dynamics in ventricular fibrillation. Am J Physiol Heart Circ Physiol 286(5): H1836-1844.

Ong AC, Ward CJ, Butler RJ, Biddolph S, Bowker C, Torra R, Pei Y and Harris PC (1999). Coordinate expression of the autosomal dominant polycystic kidney disease proteins, polycystin-2 and polycystin-1, in normal and cystic tissue. Am J Pathol 154(6): 1721-1729.

Ono K and Iijima T (2010). Cardiac T-type Ca(2+) channels in the heart. J Mol Cell Cardiol 48(1): 65-70.

Oosterhoff P, Tereshchenko LG, van der Heyden MA, Ghanem RN, Fetics BJ, Berger RD and Vos MA (2011). Short-term variability of repolarization predicts ventricular tachycardia and sudden cardiac death in patients with structural heart disease: a comparison with QT variability index. Heart Rhythm 8(10): 1584-1590.

Palanca V, Quesada A, Trigo A and Jimenez J (2006). [Arrhythmic storm induced by AICD discharge in a patient with catecholaminergic polymorphic ventricular tachycardia]. Rev Esp Cardiol 59(10): 1079-1080.

Paredes RM, Etzler JC, Watts LT, Zheng W and Lechleiter JD (2008). Chemical calcium indicators. Methods 46(3): 143-151.

Pastore JM, Girouard SD, Laurita KR, Akar FG and Rosenbaum DS (1999). Mechanism linking T-wave alternans to the genesis of cardiac fibrillation. Circulation 99(10): 1385-1394.

Patterson E, Szabo B, Scherlag BJ and Lazzara R (1990). Early and delayed afterdepolarizations associated with cesium chloride-induced arrhythmias in the dog. J Cardiovasc Pharmacol 15(2): 323-331.

Paul BM, Consugar MB, Ryan Lee M, Sundsbak JL, Heyer CM, Rossetti S, Kubly VJ, Hopp K, Torres VE, Coto E, Clementi M, Bogdanova N, de Almeida E, Bichet DG and Harris PC (2013). Evidence of a third ADPKD locus is not supported by re-analysis of designated PKD3 families. Kidney Int.

Pei Y, Obaji J, Dupuis A, Paterson AD, Magistroni R, Dicks E, Parfrey P, Cramer B, Coto E, Torra R, San Millan JL, Gibson R, Breuning M, Peters D and Ravine D (2009). Unified criteria for ultrasonographic diagnosis of ADPKD. J Am Soc Nephrol 20(1): 205-212.

Peracchia C (2004). Chemical gating of gap junction channels; roles of calcium, pH and calmodulin. Biochim Biophys Acta 1662(1-2): 61-80.

Periasamy M and Janssen PM (2008). Molecular basis of diastolic dysfunction. Heart Fail Clin 4(1): 13-21.

Perrone RD, Ruthazer R and Terrin NC (2001). Survival after end-stage renal disease in autosomal dominant polycystic kidney disease: contribution of extrarenal complications to mortality. Am J Kidney Dis 38(4): 777-784.

Persu A, Duyme M, Pirson Y, Lens XM, Messiaen T, Breuning MH, Chauveau D, Levy M, Grunfeld JP and Devuyst O (2004). Comparison between siblings and twins supports a role for modifier genes in ADPKD. Kidney Int 66(6): 2132-2136.

Peterson RT, Shaw SY, Peterson TA, Milan DJ, Zhong TP, Schreiber SL, MacRae CA and Fishman MC (2004). Chemical suppression of a genetic mutation in a zebrafish model of aortic coarctation. Nat Biotechnol 22(5): 595-599.

Picht E, DeSantiago J, Blatter LA and Bers DM (2006). Cardiac alternans do not rely on diastolic sarcoplasmic reticulum calcium content fluctuations. Circ Res 99(7): 740-748.

Pieske B and Kockskamper J (2002). Alternans goes subcellular: a "disease" of the ryanodine receptor? Circ Res 91(7): 553-555.

Pieske B, Kretschmann B, Meyer M, Holubarsch C, Weirich J, Posival H, Minami K, Just H and Hasenfuss G (1995). Alterations in intracellular calcium handling associated with the inverse force-frequency relation in human dilated cardiomyopathy. Circulation 92(5): 1169-1178.

Pirson Y (2010). Extrarenal manifestations of autosomal dominant polycystic kidney disease. Adv Chronic Kidney Dis 17(2): 173-180.

Pizzale S, Gollob MH, Gow R and Birnie DH (2008). Sudden death in a young man with catecholaminergic polymorphic ventricular tachycardia and paroxysmal atrial fibrillation. J Cardiovasc Electrophysiol 19(12): 1319-1321.

Poss KD, Wilson LG and Keating MT (2002). Heart regeneration in zebrafish. Science 298(5601): 2188-2190.

Priori SG, Napolitano C, Di Pasquale E and Condorelli G (2013). Induced pluripotent stem cell-derived cardiomyocytes in studies of inherited arrhythmias. J Clin Invest 123(1): 84-91.

Priori SG, Napolitano C, Tiso N, Memmi M, Vignati G, Bloise R, Sorrentino V and Danieli GA (2001). Mutations in the cardiac ryanodine receptor gene (hRyR2) underlie catecholaminergic polymorphic ventricular tachycardia. Circulation 103(2): 196-200.

Pruvot EJ, Katra RP, Rosenbaum DS and Laurita KR (2004). Role of calcium cycling versus restitution in the mechanism of repolarization alternans. Circ Res 94(8): 1083-1090.

Qian L and Srivastava D (2013). Direct cardiac reprogramming: from developmental biology to cardiac regeneration. Circ Res 113(7): 915-921.

Qian Q, Li M, Cai Y, Ward CJ, Somlo S, Harris PC and Torres VE (2003). Analysis of the polycystins in aortic vascular smooth muscle cells. J Am Soc Nephrol 14(9): 2280-2287.

Ravine D, Gibson RN, Walker RG, Sheffield LJ, Kincaid-Smith P and Danks DM (1994). Evaluation of ultrasonographic diagnostic criteria for autosomal dominant polycystic kidney disease 1. Lancet 343(8901): 824-827.

Reeders ST, Breuning MH, Davies KE, Nicholls RD, Jarman AP, Higgs DR, Pearson PL and Weatherall DJ (1985). A highly polymorphic DNA marker linked to adult polycystic kidney disease on chromosome 16. Nature 317(6037): 542-544.

Reid DS, Tynan M, Braidwood L and Fitzgerald GR (1975). Bidirectional tachycardia in a child. A study using His bundle electrography. Br Heart J 37(3): 339-344.

Restrepo JG, Weiss JN and Karma A (2008). Calsequestrin-mediated mechanism for cellular calcium transient alternans. Biophys J 95(8): 3767-3789.

Ridgway EB and Ashley CC (1967). Calcium transients in single muscle fibers. Biochem Biophys Res Commun 29(2): 229-234.

Rohr S (2004). Role of gap junctions in the propagation of the cardiac action potential. Cardiovasc Res 62(2): 309-322.

Romeo G, Devoto M, Costa G, Roncuzzi L, Catizone L, Zucchelli P, Germino GG, Keith T, Weatherall DJ and Reeders ST (1988). A second genetic locus for autosomal dominant polycystic kidney disease. Lancet 2(8601): 8-11.

Rosenbaum DS, Jackson LE, Smith JM, Garan H, Ruskin JN and Cohen RJ (1994). Electrical alternans and vulnerability to ventricular arrhythmias. N Engl J Med 330(4): 235-241.

Roses-Noguer F, Jarman JW, Clague JR and Till J (2013). Outcomes Of Defibrillator Therapy In Catecholaminergic Polymorphic Ventricular Tachycardia. Heart Rhythm.

Rossetti S, Burton S, Strmecki L, Pond GR, San Millan JL, Zerres K, Barratt TM, Ozen S, Torres VE, Bergstralh EJ, Winearls CG and Harris PC (2002). The position of the polycystic kidney disease 1 (PKD1) gene mutation correlates with the severity of renal disease. J Am Soc Nephrol 13(5): 1230-1237.

Rossetti S, Chauveau D, Kubly V, Slezak JM, Saggar-Malik AK, Pei Y, Ong AC, Stewart F, Watson ML, Bergstralh EJ, Winearls CG, Torres VE and Harris PC (2003). Association of mutation position in polycystic kidney disease 1 (PKD1) gene and development of a vascular phenotype. Lancet 361(9376): 2196-2201.

Rossetti S, Consugar MB, Chapman AB, Torres VE, Guay-Woodford LM, Grantham JJ, Bennett WM, Meyers CM, Walker DL, Bae K, Zhang QJ, Thompson PA, Miller JP and Harris PC (2007). Comprehensive molecular diagnostics in autosomal dominant polycystic kidney disease. J Am Soc Nephrol 18(7): 2143-2160.

Rossetti S, Kubly VJ, Consugar MB, Hopp K, Roy S, Horsley SW, Chauveau D, Rees L, Barratt TM, van't Hoff WG, Niaudet P, Torres VE and Harris PC (2009). Incompletely penetrant PKD1 alleles suggest a role for gene dosage in cyst initiation in polycystic kidney disease. Kidney Int 75(8): 848-855.

Rossetti SA, M.; Kubly, V.; Consugar, M.B.; Torres, V.E.; Harris, P.C. (2007). An Olmsted County population-based study indicates that PKD2 is more common than previously described. J.Am.Soc.Nephrol. 18.

Rosso R, Kalman JM, Rogowski O, Diamant S, Birger A, Biner S, Belhassen B and Viskin S (2007). Calcium channel blockers and beta-blockers versus beta-blockers alone for preventing exercise-induced arrhythmias in catecholaminergic polymorphic ventricular tachycardia. Heart Rhythm 4(9): 1149-1154.

Rosso R, Kalman JM, Rogowski O, Diamant S, Birger A, Biner S, Belhassen B and Viskin S (2010). Long-term effectiveness of beta blocker and calcium blocker combination therapy in patients with CPVT (abstract). Heart Rhythm(7): S423.

Roux-Buisson N, Cacheux M, Fourest-Lieuvin A, Fauconnier J, Brocard J, Denjoy I, Durand P, Guicheney P, Kyndt F, Leenhardt A, Le Marec H, Lucet V, Mabo P, Probst V, Monnier N, Ray PF, Santoni E, Tremeaux P, Lacampagne A, Faure J, Lunardi J and Marty I (2012). Absence of triadin, a protein of the calcium release complex, is responsible for cardiac arrhythmia with sudden death in human. Hum Mol Genet 21(12): 2759-2767.

Sabir IN, Ma N, Jones VJ, Goddard Ca, Zhang Y, Kalin A, Grace Aa and Huang CL-H (2010). Alternans in genetically modified langendorff-perfused murine hearts modeling catecholaminergic polymorphic ventricular tachycardia. Frontiers in physiology 1: 126.

Salerno-Uriarte JA, De Ferrari GM, Klersy C, Pedretti RF, Tritto M, Sallusti L, Libero L, Pettinati G, Molon G, Curnis A, Occhetta E, Morandi F, Ferrero P and Accardi F (2007). Prognostic value of T-wave alternans in patients with heart failure due to nonischemic cardiomyopathy: results of the ALPHA Study. J Am Coll Cardiol 50(19): 1896-1904.

Samie FH and Jalife J (2001). Mechanisms underlying ventricular tachycardia and its transition to ventricular fibrillation in the structurally normal heart. Cardiovasc Res 50(2): 242-250.

Sammels E, Devogelaere B, Mekahli D, Bultynck G, Missiaen L, Parys JB, Cai Y, Somlo S and De Smedt H (2010). Polycystin-2 activation by inositol 1,4,5-trisphosphate-induced Ca2+ release requires its direct association with the inositol 1,4,5-trisphosphate receptor in a signaling microdomain. J Biol Chem 285(24): 18794-18805.

Sassone-Corsi P (2012). The cyclic AMP pathway. Cold Spring Harbor perspectives in biology 4(12).

Schillinger W, Schneider H, Minami K, Ferrari R and Hasenfuss G (2002). Importance of sympathetic activation for the expression of Na+-Ca2+ exchanger in end-stage failing human myocardium. Eur Heart J 23(14): 1118-1124.

Schlotthauer K and Bers DM (2000). Sarcoplasmic reticulum Ca(2+) release causes myocyte depolarization. Underlying mechanism and threshold for triggered action potentials. Circ Res 87(9): 774-780.

Schmitt JP, Kamisago M, Asahi M, Li GH, Ahmad F, Mende U, Kranias EG, MacLennan DH, Seidman JG and Seidman CE (2003). Dilated cardiomyopathy and heart failure caused by a mutation in phospholamban. Science 299(5611): 1410-1413.

Schmittgen TD and Livak KJ (2008). Analyzing real-time PCR data by the comparative C(T) method. Nat Protoc 3(6): 1101-1108.

Schneider HE, Steinmetz M, Krause U, Kriebel T, Ruschewski W and Paul T (2013). Left cardiac sympathetic denervation for the management of life-threatening ventricular tachyarrhythmias in young patients with catecholaminergic polymorphic ventricular tachycardia and long QT syndrome. Clin Res Cardiol 102(1): 33-42.

Schrier RW, McFann KK and Johnson AM (2003). Epidemiological study of kidney survival in autosomal dominant polycystic kidney disease. Kidney Int 63(2): 678-685.

Sedej S, Schmidt A, Denegri M, Walther S, Matovina M, Arnstein G, Gutschi EM, Windhager I, Ljubojevic S, Negri S, Heinzel FR, Bisping E, Vos MA, Napolitano C, Priori SG, Kockskamper J and Pieske B (2013). Subclinical abnormalities in sarcoplasmic reticulum Ca2+ release promote eccentric myocardial remodeling and pump failure death in response to pressure overload. J Am Coll Cardiol.

Shiferaw Y, Watanabe MA, Garfinkel A, Weiss JN and Karma A (2003). Model of intracellular calcium cycling in ventricular myocytes. Biophys J 85(6): 3666-3686.

Shusterman V, Goldberg A and London B (2006). Upsurge in T-wave alternans and nonalternating repolarization instability precedes spontaneous initiation of ventricular tachyarrhythmias in humans. Circulation 113(25): 2880-2887.

Shusterman V, Lampert R and London B (2009). The many faces of repolarization instability: which one is prognostic? J Electrocardiol 42(6): 511-516.

Sicouri S and Antzelevitch C (1991). A subpopulation of cells with unique electrophysiological properties in the deep subepicardium of the canine ventricle. The M cell. Circ Res 68(6): 1729-1741.

Signore S, Sorrentino A, Ferreira-Martins J, Kannappan R, Shafaie M, Del Ben F, Isobe K, Arranto C, Wybieralska E, Webster A, Sanada F, Ogorek B, Zheng H, Liu X, Del Monte F, D'Alessandro DA, Wunimenghe O, Michler RE, Hosoda T, Goichberg P, Leri A, Kajstura J, Anversa P and Rota M (2013). Inositol 1, 4, 5-Triphosphate Receptors and Human Left Ventricular Myocytes. Circulation.

Sinnecker D, Goedel A, Laugwitz KL and Moretti A (2013). Induced pluripotent stem cell-derived cardiomyocytes: a versatile tool for arrhythmia research. Circ Res 112(6): 961-968.

Smith JM, Clancy EA, Valeri CR, Ruskin JN and Cohen RJ (1988). Electrical alternans and cardiac electrical instability. Circulation 77(1): 110-121.

Song L, Alcalai R, Arad M, Wolf CM, Toka O, Conner DA, Berul CI, Eldar M, Seidman CE and Seidman JG (2007). Calsequestrin 2 (CASQ2) mutations increase expression of calreticulin and ryanodine receptors, causing catecholaminergic polymorphic ventricular tachycardia. J Clin Invest 117(7): 1814-1823.

Song LS, Sobie EA, McCulle S, Lederer WJ, Balke CW and Cheng H (2006). Orphaned ryanodine receptors in the failing heart. Proc Natl Acad Sci U S A 103(11): 4305-4310.

Sossalla S, Fluschnik N, Schotola H, Ort KR, Neef S, Schulte T, Wittkopper K, Renner A, Schmitto JD, Gummert J, El-Armouche A, Hasenfuss G and Maier LS (2010). Inhibition of elevated Ca2+/calmodulin-dependent protein kinase II improves contractility in human failing myocardium. Circ Res 107(9): 1150-1161.

Spencer CI and Sham JS (2003). Effects of Na+/Ca2+ exchange induced by SR Ca2+ release on action potentials and afterdepolarizations in guinea pig ventricular myocytes. Am J Physiol Heart Circ Physiol 285(6): H2552-2562.

Spira ME and Hai A (2013). Multi-electrode array technologies for neuroscience and cardiology. Nat Nanotechnol 8(2): 83-94.

Staudt D and Stainier D (2012). Uncovering the molecular and cellular mechanisms of heart development using the zebrafish. Annu Rev Genet 46: 397-418.

Suetomi T, Yano M, Uchinoumi H, Fukuda M, Hino A, Ono M, Xu X, Tateishi H, Okuda S, Doi M, Kobayashi S, Ikeda Y, Yamamoto T, Ikemoto N and Matsuzaki M (2011). Mutation-linked defective interdomain interactions within ryanodine receptor cause aberrant Ca(2)(+)release leading to catecholaminergic polymorphic ventricular tachycardia. Circulation 124(6): 682-694.

Sun Z, Amsterdam A, Pazour GJ, Cole DG, Miller MS and Hopkins N (2004). A genetic screen in zebrafish identifies cilia genes as a principal cause of cystic kidney. Development 131(16): 4085-4093.

Swan H, Laitinen P, Kontula K and Toivonen L (2005). Calcium channel antagonism reduces exercise-induced ventricular arrhythmias in catecholaminergic polymorphic ventricular tachycardia patients with RyR2 mutations. J Cardiovasc Electrophysiol 16(2): 162-166.

Swan H, Piippo K, Viitasalo M, Heikkila P, Paavonen T, Kainulainen K, Kere J, Keto P, Kontula K and Toivonen L (1999). Arrhythmic disorder mapped to chromosome 1q42-q43 causes malignant polymorphic ventricular tachycardia in structurally normal hearts. J Am Coll Cardiol 34(7): 2035-2042.

Taggart P and Lab M (2008). Cardiac mechano-electric feedback and electrical restitution in humans. Prog Biophys Mol Biol 97(2-3): 452-460.

Takahashi K, Tanabe K, Ohnuki M, Narita M, Ichisaka T, Tomoda K and Yamanaka S (2007). Induction of pluripotent stem cells from adult human fibroblasts by defined factors. Cell 131(5): 861-872.

Takahashi K and Yamanaka S (2006). Induction of pluripotent stem cells from mouse embryonic and adult fibroblast cultures by defined factors. Cell 126(4): 663-676.

Tan YC, Blumenfeld J and Rennert H (2011). Autosomal dominant polycystic kidney disease: genetics, mutations and microRNAs. Biochim Biophys Acta 1812(10): 1202-1212.

Tang Y, Tian X, Wang R, Fill M and Chen SR (2012). Abnormal termination of Ca2+ release is a common defect of RyR2 mutations associated with cardiomyopathies. Circ Res 110(7): 968-977.

ter Keurs HE (2012). The interaction of Ca2+ with sarcomeric proteins: role in function and dysfunction of the heart. Am J Physiol Heart Circ Physiol 302(1): H38-50.

Tester DJ, Dura M, Carturan E, Reiken S, Wronska A, Marks AR and Ackerman MJ (2007). A mechanism for sudden infant death syndrome (SIDS): stress-induced leak via ryanodine receptors. Heart Rhythm 4(6): 733-739.

Thomas P and Smart TG (2005). HEK293 cell line: a vehicle for the expression of recombinant proteins. J Pharmacol Toxicol Methods 51(3): 187-200.

Tomaselli GF, Beuckelmann DJ, Calkins HG, Berger RD, Kessler PD, Lawrence JH, Kass D, Feldman AM and Marban E (1994). Sudden cardiac death in heart failure. The role of abnormal repolarization. Circulation 90(5): 2534-2539.

Torres VE, Chapman AB, Devuyst O, Gansevoort RT, Grantham JJ, Higashihara E, Perrone RD, Krasa HB, Ouyang J, Czerwiec FS and Investigators TT (2012). Tolvaptan in patients with autosomal dominant polycystic kidney disease. N Engl J Med 367(25): 2407-2418.

Torres VE and Harris PC (2006). Mechanisms of Disease: autosomal dominant and recessive polycystic kidney diseases. Nat Clin Pract Nephrol 2(1): 40-55; quiz 55.

Torres VE and Harris PC (2009). Autosomal dominant polycystic kidney disease: the last 3 years. Kidney Int 76(2): 149-168.

Torres VE, Harris PC and Pirson Y (2007). Autosomal dominant polycystic kidney disease. Lancet 369(9569): 1287-1301.

Tsai CT, Wu CK, Chiang FT, Tseng CD, Lee JK, Yu CC, Wang YC, Lai LP, Lin JL and Hwang JJ (2011). In-vitro recording of adult zebrafish heart electrocardiogram - a platform for pharmacological testing. Clin Chim Acta 412(21-22): 1963-1967.

Tsien RY (1980). New calcium indicators and buffers with high selectivity against magnesium and protons: design, synthesis, and properties of prototype structures. Biochemistry 19(11): 2396-2404.

Tsiokas L, Kim S and Ong EC (2007). Cell biology of polycystin-2. Cell Signal 19(3): 444-453.

van der Werf C, Hofman N, Tan HL, van Dessel PF, Alders M, van der Wal AC, van Langen IM and Wilde AA (2010). Diagnostic yield in sudden unexplained death and aborted cardiac arrest in the young: the experience of a tertiary referral center in The Netherlands. Heart Rhythm 7(10): 1383-1389.

van der Werf C, Kannankeril PJ, Sacher F, Krahn AD, Viskin S, Leenhardt A, Shimizu W, Sumitomo N, Fish FA, Bhuiyan ZA, Willems AR, van der Veen MJ, Watanabe H, Laborderie J, Haissaguerre M, Knollmann BC and Wilde AA (2011). Flecainide therapy reduces exercise-induced ventricular arrhythmias in patients with catecholaminergic polymorphic ventricular tachycardia. J Am Coll Cardiol 57(22): 2244-2254.

van der Werf C and Wilde AA (2013). Catecholaminergic polymorphic ventricular tachycardia: from bench to bedside. Heart 99(7): 497-504.

van der Werf C, Zwinderman AH and Wilde AA (2012). Therapeutic approach for patients with catecholaminergic polymorphic ventricular tachycardia: state of the art and future developments. Europace 14(2): 175-183.

Varkevisser R, Wijers SC, van der Heyden MA, Beekman JD, Meine M and Vos MA (2012). Beat-to-beat variability of repolarization as a new biomarker for proarrhythmia in vivo. Heart Rhythm 9(10): 1718-1726.

Vassilev PM, Guo L, Chen XZ, Segal Y, Peng JB, Basora N, Babakhanlou H, Cruger G, Kanazirska M, Ye C, Brown EM, Hediger MA and Zhou J (2001). Polycystin-2 is a novel cation channel implicated in defective intracellular Ca(2+) homeostasis in polycystic kidney disease. Biochem Biophys Res Commun 282(1): 341-350.

Viitasalo M, Oikarinen L, Swan H, Glatter KA, Vaananen H, Fodstad H, Chiamvimonvat N, Kontula K, Toivonen L and Scheinman MM (2006). Ratio of late to early T-wave peak amplitude in 24-h electrocardiographic recordings as indicator of symptom history in patients with long-QT Syndrome types 1 and 2. J Am Coll Cardiol 47(1): 112-120.

Viitasalo M, Oikarinen L, Vaananen H, Kontula K, Toivonen L and Swan H (2008). U-waves and T-wave peak to T-wave end intervals in patients with catecholaminergic polymorphic ventricular tachycardia, effects of beta-blockers. Heart Rhythm 5(10): 1382-1388.

Virág L, Iost N, Opincariu M, Szolnoky J, Szécsi J, Bogáts G, Szenohradszky P, Varró A and Papp JG (2001). The slow component of the delayed rectifier potassium current in undiseased human ventricular myocytes. Cardiovasc Res 49(4): 790-797.

Volders PG, Kulcsar A, Vos MA, Sipido KR, Wellens HJ, Lazzara R and Szabo B (1997). Similarities between early and delayed afterdepolarizations induced by isoproterenol in canine ventricular myocytes. Cardiovasc Res 34(2): 348-359.

Volders PG, Vos MA, Szabo B, Sipido KR, de Groot SH, Gorgels AP, Wellens HJ and Lazzara R (2000). Progress in the understanding of cardiac early afterdepolarizations and torsades de pointes: time to revise current concepts. Cardiovasc Res 46(3): 376-392.

Volk T, Schwoerer AP, Thiessen S, Schultz JH and Ehmke H (2003). A polycystin-2-like large conductance cation channel in rat left ventricular myocytes. Cardiovasc Res 58(1): 76-88.

Wagner E, Lauterbach MA, Kohl T, Westphal V, Williams GS, Steinbrecher JH, Streich JH, Korff B, Tuan HT, Hagen B, Luther S, Hasenfuss G, Parlitz U, Jafri MS, Hell SW, Lederer WJ and Lehnart SE (2012). Stimulated emission depletion live-cell super-resolution imaging shows proliferative remodeling of T-tubule membrane structures after myocardial infarction. Circ Res 111(4): 402-414.

Wang Q, Dai XQ, Li Q, Wang Z, Cantero Mdel R, Li S, Shen J, Tu JC, Cantiello H and Chen XZ (2012). Structural interaction and functional regulation of polycystin-2 by filamin. PLoS One 7(7): e40448.

Wang X, Wu Y, Ward CJ, Harris PC and Torres VE (2008). Vasopressin directly regulates cyst growth in polycystic kidney disease. J Am Soc Nephrol 19(1): 102-108.

Warren KS, Baker K and Fishman MC (2001). The slow mo mutation reduces pacemaker current and heart rate in adult zebrafish. Am J Physiol Heart Circ Physiol 281(4): H1711-1719.

Watanabe H, Chopra N, Laver D, Hwang HS, Davies SS, Roach DE, Duff HJ, Roden DM, Wilde AA and Knollmann BC (2009). Flecainide prevents catecholaminergic polymorphic ventricular tachycardia in mice and humans. Nat Med 15(4): 380-383.

Watanabe MA, Fenton FH, Evans SJ, Hastings HM and Karma A (2001). Mechanisms for discordant alternans. J Cardiovasc Electrophysiol 12(2): 196-206.

Wehrens XH (2007). The molecular basis of catecholaminergic polymorphic ventricular tachycardia: what are the different hypotheses regarding mechanisms? Heart Rhythm 4(6): 794-797.

Wehrens XH, Lehnart SE and Marks AR (2005). Intracellular calcium release and cardiac disease. Annu Rev Physiol 67: 69-98.

Wehrens XH, Lehnart SE, Reiken SR, Deng SX, Vest JA, Cervantes D, Coromilas J, Landry DW and Marks AR (2004). Protection from cardiac arrhythmia through ryanodine receptor-stabilizing protein calstabin2. Science 304(5668): 292-296.

Weinstein BM, Stemple DL, Driever W and Fishman MC (1995). Gridlock, a localized heritable vascular patterning defect in the zebrafish. Nat Med 1(11): 1143-1147.

Weiss JN, Qu Z, Chen PS, Lin SF, Karagueuzian HS, Hayashi H, Garfinkel A and Karma A (2005). The dynamics of cardiac fibrillation. Circulation 112(8): 1232-1240.

Wilde AA, Bhuiyan ZA, Crotti L, Facchini M, De Ferrari GM, Paul T, Ferrandi C, Koolbergen DR, Odero A and Schwartz PJ (2008). Left cardiac sympathetic denervation for catecholaminergic polymorphic ventricular tachycardia. N Engl J Med 358(19): 2024-2029.

Wilson LD and Rosenbaum DS (2007). Mechanisms of arrythmogenic cardiac alternans. Europace 9 Suppl 6: vi77-82.

Wu G, Markowitz GS, Li L, D'Agati VD, Factor SM, Geng L, Tibara S, Tuchman J, Cai Y, Park JH, van Adelsberg J, Hou H, Jr., Kucherlapati R, Edelmann W and Somlo S (2000). Cardiac defects and renal failure in mice with targeted mutations in Pkd2. Nat Genet 24(1): 75-78.

Xiao J, Tian X, Jones PP, Bolstad J, Kong H, Wang R, Zhang L, Duff HJ, Gillis AM, Fleischer S, Kotlikoff M, Copello JA and Chen SR (2007). Removal of FKBP12.6 does not alter the conductance and activation of the cardiac ryanodine receptor or the susceptibility to stress-induced ventricular arrhythmias. J Biol Chem 282(48): 34828-34838.

Xie LH, Sato D, Garfinkel A, Qu Z and Weiss JN (2008a). Intracellular Ca alternans: coordinated regulation by sarcoplasmic reticulum release, uptake, and leak. Biophys J 95(6): 3100-3110.

Xie LH and Weiss JN (2009). Arrhythmogenic consequences of intracellular calcium waves. Am J Physiol Heart Circ Physiol 297(3): H997-H1002.

Xie Y, Ottolia M, John SA, Chen JN and Philipson KD (2008b). Conformational changes of a Ca2+-binding domain of the Na+/Ca2+ exchanger monitored by FRET in transgenic zebrafish heart. Am J Physiol Cell Physiol 295(2): C388-393.

Xu C, Rossetti S, Jiang L, Harris PC, Brown-Glaberman U, Wandinger-Ness A, Bacallao R and Alper SL (2007). Human ADPKD primary cyst epithelial cells with a novel, single codon deletion in the PKD1 gene exhibit defective ciliary polycystin localization and loss of flow-induced Ca2+ signaling. Am J Physiol Renal Physiol 292(3): F930-945.

Xu J, Zaim S and Pelleg A (1996). Effects of pinacidil, verapamil, and heart rate on afterdepolarizations in the guinea-pig heart in vivo. Heart Vessels 11(6): 289-302.

Yan GX and Antzelevitch C (1998). Cellular basis for the normal T wave and the electrocardiographic manifestations of the long-QT syndrome. Circulation 98(18): 1928-1936.

Yoshida Y and Yamanaka S (2011). iPS cells: a source of cardiac regeneration. J Mol Cell Cardiol 50(2): 327-332.

Yu J, Vodyanik MA, Smuga-Otto K, Antosiewicz-Bourget J, Frane JL, Tian S, Nie J, Jonsdottir GA, Ruotti V, Stewart R, Slukvin, II and Thomson JA (2007). Induced pluripotent stem cell lines derived from human somatic cells. Science 318(5858): 1917-1920.

Yu SP and Kerchner GA (1998). Endogenous voltage-gated potassium channels in human embryonic kidney (HEK293) cells. J Neurosci Res 52(5): 612-617.

Yuan W and Bers DM (1994). Ca-dependent facilitation of cardiac Ca current is due to Ca-calmodulin-dependent protein kinase. Am J Physiol 267(3 Pt 2): H982-993.

Zhang J, Wilson GF, Soerens AG, Koonce CH, Yu J, Palecek SP, Thomson JA and Kamp TJ (2009a). Functional cardiomyocytes derived from human induced pluripotent stem cells. Circ Res 104(4): e30-41.

Zhang L, Kelley J, Schmeisser G, Kobayashi YM and Jones LR (1997). Complex formation between junctin, triadin, calsequestrin, and the ryanodine receptor. Proteins of the cardiac junctional sarcoplasmic reticulum membrane. J Biol Chem 272(37): 23389-23397.

Zhang PC, Llach A, Sheng XY, Hove-Madsen L and Tibbits GF (2011). Calcium handling in zebrafish ventricular myocytes. Am J Physiol Regul Integr Comp Physiol 300(1): R56-66.

Zhang XH, Haviland S, Wei H, Saric T, Fatima A, Hescheler J, Cleemann L and Morad M (2013a). Ca signaling in human induced pluripotent stem cell-derived cardiomyocytes (iPS-CM) from normal and catecholaminergic polymorphic ventricular tachycardia (CPVT)-afflicted subjects. Cell Calcium.

Zhang Y, Wu J, Jeevaratnam K, King JH, Guzadhur L, Ren X, Grace AA, Lei M, Huang CL and Fraser JA (2013b). Conduction slowing contributes to spontaneous ventricular arrhythmias in intrinsically active murine RyR2-P2328S hearts. J Cardiovasc Electrophysiol 24(2): 210-218.

Zhang YH and Hancox JC (2009b). Regulation of cardiac Na+-Ca2+ exchanger activity by protein kinase phosphorylation--still a paradox? Cell Calcium 45(1): 1-10.

Zhou Q, Xiao J, Jiang D, Wang R, Vembaiyan K, Wang A, Smith CD, Xie C, Chen W, Zhang J, Tian X, Jones PP, Zhong X, Guo A, Chen H, Zhang L, Zhu W, Yang D, Li X, Chen J, Gillis AM, Duff HJ, Cheng H, Feldman AM, Song LS, Fill M, Back TG and Chen SR (2011). Carvedilol and its new analogs suppress arrhythmogenic store overload-induced Ca2+ release. Nat Med 17(8): 1003-1009.

Zissimopoulos S and Lai FA (2005). Interaction of FKBP12.6 with the cardiac ryanodine receptor C-terminal domain. J Biol Chem 280(7): 5475-5485.

Zissimopoulos S, Thomas NL, Jamaluddin WW and Lai FA (2009). FKBP12.6 binding of ryanodine receptors carrying mutations associated with arrhythmogenic cardiac disease. Biochem J 419(2): 273-278.

HELSINGIN YLIOPISTO
HELSINGFORS UNIVERSITET
UNIVERSITY OF HELSINKI

LÄÄKETIETEELLINEN TIEDEKUNTA
MEDICINSKA FAKULTETEN
FACULTY OF MEDICINE

ISBN 978-952-10-9761-4 (paperback)
ISBN 978-952-10-9762-1 (PDF)
UNIGRAFIA